Analysis of retinoblastoma protein function in the regulation of apoptosis

Analyse der Funktion des Retinoblastoma-Proteins in der Apoptose-Regulation

Dissertation
zur Erlangung des akademischen Grades
doctor rerum naturalium (Dr. rer. nat.)

vorgelegt dem Rat der Biologisch-Pharmazeutischen Fakultät der Friedrich-Schiller-Universität Jena

**von Diplom-Biochemikerin
Anja Masselli**

geboren am 25.07.1976 in Göttingen

Jena, 2005

Table of contents

1 Introduction

1.1 Apoptosis as cell fate and cellular stress response

Programmed cell death is a process that is indispensable for the normal development of multicellular organisms and is of vital importance throughout their life. During embryonic development, elimination of surplus cells is required for the proper shaping of organs and body parts and the creation of complex multicellular tissues. In the developing vertebrate nervous system, for instance, most types of neurons are initially produced in excess. Surplus neurons will eventually be eliminated after reaching their target tissue, based on competition for survival factors that are released by the target cells in limited amounts. This allows the number of neurons to be exactly matched to the number of target cells. Similar mechanisms are thought to operate both during development and adulthood of metazoans to balance the numbers of different cell types in other complex tissues and organs, such as the blood and the lymphoid system.

In the adult organism, tissue maintenance requires the constant replacement of aged or damaged cells. This is achieved by the continuous proliferation of stem cell populations, from which different cell types are generated, and the predestined death of terminal differentiated cells. The normal lifespan of a differentiated cell depends on its function in the organism and ranges from several days (for instance, in the case of epithelia cells that form the lining of the small intestine) to many years (sensory receptor cells or neurons in the central nervous system, for example, have to last a lifetime). In contrast, cells with proliferative potential need to be eradicated immediately in case of damage to their genome, in order to prevent the passage of faulty genetic information to their progeny. In addition, programmed cell death is of particular importance in the immune system, for instance, to prevent the spreading of pathogens and to eliminate T-cells that are directed against endogenous proteins.

Apoptosis - after the Greek word for "falling off" - is the prevailing form of programmed cell death and is characterized by the traceless removal of the apoptotic cell in the absence of an inflammatory response. Apoptosis is defined by stereotypical morphological changes including chromatin condensation, plasma membrane blebbing and cell shrinkage, followed by fragmentation into membrane-enclosed vesicles (Kerr *et al.* 1972). These visible transformations are the effects of biochemical changes including the fragmentation of chromosomal DNA and the

cleavage of a defined set of cellular proteins that includes major structural components of the cell (Earnshaw *et al.* 1999). Concurrent alterations on the cell surface, such as the exposure of specific phospholipids, mark the cell for recognition by phagocytic cells. Together, these processes prepare the apoptotic cell for engulfment and the efficient recycling of biochemical resources. The apoptotic core machinery responsible for these intricate processes is conserved in all metazoans.

Apoptosis can be induced by different kinds of stimuli, of which two principal classes can be distinguished: 1) signals from the cells environment, such as lack of growth factors or survival signals, loss of matrix or cell-to-cell contact, and death signals through cytokines, and 2) various intracellular stress signals, created for example by the lack of nutrients, damage to the genome or the activation of oncogenes. In the adult organism proliferation and cell death are normally balanced to maintain equal cell numbers and tissue homeostasis. Defects in apoptosis regulation can therefore lead to the development of cancer, autoimmune disorders and acute or chronic degenerative diseases.

1.2   Central mediators of the apoptotic program

On the molecular level, apoptosis is characterized by the activation of the caspase family of cysteine proteases, in which a cysteine residue serves as the catalytic nucleophile. The name caspases refers to the cleavage of their substrates after a specific aspartate residue (Alnemri *et al.* 1996). Caspases reside in the cell as inactive precursors, referred to as pro-caspases, that are activated in a proteolytic cascade upon an apoptotic stimulus. They posses a large and a small subunit preceded by an N-terminal pro-domain. Structural and biochemical evidence indicates that active caspases are dimers of identical catalytic units each containing an active site (Boatright and Salvesen 2003).

According to their position in the apoptotic cascade mammalian caspases are classified as initiator or executioner caspases, also referred to as effector caspases (Thornberry and Lazebnik 1998). Initiator caspases are activated by recruitment to protein scaffolding complexes through proximity-induced dimerization (Boatright and Salvesen 2003). They are characterized by long pro-domains containing homophilic protein interaction motifs: caspase recruitment domains (CARDs) or death effector domains (DEDs). Via these motifs they can be recruited to caspase-activating scaffolding complexes at the plasma membrane and in the cytoplasm by DED or

CARD-containing adaptor molecules (Thornberry and Lazebnik 1998). Once activated, initiator caspases cleave and thereby activate the downstream effector caspases. Effector caspases have small or no pro-domains, lack the interaction motifs typical for initiator caspases and can instead be activated by cleavage through an upstream caspase, which separates their large and small subunits and removes the pro-domain (Earnshaw *et al.* 1999). In addition to upstream caspases, activated effector caspases can perform this cleavage, thereby allowing further amplification of the apoptotic signal. Crystallographic studies revealed that one large and one small subunit associate to form the active site of the enzyme (Shi 2002).

Among the numerous substrates of effector caspases are cytoskeletal proteins, nuclear structural proteins, components of the DNA repair machinery, protein kinases and other signaling molecules (Earnshaw *et al.* 1999). Proteolysis of these proteins eventually leads to chromatin degradation into nucleosomes, organelle destruction and other transformations that prepare the apoptotic cell for phagocytosis and allow the efficient recycling of its components (Salvesen and Dixit 1997; Budihardjo *et al.* 1999). Thus, the concerted action of effector caspases ultimately leads to the disassembly of the cell. Based on the different initiation of the caspase cascade, two alternative apoptotic pathways are distinguished: the intrinsic apoptosis pathway and the extrinsic, or death receptor apoptosis pathway (Figure 1 and 2).

1.3   The intrinsic apoptosis pathway

The intrinsic or mitochondrial apoptosis pathway is activated in response to various cellular stress factors, such as damage to the genome or other irreparable internal damage, and certain developmental cues, such as lack of growth or survival factors (Figure 1). These signals activate pro-apoptotic members of the BCL-2 family, which are termed BH3-only proteins, due to their possession of only one type of BCL-2 homology (BH) domains. Members include BAD, BID, BIM (BCL-2-interacting mediator of cell death), NOXA and PUMA (Huang and Strasser 2000). These proteins selectively respond to specific death signals: NOXA and PUMA, for example, are induced by p53 activity in response to DNA damage (Oda *et al.* 2000; Nakano and Vousden 2001); BAD is activated through dephosphorylation in response to a lack of
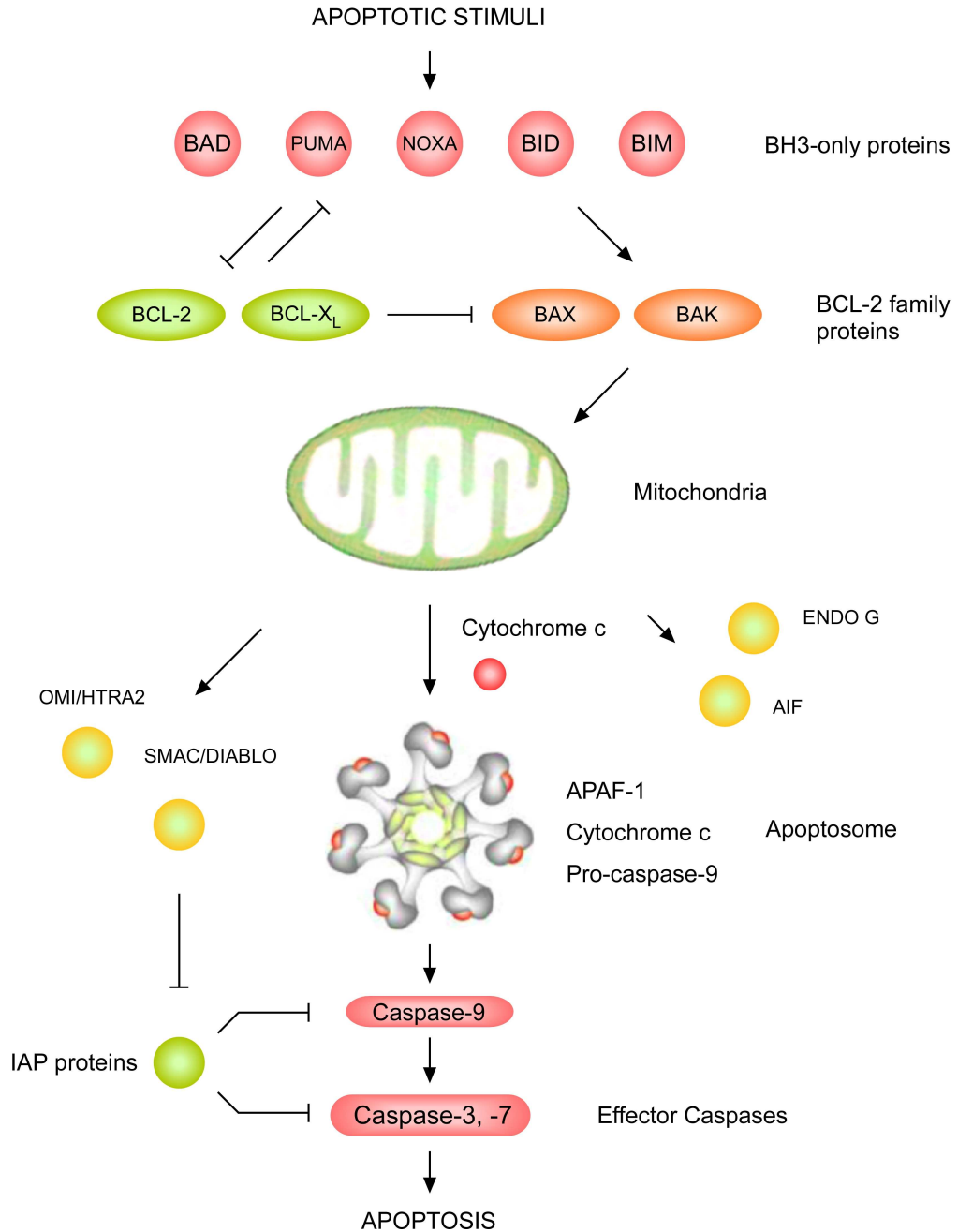
Figure 1. The intrinsic apoptosis pathway

Various cellular stresses and developmental death cues induce the release of cytochrome c from mitochondria via the activation of pro-apoptotic members of the BCL2-family. Different pro-apoptotic BH3-only proteins (*e.g.* BAD, BIM, BID, PUMA) bind A) to anti-apoptotic BCL-2-family members (BCL-2, BCL-XL) and prevent them from interacting with BAX or BAK, which allows BAX/BAK to oligomerize and promote cytochrome c release from the mitochondria, and bind B) to BAX/BAK to promote their oligomerization. Cytosolic cytochrome c triggers apoptosome formation and activation of caspase-9, which in turn activates effector caspases. Caspase activation is inhibited by IAP proteins, which are counteracted by pro-apoptotic proteins that are released from the mitochondria (SMAC/DIABLO, OMI/HTRA2). Additional proteins (ENDO G, AIF) released from the mitochondria promote caspase-independent cell death pathways.

growth factors or survival signals (Zha *et al.* 1996). BH3-only proteinsinitiate the mitochondrial apoptosis pathway by promoting cytochrome c release from the mitochondria via other pro-apoptotic BCL2-family members, BAX or BAK (Eskes *et al.* 2000). Normally, BAX is located in the cytosol or is loosely attached to membranes; while BAK is bound to the mitochondria resident voltage-dependent anion channel protein 2 (VDAC2) (Danial and Korsmeyer 2004). In response to apoptotic stimuli, BAX and BAK can oligomerize and insert into the mitochondrial membrane (Danial and Korsmeyer 2004). Different BH-3 proteins are responsible for binding anti-apoptotic BCL-2-like proteins, such as BCL-X$_L$, thereby releasing BAX/BAK from inhibition, and for binding and activating BAX/BAK to promote their oligomerization (Huang and Strasser 2000; Kuwana *et al.* 2005). BH3-only protein-induced oligomerization of BAX or BAK causes the concerted and complete release of cytochrome c and other apoptosis-promoting proteins from the entire mitochondria of the cell (Desagher *et al.* 1999; Goldstein *et al.* 2000; Wei *et al.* 2001). Cytosolic cytochrome c binds Apaf-1 (apoptotic protease activating factor 1); this induces Apaf-1 oligomerization and formation of a caspase 9-activating protein complex known as the apoptosome.

The apoptosome is a wheel-like structure consisting of seven Apaf-1 molecules in complex with cytochrome c (Acehan *et al.* 2002). Pro-caspase-9 is recruited to this complex via the Apaf-1 CARD domain, which becomes exposed on the apoptosome during its assembly (Srinivasula *et al.* 1998; Zou *et al.* 1999) Apoptosome-bound active caspase-9 cleaves and thereby activates the effector pro-caspases-3 and -7 (Rodriguez and Lazebnik 1999). Thus, the activation of the caspase cascade through the intrinsic apoptosis pathway is initiated by mitochondria permeabilization, which induces the cytochrome c-dependent formation of a scaffolding complex for initiator caspase activation. The significance of this pathway for the response to intrinsic apoptosis stimuli is illustrated by the fact that cells lacking cytochrome c, Apaf-1 or caspase-9 are to a great extent resistant to stress-induced apoptosis (Green and Reed 1998).

Recent work suggests that caspase-2 can function as initiator and effector caspase in the apoptotic response to selected intrinsic stimuli, including DNA damage and growth factor deprivation (Troy and Shelanski 2003). In contrast to caspase-9, pro-caspase-2 was proposed to be activated upstream of the mitochondria, by CARD-dependent recruitment to a protein complex containing the adaptor proteins PIDD

(p53-induced protein with DD) and RAIDD (RIP1-associated apoptosis inducer with DD) (Tinel and Tschopp 2004) and seemed to be required for BAX-mediated cytochrome c release in response to DNA damage (Lassus *et al.* 2002). However, the absence of stress-induced caspase-2 activation in Bax/Bak double-deficient cells casts doubt on this notion (Ruiz-Vela *et al.* 2005). A direct role in promoting DNA damage-induced mitochondrial cytochrome c release has also been reported for cytoplasmic p53, which was shown to induce BAX oligomerization (Chipuk *et al.* 2004) and histone H1.2, which induced cytochrome c release via BAK oligomerization in cells treated with ionizing radiation (Konishi *et al.* 2003). Translocation of apoptosis-promoting proteins such as capasase-2, p53 or histone H1.2 to the mitochondria is a conceivable mechanism through which a death signal generated in the nucleus can be relayed to the apoptotic machinery in the cytoplasm.

Some apoptotic stimuli including DNA damage and oxidative stress apparently require the activation of BAX or BAK at the endoplasmatic reticulum, where they mediate Ca^{++} release to promote cell death (Scorrano *et al.* 2003). In summary, the intrinsic apoptosis pathway is initiated by BH3-only proteins and involves the BAX/BAK-dependent release of apoptosis promoting factors from organelles, most prominently the release of cytochrome c from the mitochondria.

1.4   Death receptor-induced apoptosis

Death receptor-induced apoptosis, also known as the extrinsic apoptosis pathway, is an important mechanism for the elimination of surplus cells during development. Receptor-mediated cell death is especially prominent in the immune system, where it mediates the negative selection of self-reactive T-cells and continues to have a vital role in the adult organism, for example, in the killing of virus-infected cells or cancer cells and the elimination of T cells at the end of an immune response (Osborne *et al.* 1996; Nagata 1997). The extrinsic apoptosis pathway is initiated by ligation of a death receptor on the plasma membrane (Ashkenazi and Dixit 1998) (Figure 2). Death receptors belong to the tumor necrosis factor (TNF) receptor superfamily of trans-membrane proteins, whose defining feature is the possession of characteristic cysteine-rich extracellular domains (Smith *et al.* 1994); the death receptors contain an additional intracellular protein interaction motif termed death domain (DD). The death receptor subfamily includes Fas (also known as APO-1 or CD95), TNFR1 (TNF

receptor 1) and TRAIL (TNF—related apoptosis inducing ligand) receptor 1 and 2 (Ashkenazi and Dixit 1998).

Ligand binding induces either trimerization of receptor monomers or conformational changes in pre-formed receptor trimers, which converts their intracellular domains into a signaling platform that recruits adaptor proteins to form a death-inducing signaling complex (DISC) (Kischkel *et al.* 1995). Death domain-containing adaptor proteins, such as FADD (Fas-associated death domain protein) and TRADD (TNFR-associated death domain protein), bind to the cytoplasmatic receptor tail via homophilic interaction with the receptor death domains. These proteins in turn recruit signaling molecules and the initiator pro-caspase-8 (and in humans, pro-caspase 10) via DED protein binding motifs to a caspase-activating complex (Medema *et al.* 1997). Dependent on receptor type, caspase activation occurs directly at the membrane-associated DISC (for example in the well-studied FAS signaling pathway), or, alternatively, by association with a second TRADD-based signaling complex that is assembled in the cytosol after dissociation from the receptor, as has been shown for the TNFR1 signaling pathway (Harper *et al.* 2003; Micheau and Tschopp 2003). Once activated, caspase-8 and caspase-10 in turn activate effector pro-caspases 3 and 7, thereby initiating apoptosis.

Depending on the context, however, direct effector caspase activation by caspase-8 varies in efficiency and is in certain cell types not sufficient for apoptosis execution (Scaffidi *et al.* 1998). In these cells, sometimes referred to as type II cells, cleavage of the BCL2 family protein BID by death receptor-activated caspase-8 is required for apoptosis. Upon cleavage, truncated BID translocates to the mitochondria to induce cytochrome c release via BAX/BAK oligomerization (Li *et al.* 1998; Luo *et al.* 1998; Desagher *et al.* 1999; Wei *et al.* 2001). In this way, the death receptor-initiated apoptosis response can be executed via the intrinsic apoptosis pathway. Thus, the extrinsic apoptosis pathway can initiate the caspase cascade both directly, via death receptor-induced formation of caspase-8 activating scaffolding complexes, and via caspase-8 mediated cleavage of BID, which activates the mitochondria pathway of caspase activation.
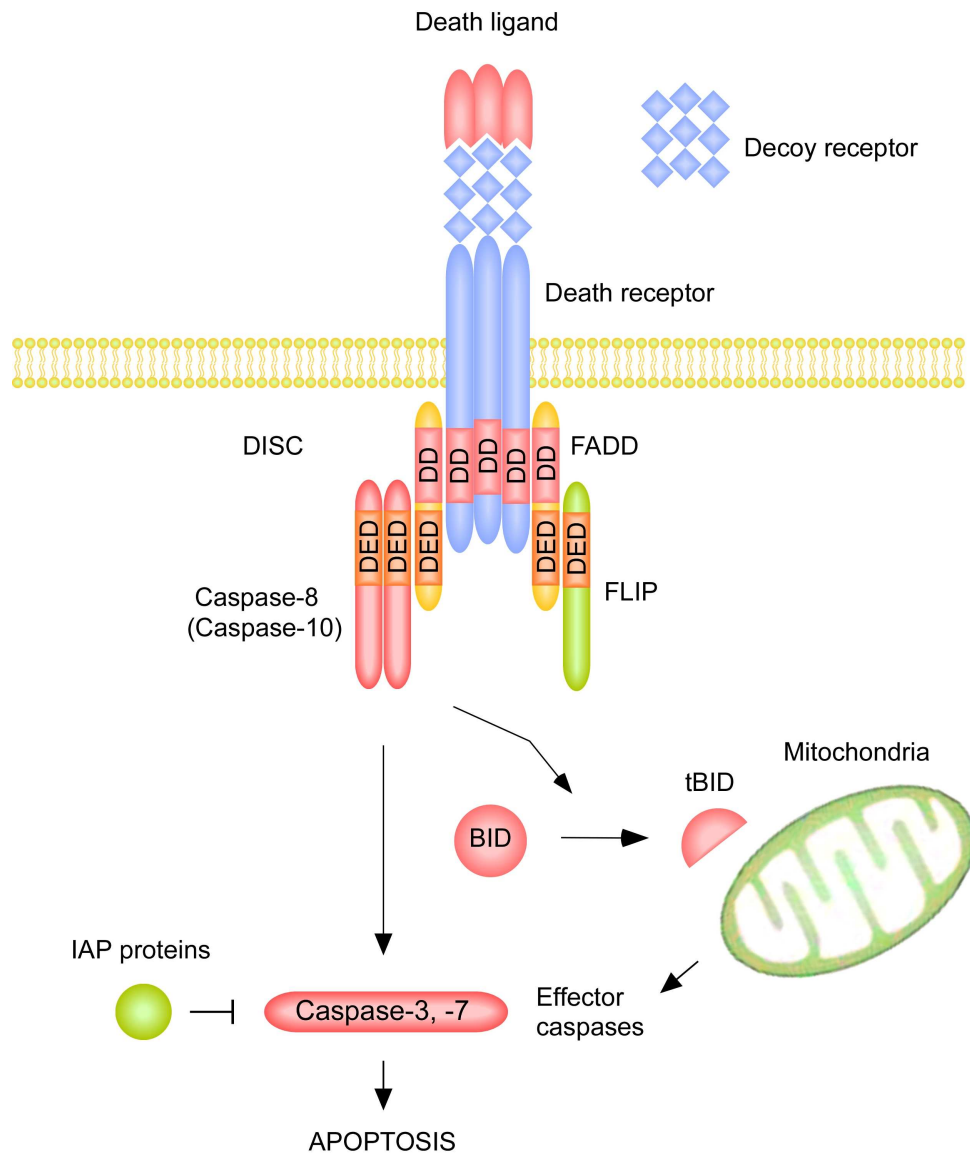
Figure 2. The extrinsic (death receptor) apoptosis pathway

Binding of death ligands to their cognate receptors leads to the formation of a death inducing signaling complex (DISC) at their intracellular domains, which contain docking sites for death domain (DD) containing adaptor proteins, such as FADD. Pro-caspase-8 is recruited by FADD via interaction of their death effector domains (DEDs). Caspase-8 is activated by proximity-induced dimerization and can activate effector caspases directly through cleavage and via the mitochondrial pathway through the cleavage of BID. Caspase-8 activation at the DISC is regulated by FLIP, which can form hetero-dimers with caspase-8 or occupy caspase-8 binding sites at the DISC; effector caspase activity is inhibited by IAPs. Ligand binding to decoy receptors can prevent the activation of death receptors on the cell surface.

1.5 Regulation of apoptosis pathways

The process of apoptosis is subject to intricate regulation in manifold ways. Generally, apoptosis is counteracted by the parallel activation of survival pathways. Thus, the decision between survival and apoptosis generally results from the integration of multiple signals received by the cell. One important way of regulating the initiation of apoptosis is transcriptional and post-translational control of pro- and anti-apoptotic proteins. A critical control point in the intrinsic cell death pathway in mammals is the activity of pro-apoptotic and anti-apoptotic members of the BCL-2 protein family (Danial and Korsmeyer 2004).

The pro-apoptotic members are grouped into multi-domain pro-apoptotic proteins, which possess three out of four conserved, function-defining regions termed BCL-2 homology (BH) domains, and BH3-only proteins, which possess only the amphipathic α helix of the BH3 domain (Adams and Cory 2001; Martinou and Green 2001). Multi-domain pro-apoptotic proteins, including BAX and BAK, mediate cytochrome c release from the mitochondria as homo-oligomers; BH3-proteins, such as BID, BAD and PUMA, initiate the intrinsic apoptosis pathway by promoting BAX/BAK activation (Huang and Strasser 2000). The activity of BH3 proteins is subject to transcriptional control and post-translational modification. PUMA and NOXA, for instance, are induced by p53 (Oda *et al.* 2000; Nakano and Vousden 2001). BAD is activated by phosphorylation in response to a lack of survival signals (Zha *et al.* 1996) and BID is converted to its active form via caspase cleavage upon death receptor triggering (Li *et al.* 1998; Luo *et al.* 1998).

The activity of BAX and BAK is negatively regulated by the anti-apoptotic members of the BCL-2 family, including BCL-2, BCL-XL and MCL-1, which show homology in all four BCL-2 homology domains. The founding member of the BCL-2 family, the BCL-2 proto-oncogene identified in B-cell lymphomas, was found to block apoptosis following multiple physiological and pathological stimuli (Vaux *et al.* 1988; McDonnell *et al.* 1989). Accordingly, Bcl-2 deficient mice display excessive apoptosis of lymphocytes in thymus and spleen (Veis *et al.* 1993). Anti-apoptotic BCL-2 proteins are thought to bind and sequester BH3-only proteins to prevent BAX/BAK activation, and to directly bind to BAX and BAK to keep them in their inactive conformation (Cheng *et al.* 2001; Martinou and Green 2001) (Figure 1). Because of the mutual inhibition of BCL-2 and BH-3 only proteins, the ratio of these molecules within a cell is a crucial determinant of the cells susceptibility to intrinsic

death signals. There is ample evidence that cells double-deficient for BAX and BAK are resistant to all stimuli that trigger death via the mitochondrial apoptosis pathway (Lindsten *et al.* 2000; Wei *et al.* 2001). This supports the notion that BAX and BAK are a requisite gateway to the intrinsic apoptosis pathway (Wei *et al.* 2001; Danial and Korsmeyer 2004).

A second group of regulatory proteins, inhibitors of apoptosis proteins (IAPs), controls caspase activity downstream of cytochrome c release. Like BCL-2 family proteins, they are subject to transcriptional regulation and post-translational modifications. For instance, IAPs are induced by survival signals through activation of the NF-κB group of transcription factors (Wang *et al.* 1998) and can be inactivated by proteolytic cleavage. IAPs were initially characterized as baculovirus-encoded proteins that suppressed apoptosis in infected host cells (Clem 2001). They are characterized by zinc-binding baculoviral IAP repeat (BIR) domains. Mammalian homologues include c-IAP-1, c-IAP-2 and XIAP, which inhibit the activity of caspase-3, -7 and -9 (Salvesen and Duckett 2002; Shi 2002; Riedl and Shi 2004). XIAP (X-linked IAP) and c-IAP-1 and -2 inhibit active caspases-3 and -7 by blocking the enzyme's substrate binding site (Roy *et al.* 1997; Deveraux *et al.* 1998; Riedl *et al.* 2001; Suzuki *et al.* 2001; Scott *et al.* 2005). XIAP potently inhibits caspase-9 by trapping it in a catalytically inactive conformation (Srinivasula *et al.* 2001; Shiozaki *et al.* 2003).

In mammals, the inhibition of caspases by IAPs is antagonized by binding of SMAC/DIABLO and OMI/HTRA2, two mitochondrial proteins released during apoptosis (Du *et al.* 2000; Suzuki *et al.* 2001; Verhagen *et al.* 2002). Both molecules possess conserved tetrapeptide IAP binding motifs (Wu *et al.* 2000; Hegde *et al.* 2002). Omi/HTRA2 is a serine protease that neutralizes IAPs, presumably by cleavage (Suzuki *et al.* 2004). SMAC binds IAPs, thereby preventing them from targeting caspases (Wu *et al.* 2000; Yang and Du 2004) (Figure 1). Thus, the balance between IAPs and IAP antagonizing proteins is an important control factor for effector caspase activation. In addition, caspases themselves and other proteins that promote apoptosis downstream of cytochrome c release, are subject to transcriptional regulation (Earnshaw *et al.* 1999). Caspase-3 and Apaf-1, for instance, are under transcriptional control of E2F-1 (Muller *et al.* 2001).

The activation of initiator caspases by death receptors is regulated by the expression of FLIP (FLICE-like inhibitory protein; FLICE, FADD-like ICE like protease, one of the original names for caspase-8) (Krueger *et al.* 2001). FLIP is a caspase-8 homolog that lacks the catalytic cysteine, but can form hetero-dimers with caspase-8 that are catalytically active (Micheau *et al.* 2002). This mechanism appears to enhance caspase-8 activation at the DISC at low concentrations of FLIP, while high levels of FLIP inhibit activation of caspase-8 and -10, presumably by occupying caspase binding sites at the activation complex (Chang *et al.* 2002; Micheau and Tschopp 2003) (Figure 2). In addition, the very first step of the extrinsic apoptosis pathway – the activation of a death receptor - can be inhibited by the expression of decoy receptors - extracellular, truncated versions of death receptors that compete with receptors on the cell surface for ligand binding (Igney and Krammer 2002).

Moreover, survival signals and death signals can be transduced by the same receptor. The most prominent example is provided by TNFR1, which activates an NF-κB-dependent survival pathway but can also induce apoptosis (Karin 1998; Van Antwerp *et al.* 1998) (Figure 3). Cells deficient for components of the NF-κB pathway are sensitized to TNF-induced apoptosis (Wajant *et al.* 2003), indicating that NF-κB promotes survival in response to TNF. The decision between life and death appears to be governed by differential complex formation between various DD and DED containing adaptor proteins (Danial and Korsmeyer 2004). Upon TNFR1 activation, the receptor DISC containing TRADD, TRAF2, c-IAP1 and the kinase RIP1, recruits and activates the IKK (Inhibitor of NF-κB kinase) complex (Micheau and Tschopp 2003; Wajant *et al.* 2003). The resulting activation of NF-κB transcription factors induces the expression of anti-apoptotic proteins, such as c-IAP and FLIP (Van Antwerp *et al.* 1998), which interfere with caspase-8 activation in a TRADD-based cytosolic complex (Micheau and Tschopp 2003). The TNFR1 DISC also activates another major transcription factor, c-Jun/AP1, via activation of Jun kinase (JNK). However, the role of c-Jun/AP1 activity for cell survival remains to be clarified. Both pro-and anti-apoptotic effects have been reported (Liu 2003; Varfolomeev and Ashkenazi 2004).

In addition to the mechanisms described so far, recent evidence suggests that the cleavage of effector caspase substrates constitutes an important control point in apoptosis regulation (Chau and Wang 2003). The cleavage of proteins, which
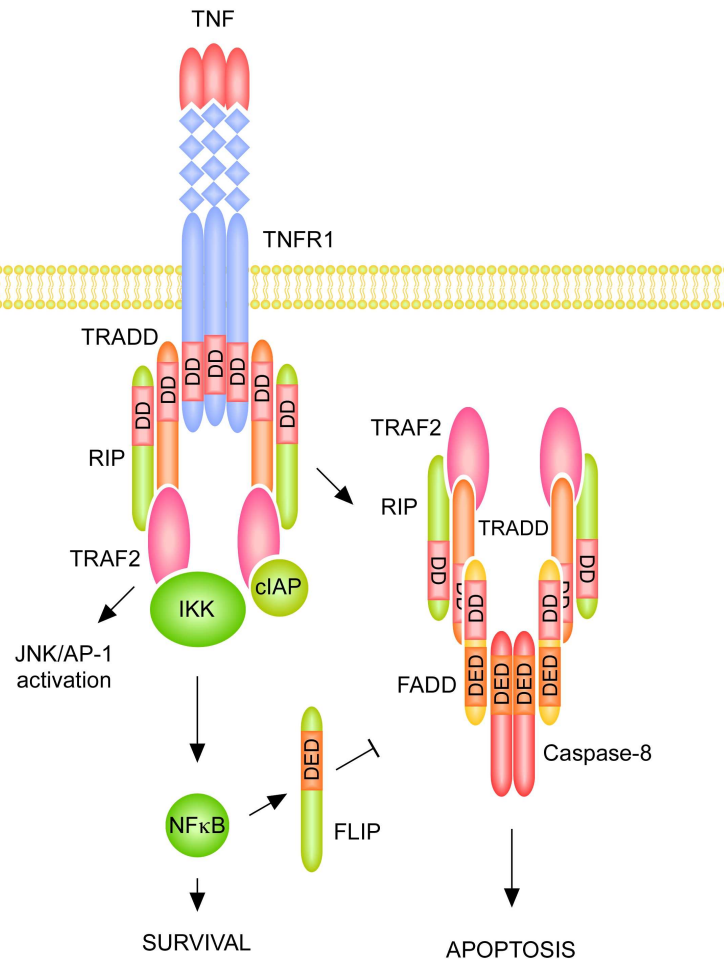
Figure 3. TNFR1 signaling pathways
Engagement of TNF with TNFR1 results in the formation of a receptor-proximal complex containing the adaptor proteins TRADD, RIP and TRAF2, which in turn recruit c-IAP proteins and IKK. This signaling complex initiates NFκB and JNK activation. A second complex based on TRADD, RIP and TRAF2 is formed in the cytosol and recruits FADD and pro-caspase-8. Caspase-8 activation in this complex initiates the apoptotic caspase cascade. Caspase-8 activation is inhibited by NF-κB-induced expression of FLIP and other anti-apoptotic proteins.

normally inhibit caspase activation, seems to create a positive feedback loop that drives further caspase activation (Chau and Wang 2003). An IKK mutant resistant to cleavage by effector caspases, for instance, was able to protect cells from TNF-induced apoptosis (Tang *et al.* 2001). Likewise, a caspase-cleavage resistant variant of the Retinoblastoma protein can suppress caspase activation and apoptosis in several cellular contexts (Harbour 2000; Chau and Wang 2003). These data indicated that cleavage of certain key substrates may be a required step in the execution of apoptosis.

In summary, apoptosis pathways are regulated by various mechanisms at several control points, whose relative importance depends on the apoptotic stimulus and the cellular context. Negative regulation of apoptosis is usually the effect of the simultaneous activity of survival pathways Key regulators of the mitochondria apoptosis pathway are pro- and anti-apoptotic proteins of the BCL-2 family. IAP proteins and IAP antagonizing proteins control caspase activation downstream of cytochrome c release..

1.6 The retinoblastoma protein as a regulator of proliferation and apoptosis

RB, the product of the retinoblastoma-susceptibility gene (*RB*), was the first tumor suppressor protein to be identified (Sherr 1996). In individuals heterozygous for a germline mutation in the *RB* gene, acquisition of a second mutation in the wild-type *RB* allele in embryonic retinoblasts results in the development of retinoblastoma in early childhood, a mechanism that was first suggested by a pioneering statistical study of human retinoblastomas (Knudson 1971). The tumor suppressor function of *RB* is consistent with the critical role of the Rb protein in cell cycle regulation (Figure 3). RB inhibits proliferation by repressing transcription of genes required for DNA synthesis through its interaction with the E2F family of transcription factors (Nevins *et al.* 1997; Harbour 2000). Active RB binds E2Fs and converts them into transcriptional repressors by recruiting chromatin-modifying enzymes (Harbour 2000; Nielsen *et al.* 2001). Mitogenic signaling drives cell cycle progression through the activation of cyclin-dependent kinases (CDKs), which phosphorylate RB (Morgan *et al.* 1998). The hyperphosphorylation of RB by cyclin D-CDK4/6 complexes in mid G1 inactivates its transcriptional repressor activity by disrupting the interaction with E2F and chromatin modifying enzymes (Bremner *et al.* 1995; Knudsen and Wang 1996; Mittnacht 1998).

The elimination of *Rb* by gene targeting in mice was found to result in embryonic lethality (around embryonic day 13.5) and revealed additional functions of Rb during development (Clarke *et al.* 1992; Jacks *et al.* 1992; Lee *et al.* 1992). *Rb-null* mutant embryos suffer from ectopic proliferation in the developing central nervous system (CNS), consistent with the established role of Rb-E2F in cell cycle regulation. Intriguingly, *Rb* deficient embryos also display massive apoptosis in
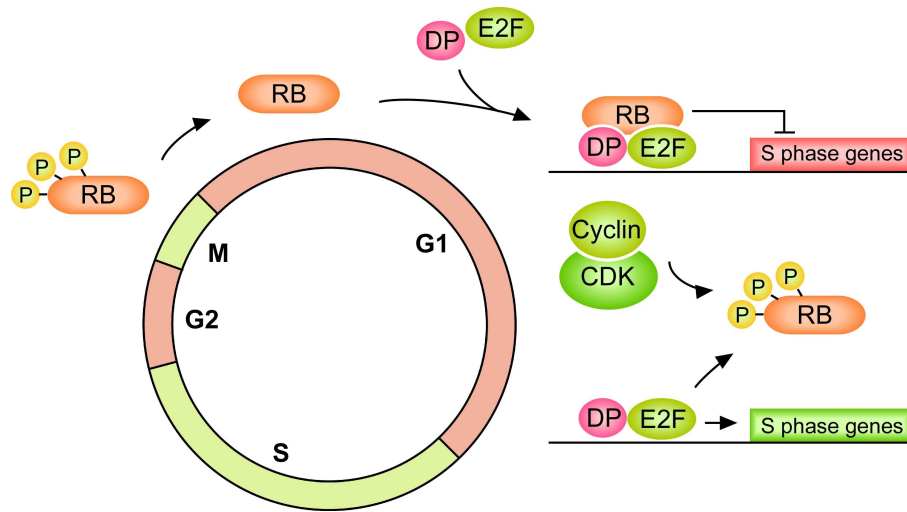
Figure 4. Inhibition of cell cycle progression by RB

Hypophosphorylated RB binds the E2F transcription factor, a hetero-dimer of DP and E2F, and recruits chromatin-modifying enzymes to form a complex, which suppresses "S phase genes", whose transcription is required for DNA synthesis. Upon phosphorylation by CDKs in mid G1, RB dissociates from E2F, which then activates the transcription of S-phase genes. RB is re-activated through dephosphorylation at the end of mitosis.

the CNS and exhibit defects in the terminal differentiation of myocytes and erythrocytes. These observations strongly indicated additional roles for RB in the process of terminal differentiation and apoptosis regulation. The terminal differentiation of a progenitor cell into a quiescent post-mitotic cell is usually accompanied with the loss of its proliferative potential, a characteristic effectively preventing tumor development. Thus, the promotion of terminal differentiation, which has been confirmed in several contexts (Lipinski and Jacks 1999; Ferguson and Slack 2001), is another mechanism potentially contributing to the tumor suppressor activity of RB. At the same time, the phenotype of Rb-deficient mice, which indicated that RB is normally required to inhibit apoptosis, seemed to contradict RB's well-established growth suppressing function. Despite this apparent conundrum, several lines of evidence now support the ability of RB to suppress apoptosis (Harbour 2000; Chau and Wang 2003). Together, these studies revealed an intriguing dual role of RB: as an inhibitor of both cell growth and death (Chau and Wang 2003).

In addition to E2F transcription factors and chromatin modifying enzymes, RB interacts with an astounding variety of cellular proteins (Morris and Dyson 2001). The affinity of RB to its binding partners was shown to be intricately regulated: three distinct peptide-binding pockets have been identified in RB to bind (a) the C-terminal region of E2F (Xiao *et al.* 2003), (b) the LxCxE peptide motif, *e.g.* in viral E7 protein or cellular histone methyl-transferase (Lee *et al.* 1998; Robertson *et al.* 2000), and (c) the PENF homology motif, e.g., in cellular proteins such as c-Abl tyrosine kinase and Serpin 2B (Darnell *et al.* 2003). Each of these peptide-binding pockets is independently regulated by specific CDK phosphorylation sites (Knudsen and Wang 1996). Mutation of nine out of sixteen CDK sites is required to create an RB variant with constitutive growth suppressing function (Knudsen and Wang 1997). This variant, termed PSM-RB (phosphorylation site mutated RB), lacks seven phosphorylation sites in the C-region and two phosphorylation sites in the insert region of RB (Knudsen and Wang 1997) (Figure 5). PSM-RB is a potent inhibitors of proliferation in various cellular contexts (Knudsen and Wang 1997; Knudsen *et al.* 1998; Sever-Chroneos *et al.* 2001).

In addition to changes in its phosphorylation status, regulated cleavage and degradation control the activity of the RB protein. RB is an effector caspase substrate and caspase cleavage induces its degradation during apoptosis (Tan and Wang 1998). Mutation of the C-terminal caspase cleavage site (Figure 5) generates a protein termed RB-MI (mutated in ICE-site) that is resistant to caspase cleavage and can suppress apoptosis in response to various stimuli (Tan and Wang 1998). The MI mutation has moreover been introduced into the mouse *Rb-1* gene by gene targeting to create $Rb^{MI/MI}$ 'knockin' mice (Chau *et al.* 2002). In these animals, Rb-MI conferred tissue-specific protection from endotoxin-induced apoptosis. Moreover, fibroblasts derived from these animals were specifically protected from TNFR1- induced apoptosis, but remained sensitive to apoptosis in response to DNA damage (Chau *et al.* 2002). These observations indicate that elimination of RB is a required step in selective apoptosis pathways. A fundamental question in this context is, whether apoptosis suppression by RB is connected to its growth suppressing activity and may thus be antagonized by phosphorylation as well as degradation. In particular, the role of E2F-dependent cell-cycle regulation for apoptosis suppression by RB is not fully understood. The ectopic
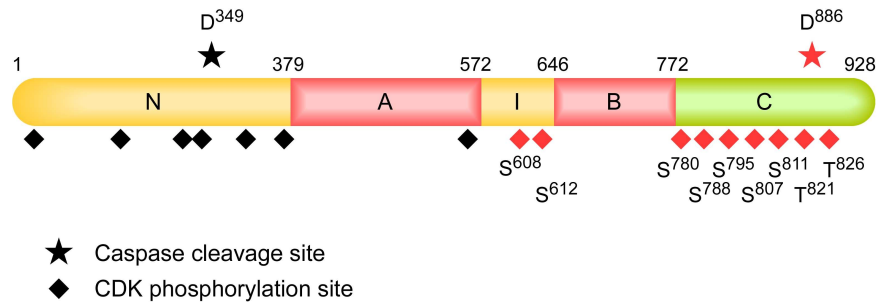
Figure 5. Domain structure of the Retinoblastoma protein

The A and B pocket domains are shaded in red; CDK phosphorylation sites are indicated by diamonds. Two conserved caspase consensus sites are indicated by stars, one -DEAD^{886}G- at the C terminus (Tan *et al.* 1997), the other - DSID^{349}- in the N-terminal domain (Fattman *et al.* 2001). Residues that are mutated in RB-MI or PSM-RB are shown in red.

S-phase entry and enhanced apoptosis of cells in the developing CNS of *Rb$^{-/-}$* embryos are absent *in Rb$^{-/-}$E2F1$^{-/-}$* double null mutant animals (Tsai *et al.* 1998). Moreover, E2F1 was shown to control the expression of both S-phase- specific and apoptosis-promoting genes, including Apaf-1 and caspase-3 (Muller *et al.* 2001). These data suggest that RB controls developmental apoptosis by suppressing the transcription of E2F regulated pro-apoptotic genes. On the other hand, RB is able to block the TNF-induced apoptosis pathway, which is independent of transcription (Chau and Wang 2003). Thus, the central question remains, whether apoptosis suppression by RB obligatory depends on the regulation of gene expression, or if RB can act through other mechanisms to inhibit apoptosis. Moreover, the relative significance of RB-dependent apoptosis suppression for each of the various apoptosis pathways in developmentally mature cells remains to be elucidated.

1.7   Objectives

The first aim of this work was to examine the role of RB in the negative regulation of different cell death pathways. To this end, it was intended to examine the potential of constitutively active RB variants to inhibit apoptosis induced by DNA damage, general kinase inhibition and tumor necrosis factor-α. Cell lines with stable expression of RB variants that were resistant to CDK-mediated phosphorylation, caspase-induced degradation, or both, were to be generated. The growth inhibitory activity of CDK-phosphorylation resistant variants required the use of a cell line that allowed inducible gene expression (TET off system). This system was expected to allow a comprehensive analysis of the effects of RB-induced growth arrest and caspase-resistant RB activity on the cellular response to different apoptotic stimuli.

The second aim was to elucidate the mechanism for RB-dependent regulation of apoptosis in response to extracellular death stimuli. In particular, it was intended to identify the control point for the inhibition of TNFR1-induced apoptosis in fibroblasts derived from mice expressing caspase-resistant Rb (Rb-MI). To identify putative Rb-dependent changes in the expression of apoptosis-related genes, it was decided to conduct a microarray-based gene expression analysis of TNF-treated $Rb^{MI/MI}$ cells. The alternative possibility of a post-transcriptional anti-apoptotic function of Rb-MI was to be addressed by a step-wise analysis of the mitochondrial apoptosis pathway in $Rb^{MI/MI}$ cells. This approach implied a detailed *in vitro* analysis of the cytochrome c release capacity of cytosolic extracts from TNF-treated cells. In summary, this study aimed to gain insights into the regulation of apoptosis by RB to shed light on the dual role of RB as a regulator of proliferation and cell death.

2 Results

2.1 Effect of constitutively active RB variants on cell death response to different stimuli

To compare the potential of constitutively active RB variants to inhibit apoptosis in response to different types of stimuli, cell lines with stable expression of RB variants were generated. The growth inhibitory activity of CDK-phosphorylation resistant variants required the use of a parental cell line that allowed inducible gene expression. Therefore, the Rat fibroblast cell line Rat-16 (Sever-Chroneos *et al.* 2001) was used, which has been engineered to express the TET-VP fusion protein and provides tight control of tetracycline-regulated gene expression (TET off system). Rat fibroblasts are suitable for the analysis of inducible RB expression, because they express Rb at very low endogenous levels that are not detectable in most assays (*e.g.* Figure 2c).

Four Rat-16-based cell lines were generated that expressed wild-type RB (WT-RB), caspase site-mutated RB (RB-MI), phosphorylation site-mutated RB (PSM-RB), or PSM-RB-MI, respectively, each under the control of the tetracycline-regulated promoter. Upon switching to tetracycline-free media, expression of wild-type RB, or one of its variants, was induced in each of the four cell lines and each of the proteins localized correctly to the nucleus (Figure 1a-h). Proliferation in these cell lines was monitored through pulse labeling of replicating cells with bromodeoxyuridine (BrdU). Cells that incorporated BrdU during DNA synthesis were stained with a FITC-conjugated anti-BrdU antibody. Co-staining of all cells with propidium iodide allowed to determine the percentage of cells in S-phase. As previously reported (Knudsen and Wang 1997; Knudsen *et al.* 1998), expression of PSM-RB inhibited DNA synthesis causing the majority of the cells to arrest in G1 by 24 hr after the removal of tetracycline (Figure 2a, b). Likewise, expression of PSM-RB-MI inhibited DNA replication (Figure 2b). However, expression of WT-RB or RB-MI did not interfere with the proliferation of Rat-16 cells (Figure 2b), because these proteins could be inactivated by phosphorylation (Figure 2c).
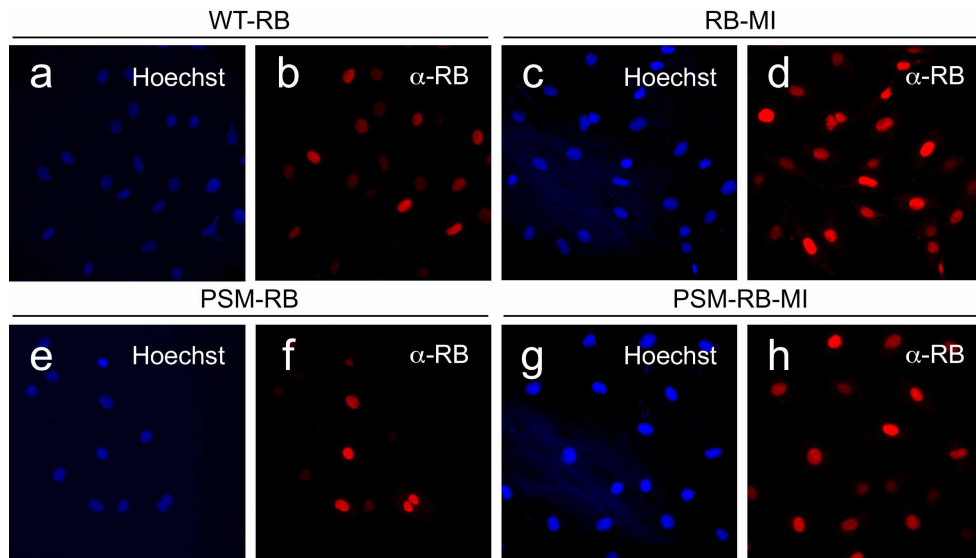
Figure 1. Induced expression and nuclear localization of RB variants in Rat-16 cells.

The indicated cell lines were seeded on coverslips and cultured in the absence of tetracycline for 24 h. Cells were fixed and RB was detected by indirect immunofluorescence. Representative pictures are shown at 60 x magnification.

2.1.1 Doxorubicin-induced activation of caspases is attenuated in Rat-16 cells arrested by PSM-RB

Having thus characterized the established cell lines, the effect of each of the four RB proteins on the cellular response to DNA damage was examined. DNA damage was induced by doxorubicin, a chemotherapeutic anti-tumor agent of the anthracyclin type. Doxorubicin acts via several mechanisms, including topoisomerase II inhibition and free radical formation, that cause DNA double strand breaks and result in inhibition of DNA replication (Panaretakis *et al.* 2002). Rat-16 fibroblasts express the p53 protein, which is stabilized in response to doxorubicin treatment (Figure 3a). In addition, doxorubicin induced cleavage of Parp to an 89 kD fragment, which is typically observed in apoptotic cells (Figure 3b). However, doxorubicin did not induce acute cell death in Rat-16 cells: after 48 hours treatment with doxorubicin the analysis of cellular membrane integrity showed no increase in the number of dead or necrotic cells (Figure 3c) and almost no cells with the sub-G1 DNA content characteristic of apoptotic cells could be detected (not shown).

a

PSM-RB

b

% BrdU positiv cells

	6 h		24 h	
	+ TET	- TET	+ TET	- TET
WT	31	28	27	24
MI	33	39	33	32
PSM	33	33	42	2
PSM-MI	20	16	20	2

c
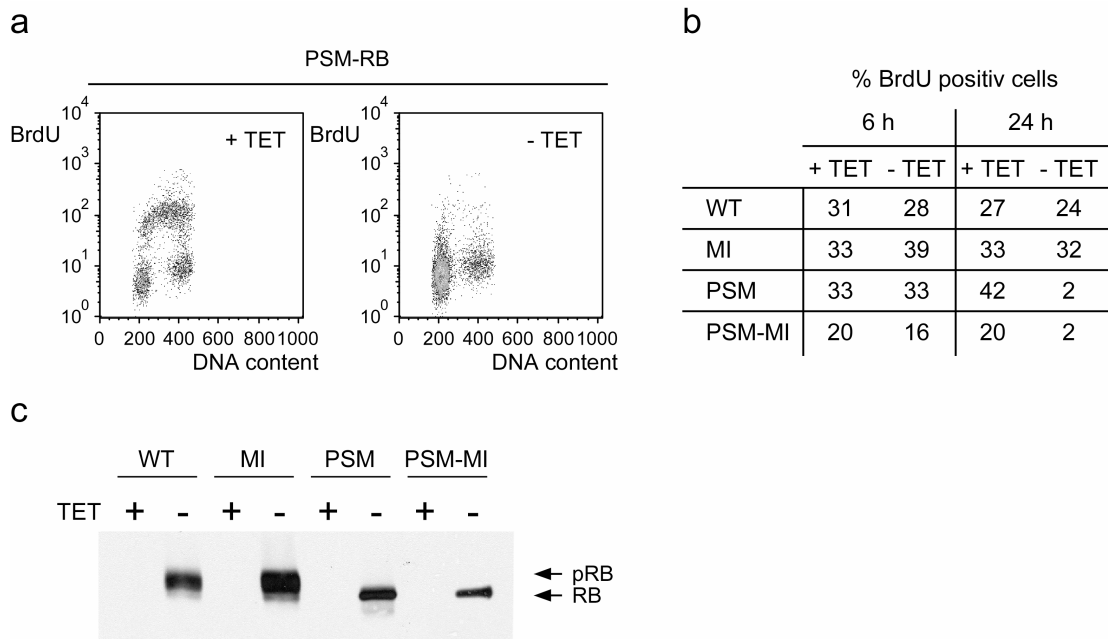
Figure 2. Effect of RB variants on Rat-16 cell cycle progression

(a) Inhibition of BrdU incorporation by PSM-RB. PSM-RB cells were cultured with (uninduced, left panel) or without (induced, right panel) tetracycline (TET) for 24 h and pulse labeled with BrdU. Cells were fixed and stained with FITC-conjugated BrdU antibody and propidium iodide and analyzed by flow cytometry. Shown are representative density plots of FITC (BrdU) and propidium iodide (DNA content) signal intensity. (b) Summary of the effect of RB variants on BrdU incorporation. The indicated cell lines (WT, WT-RB; etc.) were cultured with (uninduced) or without (induced) TET for 6 h or 24 h and analyzed as in (a). 10 000 gated events were counted and the percentage of S-Phase (BrdU-positive) cells was calculated. (c) Phosphorylation status of RB variants 24 h after induction. The indicated cell lines were cultured with (uninduced) or without (induced) TET for 24 h, and RB was detected in whole cell lysates by immunoblotting. pRB, hyperphosphorylated RB; RB, unphosphorylated RB

The resistance of Rat-16 cells to doxorubicin-induced acute cell death was not affected by induction of RB or one of its variants in any of the four cell lines (Figure 3c). However, doxorubicin did cause a drastic reduction in clonogenic survival of Rat-16 cells (Figure 4a). PSM-RB and PSM-RB-MI cells were cultured with or without tetracycline for 24 hr, and then treated with doxorubicin for 24 hours. After treatment, equal numbers of cells were replated in tetracycline-containing media and allowed to grow for one week. At that point, surviving cells were stained with crystal violet to determine the percentage of surviving doxorubicin-treated cells. Virtually no cell proliferation could be detected in the doxorubicin-treated samples (Figure 4a).

a

b

c
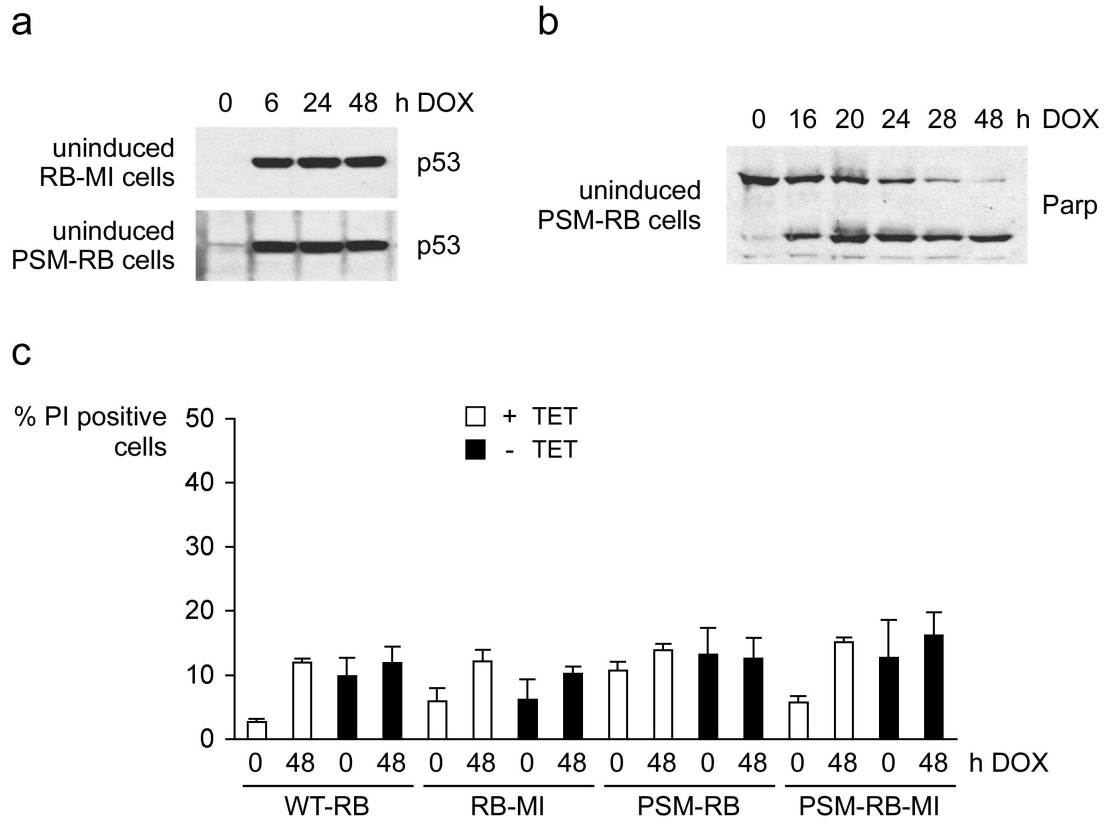
Figure 3. Doxorubicin (DOX) induces p53 accumulation and Parp cleavage but does not induce acute cell death in Rat-16 cells

(a) Stabilization of p53 protein in DOX-treated Rat-16 cells. Uninduced RB-MI and PSM-RB cells were treated with DOX for the indicated times. Equal amounts of protein from whole cell lysates were resolved by SDS-PAGE and p53 was detected by immunoblotting. (b) Cleavage of Parp in DOX-treated Rat-16 cells. Uninduced PSM-RB cells were treated as in (a) and Parp was detected by immunoblotting. (c) Quantification of cell death in Rat-16 cells. The indicated cell lines were cultured with or without TET for 24 h and subsequently treated with DOX for 48 h in the presence (white bars) or absence (black bars) of TET. Uptake of propidium iodide (PI) was analyzed by flow cytometry.

Induction of PSM-RB or PSM-RB-MI for 24 hours before and during drug treatment, did not affect clonogenic survival (Figure 3d). These results suggest that doxorubicin activates p53 to induce long-term growth arrest rather than acute apoptosis in Rat-16 cells. Growth arrest caused by PSM-RB or PSM-RB-MI prior to drug treatment had no impact on the permanent growth arrest and the resulting lack of clonogenic survival caused by the exposure to doxorubicin. Although doxorubicin did not activate apoptosis, it induced cleavage of Parp (Figure 3b) and cleavage of WT-RB and

a

clonogenic survival fraction
(% of untreated)

	uninduced		induced	
	NT	DOX	NT	DOX
PSM	100	0.08	100	0.19
PSM-MI	100	0.07	100	0.12

b
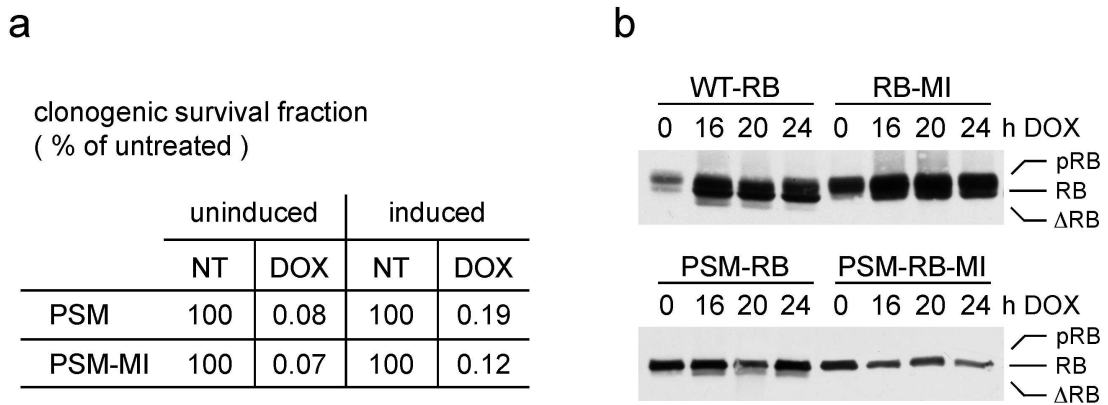
Figure 4. Doxorubicin (DOX) induces long-term growth arrest in Rat-16 cells.
(a) Lack of clonogenic survival in DOX-treated Rat-16 cell populations. The indicated cell lines were cultured with (uninduced) or without TET (induced) for 24 h and subsequently treated with DOX for 24 h in the presence (white bars) or absence (black bars) of TET. Cells were washed and replated in TET containing media and clonogenic survival was assayed after 7 days in culture. NT, no treatment (b) DOX induces dephosphorylation and cleavage of RB. The indicated cell lines were cultured without TET for 24 h and subsequently treated with DOX for the indicated times and RB was detected in whole cell lysates by immunoblotting. ΔRB, truncated RB resulting from cleavage at the C-terminal DEAD sequence; pRB, phosphorylated RB; RB, unphosphorylated RB

PSM-RB to a size corresponding to ΔRB (Figure 4b). This cleavage product was not observed with RB-MI or PSM-RB-MI (Figure 4b), confirming cleavage to be at the site that is eliminated by the MI mutation. It has previously been shown that the C-terminal cleaved ΔRB is unstable (Tan *et al.* 1997); this might explain the very faint ΔRB band on these blots. However, despite the cleavage reaction, RB protein levels were not significantly reduced in doxorubicin-treated cells. This observation suggests that the low levels of detectable ΔRB simply reflect the minor extent of RB cleavage under these conditions. While in untreated WT-RB and RB-MI cells, the majority of RB was in its hyperphosphorylated form, dephosphorylated RB accumulated in doxorubicin-treated cells (Figure 4b). The resulting change in the ratio between dephosphorylated and hyperphosphorylated forms of RB is consistent with the observation that doxorubicin induced growth arrest in Rat-16 cells.

The characteristic cleavage fragments of RB and Parp indicated that doxorubicin activated caspases despite the absence of apoptosis. To confirm this notion, caspase activity was measured in cell extracts using the synthetic tetrapeptide

a

b
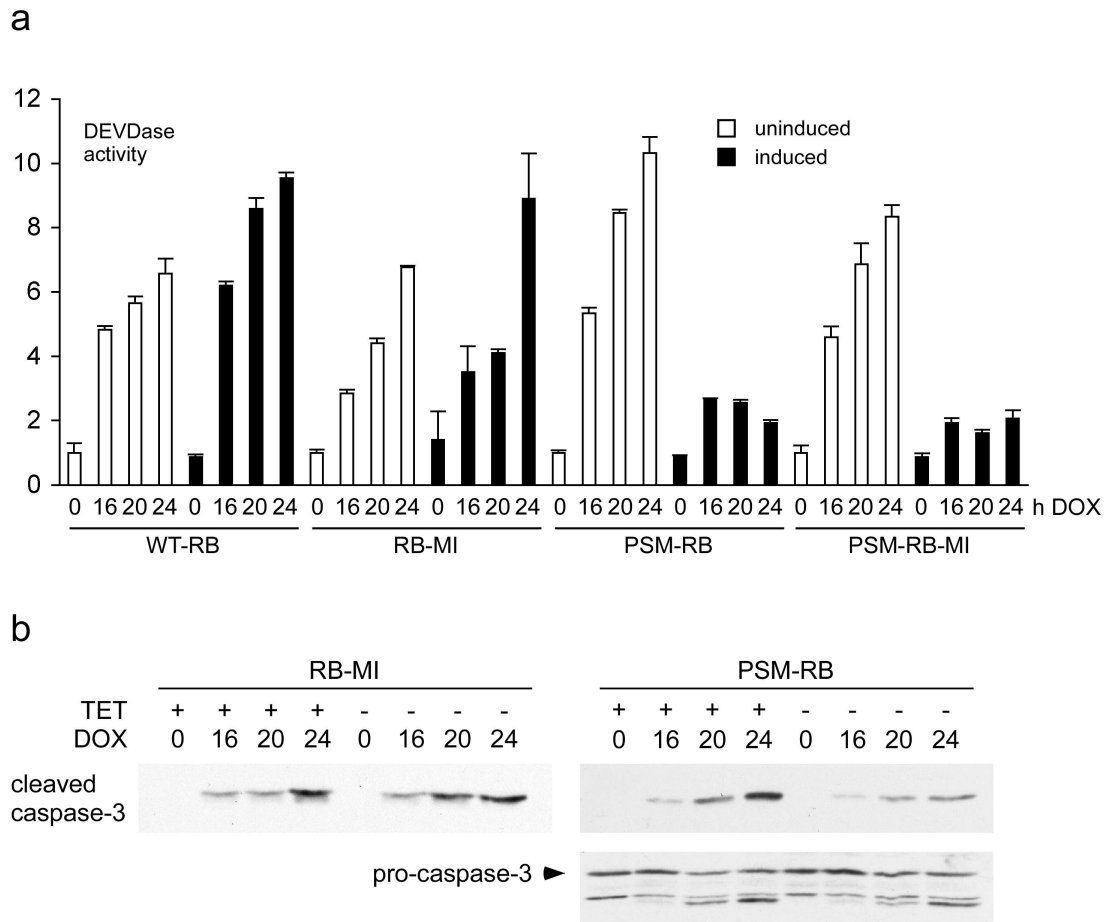
Figure 5. Inducible expression of PSM-RB or PSM-RB-MI inhibits caspase activation in response to doxorubicin (DOX)

(a) DEVDase activity in DOX-treated Rat-16 cells. The indicated cell lines were cultured with (uninduced) or without TET (induced) for 24 h and subsequently treated with DOX for the indicated times in the presence (white bars) or absence (black bars) of TET. Equal amounts of protein from whole cell lysates were incubated with a fluorogenic caspase-3 substrate (Ac-DEVD-AMC) for 30 min. For each time point, the fold increase in fluorescence intensity relative to uninduced, untreated control cells is given as DEVDase activity. (b) Levels of cleaved caspase-3 in DOX-treated Rat-16 cells. The indicated cell lines were treated as in (a). Equal amounts of protein from whole cell lysates were resolved by SDS-PAGE and cleaved caspase-3 (upper panel) and pro-caspase-3 (lower panel) were detected by immunoblotting.

substrate Ac-DEVD-AMC (Figure 5). Caspase cleavage of Ac-DEVD-AMC releases the 7-amino-4-methylcoumarin (AMC) reporter group, which can then be detected in a fluorometric assay. When cultured with tetracycline (RB expression off), DEVDase activity increased 7-10 fold after 24 hours treatment with doxorubicin in each of the four cell lines (Figure 5a, white bars). In addition, cleaved caspase-3 could be detected by immunoblotting in doxorubicin-treated samples (Figure 5b, TET + lanes, upper

panel). Interestingly, expression of PSM-RB or PSM-RB-MI for 24 hours prior to doxorubicin treatment caused a reduction in DEVDase activation while expression of WT-RB or RB-MI had no significant effect (Figure 5a, black bars). Consistently, cleaved caspase-3 accumulated to a similar level in uninduced and induced RB-MI cells, but reached considerably lower levels in cells induced for PSM-RB expression (Figure 5b, TET - lanes, upper panel). Evidently, induced expression of PSM-RB did not reduce protein levels of pro-caspase-3 (Figure 5b, lower panel). Thus, PSM-RB apparently did not interfere with pro-caspase-3 expression, but inhibited the processing of pro-caspase-3 to its active form.

To determine if the establishment of PSM-RB-induced cell cycle arrest was required for the reduction of caspase activation, PSM-RB was induced for only 6 hours prior to doxorubicin treatment. After 6 hours, PSM-RB protein accumulated to a level that was already significantly higher than the endogenous RB (Figure 6b, endogenous RB not detectable on this blot), but the percentage of cells in S-phase was still the same as in uninduced cells (Figure 2b). Doxorubicin added 6 hours after induction of PSM-RB expression caused a level of caspase activity comparable to uninduced cells (Figure 6a). This result suggested that either cell cycle arrest or an excessive level of PSM-RB was required for the attenuation of caspase activation.

In order to test, if starvation-induced cell cycle arrest can inhibit caspase activation in cells without PSM-RB expression, uninduced WT-RB cells were synchronized in quiescence by serum withdrawal prior to doxorubicin treatment. Parallel populations of quiescent cells were then treated with doxorubicin either after the re-addition of serum or under conditions of continuous serum starvation (Figure 6c). Cells that had re-entered the cell cycle (white bars) activated DEVDase to the same level as control cells that had not been serum-starved (grey bars). In contrast, cells that had remained quiescent (black bars) showed greatly reduced caspase activation in response to doxorubicin. Taken together, these results suggest that PSM-RB and PSM-RB-MI interfered with doxorubicin-induced caspase activation, most likely by blocking cell cycle progression. It should be noted that cell cycle arrest did not prevent doxorubicin from causing damage, because induction of growth arrest by PSM-RB or PSM-RB-MI did not rescue clonogenic survival of doxorubicin-treated cells (Figure 4a). Thus, PSM-RB and PSM-RB-MI affected caspase activation but not induction of permanent growth arrest by doxorubicin in Rat-16 cells.

a

b

c
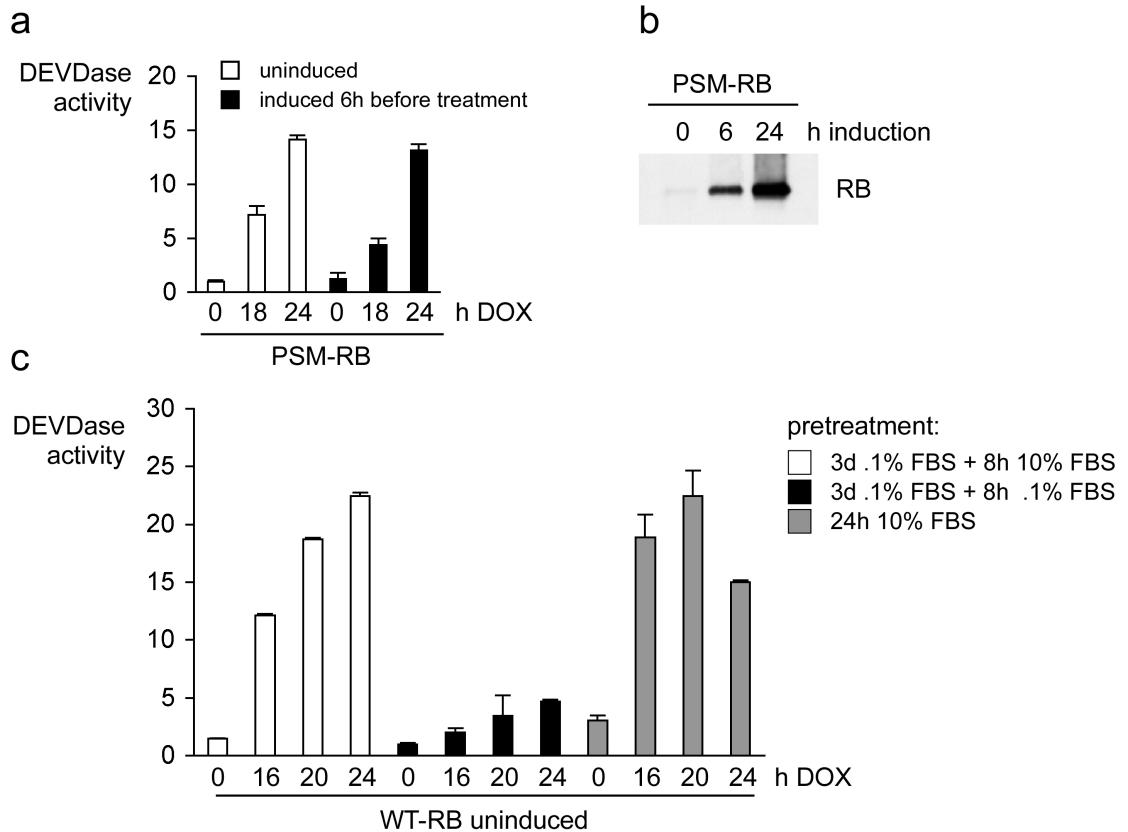
Figure 6. Cell cycle arrest inhibits caspase activation in response to doxorubicin (DOX)

(a) DEVDase activity after DOX treatment of unarrested PSM-RB cells. PSM-RB cells were cultured with (uninduced) or without TET (induced) for only 6 h and subsequently treated with DOX for the indicated times in the presence (white bars) or absence (black bars) of TET. At each time point DEVDase activity in whole cell lysates was determined as described in Figure 5. (b) PSM-RB protein levels 6 h and 24 h after induction. PSM-RB cells were treated as in (a). Equal amounts of protein from whole cell lysates were resolved by SDS-PAGE and RB was detected by immunoblotting. (c) DEVDase activity in DOX-treated WT-RB cells. WT-RB cells were cultured in the presence of TET and either serum starved for 3 days followed by 8 h culture in 10 % serum (white bars), continuously serum starved for 3 days + 8h (black bars) or cultured in 10 % serum for 24 h (grey bars). Subsequently cells were treated with DOX in 10 % (white and grey bars) or 0.1 % serum (black bars) for the indicated times. Whole cell lysates were analyzed as in (a).

2.1.2 Staurosporine-induced apoptosis of Rat-16 cells is not prevented by PSM-RB

Staurosporine (STS), a broad-spectrum inhibitor of protein kinases, is a potent inducer of apoptosis in a wide range of cell types, including Rat fibroblasts (Yoshida *et al.* 1997). Similar to DNA damage inducing agents, STS can alternatively induce growth arrest. Previous studies have suggested STS-induced G1 arrest to be mediated by RB (Schnier *et al.* 1996; Orr *et al.* 1998; Chen *et al.* 2000). Therefore, it was examined whether staurosporine-induced apoptosis of Rat-16 cells can be prevented by PSM-RB-mediated cell cycle arrest. Treatment with 1 µM staurosporine induced a high level of DEVDase activity (Figure 7a) and phosphatidyl-serine exposure (annexin-V staining) on the plasma membrane (not shown) within a few hours. The level of DEVDase activity induced by staurosporine was ten times higher than that induced by doxorubicin (compare Y-axis values in Figure 5a and 7a). Induction of cell cycle arrest by either PSM-RB or PSM-RB-MI did not affect staurosporine-induced caspase activation: levels of DEVDase activity were similar in uninduced (white bars) and induced (black bars) cells (Figure 7a).

Moreover, PSM-RB cleavage to ΔRB and, to a minor extent, alternative fragments (*RB), was observed with time in staurosporine-treated cells (Figure 7b). The *RB fragments may result from cleavage at a previously described internal caspase site (Fattman *et al.* 2001), or reflect cleavage by non-caspase apoptotic proteases. Consistently, *RB generation could not be prevented by mutation of the C-terminal caspase site and was thus also observed in staurosporine PSM-RB-MI cells. Moreover, alternative cleavage events evidently induced RB degradation and caused the loss of PSM-RB-MI, despite the fact that the MI mutation prevented the formation of ΔRB (Fig. 7b). In summary, it was shown that PSM-RB-induced G1 arrest had no effect on staurosporine-induced apoptosis in Rat-16 cells. Moreover, mutation of the C-terminal caspase site did not prevent RB degradation during staurosporine-induced apoptosis.

a

b
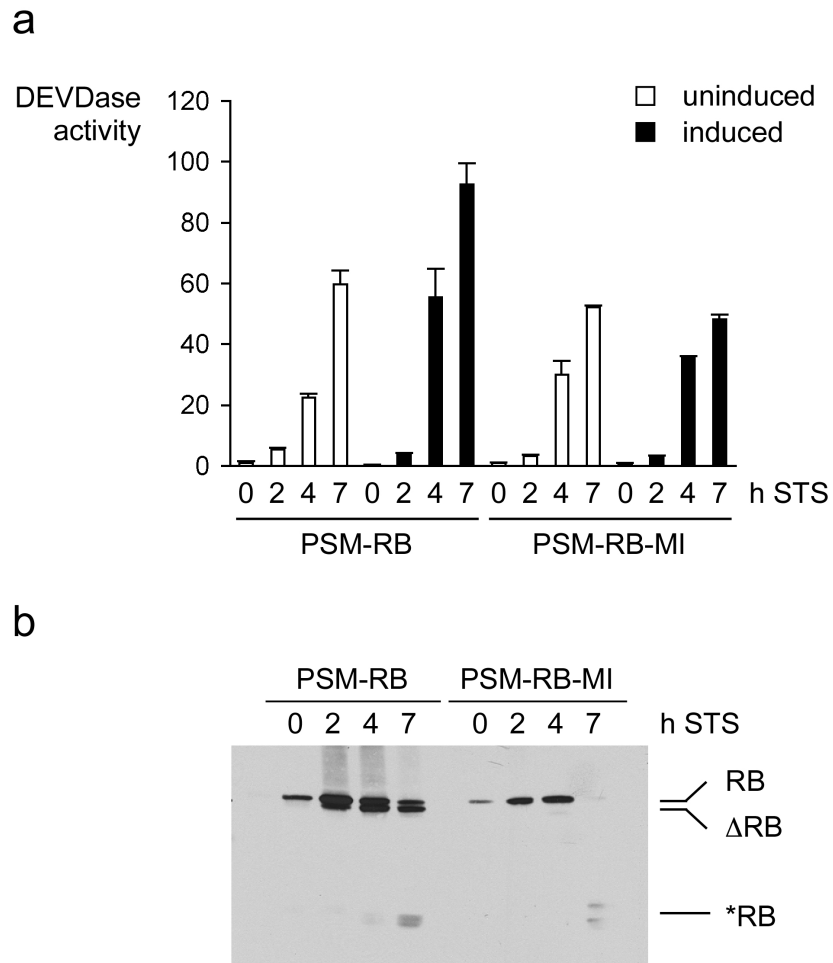
Figure 7. Staurosporine (STS)-induced caspase activation is not affected by PSM-RB variants

(a) DEVDase activity in STS-treated Rat-16 cells. PSM-RB and PSM-RB-MI cells were cultured with (uninduced) or without TET (induced) for 24 h and subsequently treated with STS for the indicated times in the presence (white bars) or absence (black bars) of TET. DEVDase activity was analyzed as in Figure 5. (b) PSM-RB and PSM-RB-MI protein degradation in STS-treated Rat-16 cells. PSM-RB and PSM-RB-MI cells were treated as in (a). Equal amounts of protein from whole cell lysates were resolved by SDS-PAGE and RB was detected by immunoblotting. ΔRB and *RB indicate cleavage fragments of RB.

2.1.3   Inducible expression of RB variants sensitizes Rat-16 cells to TNF-induced apoptosis

Tumor necrosis factor (TNF), in combination with cycloheximide (CHX), is known to induce caspase-dependent (apoptotic) and caspase-independent (necrotic) cell death in cultured fibroblasts (Liu *et al.* 1996; Humphreys and Wilson 1999; Denecker *et al.* 2001; Lin *et al.* 2004). TNF/CHX-induced death of Rat-16 cells, measured by the uptake of propidium iodide (PI), was only partially inhibited by the broad-spectrum caspase inhibitor z-VAD-fmk (Figure 8, left panel); and not associated with DNA fragmentation, as measured by sub-G1 DNA content (Fig. 9a, white bars) or caspase activity (not shown). These results suggest that Rat-16 cells undergo necrotic death in response to TNF/CHX. The percentage of PI positive cells was the same in uninduced (white bars) and induced (black bars) PSM-RB cells, indicating that PSM-induced cell-cycle arrest did not prevent TNF-induced cell death. Interestingly, the expression of PMS-RB caused a significant increase in sub-G1 DNA content following TNF/CHX treatment (Figure 9a, black bars). Increased DNA fragmentation and Parp cleavage were observed, with both mouse and human TNF (Figure 9). Expression of PSM-RB also increased nuclear condensation, which was blocked by z-VAD-fmk (Figure 8), indicating that this was a caspase-dependent process. The enhanced DNA fragmentation was not caused by the withdrawal of tetracycline in parental Rat-16 cells that did not express PSM-RB (not shown) and was thus not an unspecific effect of culture conditions. Taken together, these results indicated that PSM-RB expression enhanced the apoptotic response of Rat-16 cells to TNF.

Moreover, induction of RB variants that could be inactivated by phosphorylation (WT-RB, RB-MI) also enhanced the apoptotic response to TNF/CHX in Rat-16 cells (Figure 9 and data not shown). Mutation of the caspase-cleavage site (MI) in either RB-MI or PSM-RB-MI did not prevent or decrease the apoptosis enhancing effect (Figure 9), consistent with the observation that TNF/CHX did not cause a significant level of RB cleavage or degradation in Rat-16 cells (Figure 9b). Although the cleavage of Parp indicated caspase activation (Figure 9b, lower panel), ΔRB was not detected in cells treated with TNF/CHX (Figure 9b, upper panel). It is possible that ΔRB was rapidly degraded or that caspase activity was not high enough to allow accumulation of the cleavage product during apoptosis.
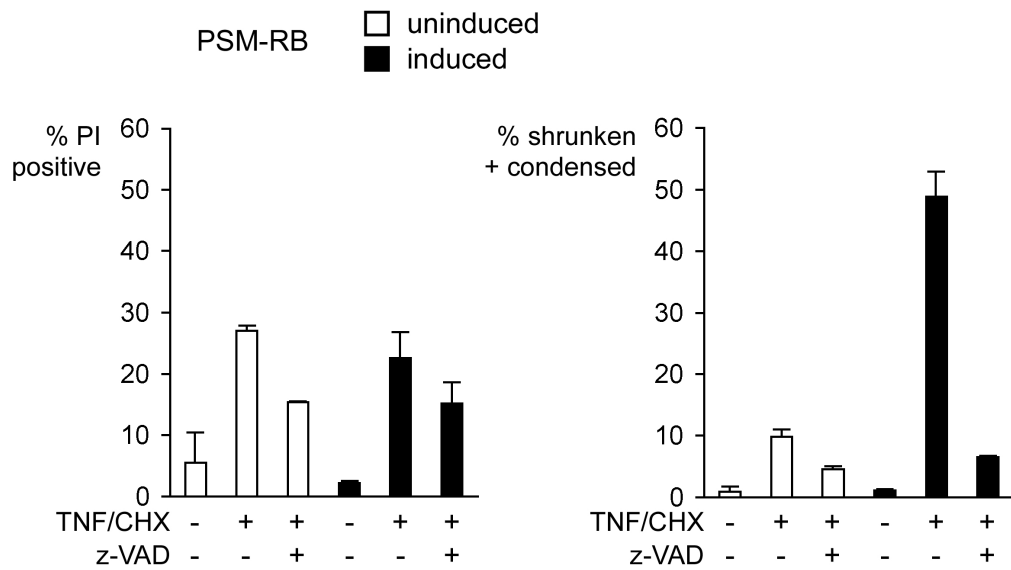
Figure 8. Caspase inhibition can prevent TNF-induced cell shrinkage but not death in PSM-RB expressing cells. PSM-RB cells were cultured with or without TET for 24 h and subsequently treated with m TNF/CHX for 48 h in the presence (white bars) or absence (black bars) of TET with (+) or without (-) prior addition of 50 μM z-VAD-fmk. Uptake of PI (a) and cell size and shape (b) were analyzed by flow cytometry

Alternatively, the C-terminal cleavage site may not be accessible to caspases in TNF/CHX-treated Rat-16 cells. Importantly, the observation that RB was cleaved at this site in cells treated with doxorubicin or staurosporine (Figure 5 and 7b, respectively) indicated that RB cleavage is not generally impaired in Rat-16 cells.

Since all four RB proteins caused a sensitization to TNF, but WT-RB and RB-MI did not inhibit proliferation (Figure 2b), the effect did not correlate with cell cycle arrest. Consistently, induction of PSM-RB expression for only 6 hours prior to TNF/CHX treatment was sufficient to sensitize cells to TNF-induced apoptosis (Figure 10a). To test how cell-cycle arrest by serum-starvation would affect the TNF response of Rat-16 cells, uninduced cells were synchronized in quiescence by serum starvation before the induction of PSM-RB. Serum-starved cells were incubated for 24 hours with or without tetracycline and subsequently treated with TNF/CHX. Clearly, serum starvation sensitized Rat-16 cells to TNF–induced apoptosis, probably due to a limitation of survival factors (Figure 10b). Induction of PSM-RB variants had no additive effect on the apoptosis sensitivity of serum-starved cells: cells that were

a
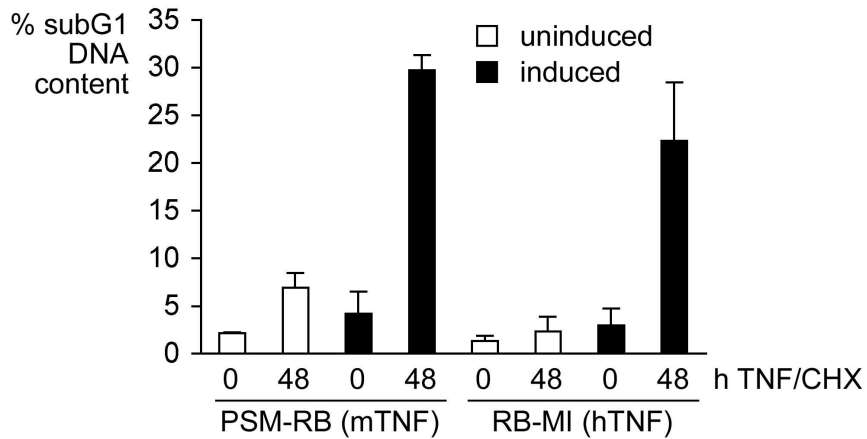
b
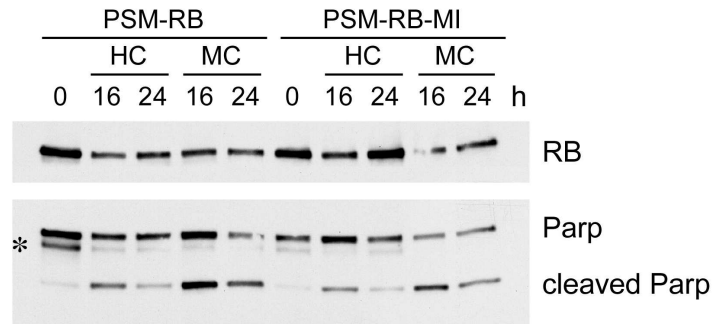
Figure 9. Induced expression of RB and its variants sensitizes to TNF-induced apoptosis

(a) Levels of cells with subG1 DNA content in TNF-treated Rat-16 cells. PSM-RB and RB-MI cells were cultured with (uninduced) or without TET (induced) for 24 h and subsequently treated with recombinant mouse or human TNF (mTNF, hTNF) and cycloheximide (CHX) for 48 h in the presence (white bars) or absence (black bars) of TET. Cells were stained with PI and analyzed by flow cytometry. (b) RB and Parp protein levels in TNF-treated PSM-RB and PSM-RB-MI expressing cells. PSM-RB and PSM-RB-MI cells were cultured without TET for 24 h and subsequently treated with mTNF/CHX (MC) or hTNF/CHX (HC) for the indicated times. Equal amounts of protein from whole cell lysates were resolved by SDS-PAGE and RB (upper panel) and Parp (lower panel) were detected by immunoblotting on the same membrane. ∗ indicates the faint RB band visible due to incomplete stripping.

a

b
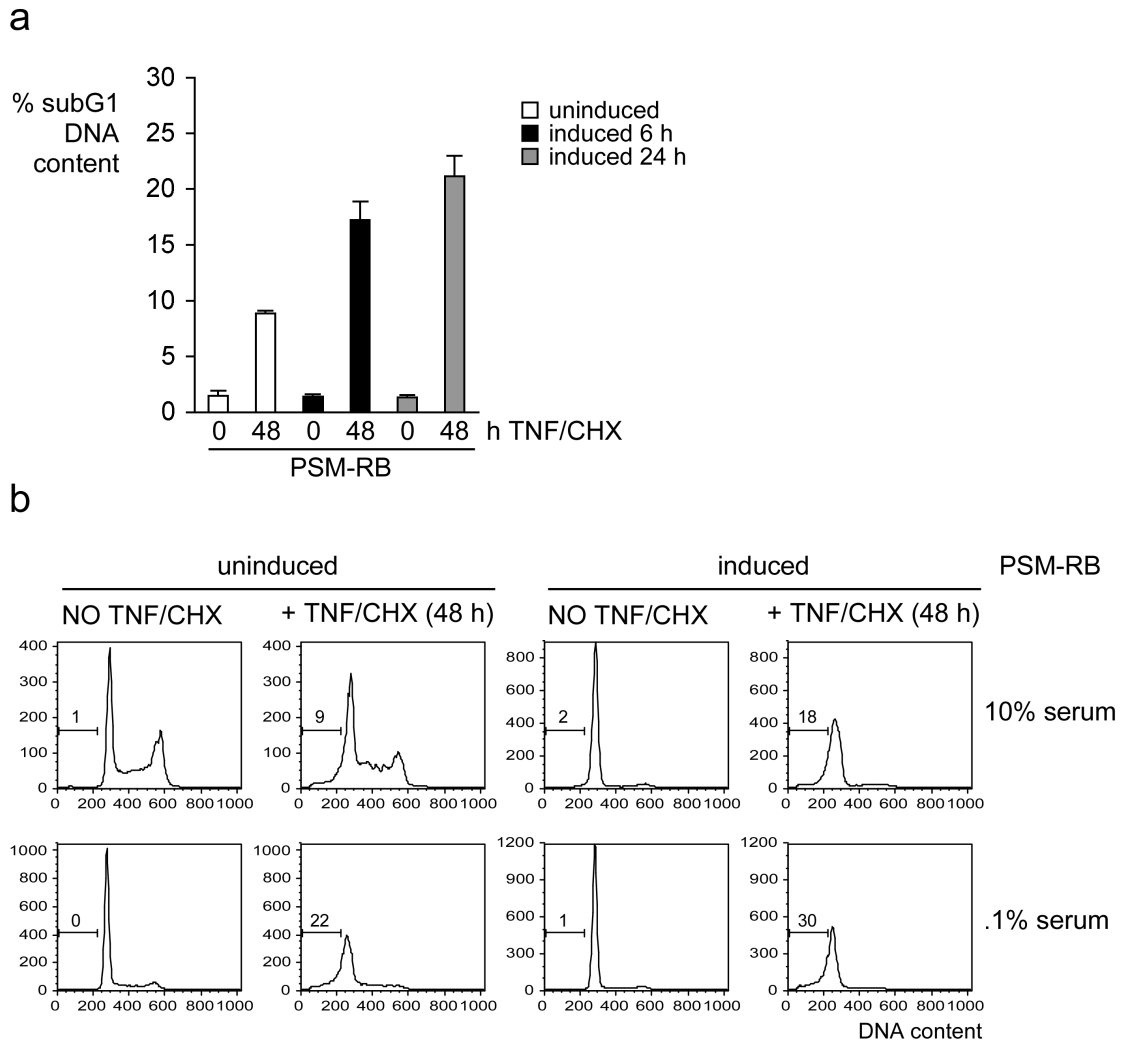
Figure 10. Effect of cell cycle arrest on sensitivity to TNF-induced apoptosis

(a) Sensitization does not correlate with PSM-RB-induced cell cycle arrest. PSM-RB cells were cultured without TET for 6 h (black bars) or 24 h (grey bars) or left uninduced (white bars) and subsequently treated with mouse TNF plus CHX (TNF/CHX) for the indicated times in the presence or absence of TET. Levels of cells with subG1 DNA content were determined by flow cytometry. (b) Sensitization by serum starvation. PSM-RB cells were cultured in 10 % serum (upper panel) or synchronized in quiescence by culture in 0.1 % serum for 3 days (lower panel) in the presence of TET. During the last 24 h, PSM-RB expression was induced in half of the samples (- TET). Subsequently, cells were treated with mouse TNF plus CHX (TNF/CHX) as indicated in the presence (+ TET) or absence (- TET) of TET and/or serum. Cell cycle distribution and subG1 DNA content were determined by flow cytometry. Shown are histograms of 10 000 gated events.
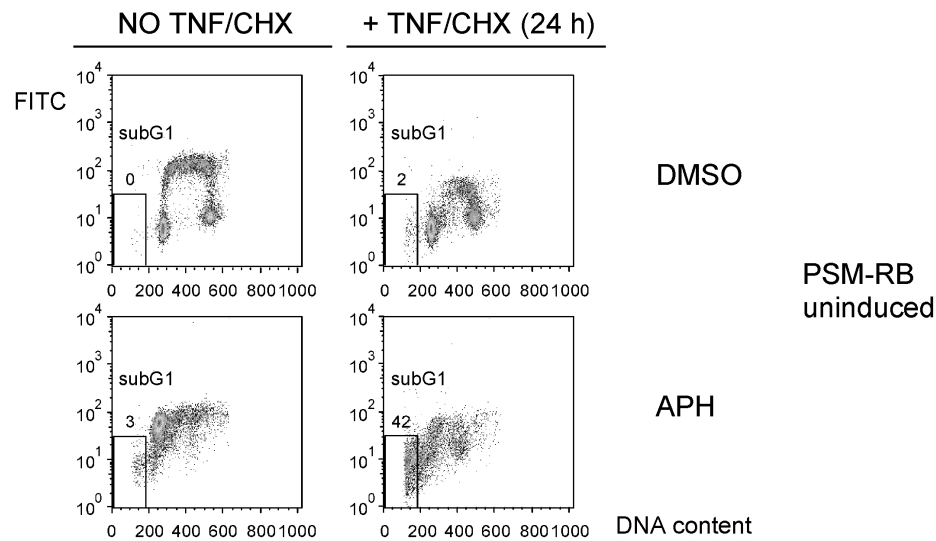
Figure 11. Sensitization to TNF-induced apoptosis by aphidicolin (APH)
Uninduced PSM-RB cells were first synchronized in quiescence by culture in 0.1 % serum for 3 days. Subsequently, cells were cultured in 10 % serum for 16 h and treated with APH (lower panel) or DMSO (upper panel) for 22 h. Cells were then treated with TNF/CHX as indicated and pulse labeled with BrdU. Cells were fixed and stained with FITC-conjugated BrdU antibody and propidium iodide and analyzed by flow cytometry. Shown are representative density plots of FITC (BrdU) and propidium iodide (DNA content) signal intensity. Cells with subG1 DNA content are indicated.

quiescent at the time of PSM-RB induction showed the same levels of apoptosis as uninduced cells (Figure 10b, lower panel), while in parallel populations, that were proliferating in 10% serum when PSM-RB was induced, the number of apoptotic cells following TNF/CHX treatment was again markedly increased compared to uninduced cells (Figure 10b, upper panel). This observation suggests that RB-dependent suppression of survival gene expression might be responsible for the sensitization to TNF-induced apoptosis. Alternatively, interference with replication fork movement, a function previously described for PSM-RB (Sever-Chroneos et al. 2001), might cause a replication stress response that enhanced the cells susceptibility to a second stress signal (Figure 27c). This notion was supported by the observation that aphidicolin-induced S-phase arrest augmented TNF-induced apoptotic DNA fragmentation in Rat-16 cells (Figure 11). Aphidicolin causes cell cycle arrest in early S-phase by selective inhibition of DNA polymerase alpha (Spadari et al. 1985). Cells were first arrested by serum starvation and then treated with aphidicolin in the presence of serum for 16 hours prior to TNF/CHX treatment. Synchronization of the population in early S-

phase was reflected by the accumulation of BrdU-positive cells with G1 DNA content and the absence of BrdU positive cells with intermediate DNA content indicative of S phase cells (Figure 11 lower left hand panel). Interestingly, treatment with TNF/CHX also prevented BrdU incorporation (Fig. 11, upper right hand panel), indicating inhibition of DNA replication by CHX, most likely due to the reduction in histone biosynthesis (Venkatesan 1977; Bonner *et al.* 1988). Again, TNF/CHX treatment did not cause apoptosis in the absence of RB overexpression (Fig. 11, upper right hand panel). Cells arrested with aphidicolin, however, underwent substantial apoptosis following treatment with TNF/CHX (Figure 11, lower right hand panel). This result is consistent with a previous report that aphidicolin sensitized fibroblastic cells to TNF-induced apoptosis (Gera *et al.* 1993) and supports the notion that G1/S arrest or replication stress can sensitize cells to TNF-induced apoptosis. In the Rat-16 expression system, sensitization to TNF-induced apoptosis might be a non-physiological activity of RB and RB variants that is associated with conditions of overexpression.

Taken together, the analysis of RB expressing Rat-16 cells showed that RB-dependent cell cycle arrest is not generally associated with resistance to apoptosis. In Rat-16 cells, PSM-RB induced G1/S arrest could inhibit DNA damage-induced caspase activation, but did not affect caspase activation in response to staurosporine. RB expression sensitized Rat-16 cells to TNF-induced apoptosis independent from the induction of cell cycle arrest. Sensitization to TNF/CHX treatment was also caused by serum starvation or the inhibition of DNA replication by aphidicolin.

2.2 Analysis of altered TNF response in $Rb^{MI/MI}$ fibroblasts

2.2.1 Response of wild-type and $Rb^{MI/MI}$ cells to selective activation of TNF receptors

Mutation of the conserved C-terminal caspase recognition site in the *Rb* sequence generates a protein (termed Rb-MI) that is resistant to caspase cleavage in several different cellular contexts (Tan and Wang 1998; Chau and Wang 2003). For example, expression of Rb-MI has been shown to protect fibroblasts from TNF-induced apoptosis (Tan *et al.* 1997) and cultured neurons from apoptosis caused by potassium deprivation (Boutillier 2000). The MI mutation has been introduced into the mouse *Rb-1* gene (Chau *et al.* 2002) in Dr. Wang's laboratory to generate $Rb^{MI/MI}$ knockin mice. In these animals, Rb-MI conferred tissue-specific protection from endotoxin-induced apoptosis (Chau *et al.* 2002). Fibroblasts derived from $Rb^{MI/MI}$ embryos were protected from apoptosis induced by human TNF (hTNF) (Chau *et al.* 2002) and this work). Interestingly, $Rb^{MI/MI}$ fibroblasts remained sensitive to apoptosis induced by murine TNF-α (mTNF) and the Rb-MI protein was degraded in mTNF-treated cells. This observation is consistent with the notion that Rb degradation is required for TNF-induced apoptosis and demonstrates that mechanisms other than C-terminal caspase cleavage can eliminate Rb during death receptor-induced apoptosis.

TNF exerts its diverse biological activities via two different receptors: type 1 TNF-α receptor (TNFR1) and type 2 TNF-α receptor (TNFR2). Both receptors belong to the death receptor family but differ in tissue distribution and intracellular signaling (Wajant *et al.* 2003). In murine cells, hTNF only activates TNFR1, while mTNF naturally triggers both types. Thus, a different response of murine cells to human and mouse TNF might be explained by the signaling of either one or both types of TNF receptors. To test this, wild-type and $Rb^{MI/MI}$ fibroblasts were treated with agonistic antibodies that specifically activate only one of the two TNF receptors (Figure 13). Analysis of cell death based on membrane integrity (PI uptake assay) showed that treatment with TNFR1-activating antibody (anti-TNFR1) plus cycloheximide (CHX) for 16 h caused massive death in wild-type, but not in $Rb^{MI/MI}$ cells (Figure 13a). Treatment with TNFR2-activating antibody (anti-TNFR2) plus CHX did not cause significant death by itself in wild-type or $Rb^{MI/MI}$ cells. Moreover, co-treatment with anti-TNFR2 did not increase the level of cell death in anti-TNFR1–treated wild-type cells. By contrast, in $Rb^{MI/MI}$ cells, which were resistant to cell death

induced by anti-TNFR1, the combined treatment with anti-TNFR1 and anti-TNFR2 (plus CHX) induced death to the same extent as in wild-type cells (Figure 13a).

The different sensitivity of wild-type and $Rb^{MI/MI}$ cells to TNFR1-induced cell death correlated with differences in caspase-3 activation (Figure 13b). In wild-type cells, treatment with both human and mouse TNF and treatment with anti-TNFR1 caused the processing of pro-caspase-3 to the active, cleaved form. Levels of cleaved caspase-3 in wild-type cells were the same after hTNF and mTNF treatment as well as anti-TNFR1 treatment and were not enhanced by co-treatment of wild-type cells with anti-TNFR1I and anti-TNFR1 (Figure 13b, left lanes). Again, $Rb^{MI/MI}$ cells did not respond to treatment with hTNF or anti-TNFR1: only mTNF or the combined treatment with both TNF receptor-activating antibodies caused a significant processing of pro-caspase 3 to the active form (Figure 13b, right lanes). Thus, the different sensitivity of wild-type and $Rb^{MI/MI}$ cells to human TNF was mirrored by a different sensitivity to TNFR1-activating antibody. Thus, the different effect of human and mouse TNF on $Rb^{MI/MI}$ cells could be attributed to their different capacity to activate the two TNF receptors. Taken together, these results show, that $Rb^{MI/MI}$ cells are specifically protected from apoptosis induced by TNFR1.

The possibility that this resistance was due to a reduced expression of TNFR1 in $Rb^{MI/MI}$ cells was ruled out by the comparison of TNFR1 protein levels in wild-type and $Rb^{MI/MI}$ cells by immunoblotting (Figure 14a). Similar levels of TNFR1 could be detected in lysates from wild-type and $Rb^{MI/MI}$ cells; the identity of the band corresponding to TNFR1 was confirmed by its absence in $TNFR1^{-/-}$ cells.

Previous studies have linked apoptosis in $Rb^{-/-}$ embryos to deregulated proliferation (Macleod *et al.* 1996). Moreover, cells in S-phase are known to be more susceptible to a number of apoptotic stimuli (Meikrantz and Schlegel 1995). To test for a possible correlation between inhibition of proliferation and protection from apoptosis in $Rb^{MI/MI}$ cells, cell cycle progression of wild-type and $Rb^{MI/MI}$ cells was analyzed by BrdU pulse labeling of replicating cells (Figure 14b). Untreated cells of both genotypes showed comparable levels of cells in S-phase (Figure 14b, 0 h). Treatment with hTNF/CHX inhibited BrdU (5-bromodeoxyuridine) incorporation in both wild-type (+/+) and $Rb^{MI/MI}$ cells (MI/MI); this effect was probably due to CHX dependent inhibition of protein and DNA synthesis (Venkatesan 1977; Bonner *et al.* 1988). Among wild-type cells, levels of proliferating cells dropped faster than with $Rb^{MI/MI}$ cells (compare +/+ and MI/MI at 6 h), which was consistent with the onset of

apoptosis in wild-type but not $Rb^{MI/MI}$ cells within this time course (Figure 13). Similar results were obtained with $Rb^{MI/MI}$ MEFS (Chau *et al.* 2002). Thus, for the apoptosis response to TNFR1 activation, the apoptosis suppressing activity of Rb-MI could be separated from its growth suppressor function.

2.2.2   Gene expression analysis of TNF response in $Rb^{MI/MI}$ cells

$Rb^{-/-}E2F\text{-}1^{-/-}$ double-deficient embryos are partially rescued from the aberrant apoptosis observed in $Rb^{-/-}$ animals (Tsai *et al.* 1998). E2F-1 has been shown to regulate several pro-apoptotic genes including Apaf-1 and caspase-3 (Muller *et al.* 2001). Consistently, the expression of Apaf-1 is deregulated in $Rb^{-/-}$ embryos (Moroni *et al.* 2001). Moreover mutation of Apaf-1 or caspase-3 can prevent ectopic apoptosis of *Rb*-deficient neurons (Guo *et al.* 2001; Simpson *et al.* 2001). These data indicate that Rb-dependent suppression of apoptosis during embryonic development is mediated by E2F1-dependent suppression of genes required for mitochondria-dependent apoptosis. Thus, the protection of $Rb^{MI/MI}$ fibroblasts from TNF-induced cell death might also be due to Rb-dependent suppression of E2F1-regulated pro-apoptotic genes. On the other hand, the observation that cell death in response to TNF is enhanced in the presence of inhibitors of transcription and translation, like actinomycin and cycloheximide, suggests that the TNF-induced apoptosis pathway does not require new gene transcription.

To directly assess the role of TNF-induced changes in gene expression in the apoptosis response of $Rb^{MI/MI}$ fibroblasts, an extensive analysis of TNF-induced changes in gene expression was conducted via DNA microarray-based gene expressing profiling. The fact that the Rb-MI protein was inactivated and degraded in mTNF-treated cells, allowed the comparison of transcriptional changes in response to TNF in the presence (during hTNF treatment) and absence (during mTNF treatment) of active Rb-MI. In this way, the response to TNF could be examined for Rb-dependent changes in gene expression in a single cell line, thus avoiding variations due to possible intrinsic differences between individual cell lines. To test whether Rb-MI regulates the transcription of apoptosis-related genes in $Rb^{MI/MI}$ fibroblasts, transcriptional changes in $Rb^{MI/MI}$ cells were therefore compared between human and

a

% PI
positive

b
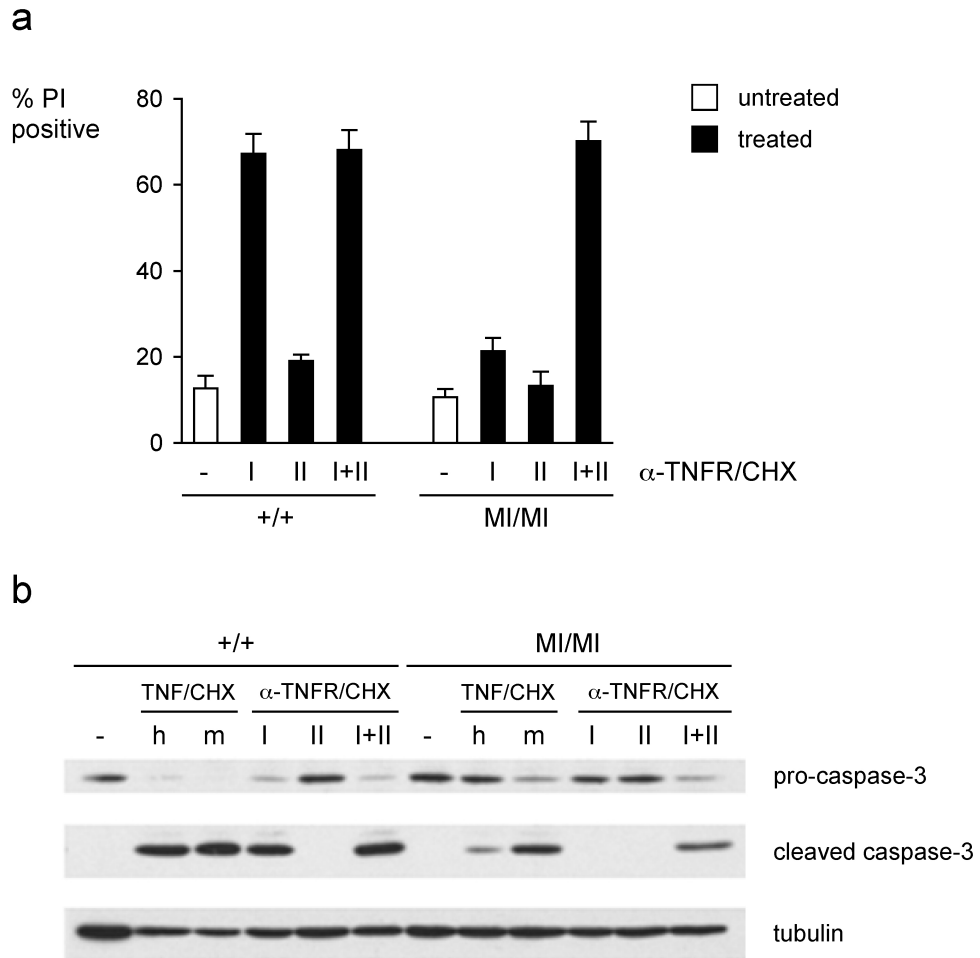
Figure 13. $Rb^{MI/MI}$ cells are resistant to apoptosis induced by TNFR1

(a) Percentage of dead (PI-positive) wild-type (+/+) and $Rb^{MI/MI}$ (MI/MI) cells after treatment with agonistic antibodies against TNF receptors. Cells were treated with the indicated antibodies (I, anti-TNFR1; II, anti-TNFR1I) for 16 h and PI positive cells were quantified by flow cytometry. (b) Differential activation of caspase-3 in wild-type and $Rb^{MI/MI}$ cells. Cells were treated as indicated with TNF (h, hTNF; m, mTNF) plus cycloheximide (CHX) for 6 h or agonistic antibodies (I, anti-TNFR1; II, anti-TNFR1I) plus CHX for 7 h. Lysates were resolved by SDS-Page and pro-caspase-3 (upper panel), cleaved caspase-3 (middle panel) and tubulin (lower panel) were detected by immunoblotting.

murine TNF treatment via an oligonucleotide microarray analysis. Briefly, biotin-labeled cRNA was generated from cellular mRNA and hybridized to a GeneChip® oligonucleotide array, representing a mouse genomic library of approximately 12 000 known genes and expressed sequences. To this end, total RNA was isolated from untreated control cells and cells treated with human or murine TNF plus cycloheximide (CHX).
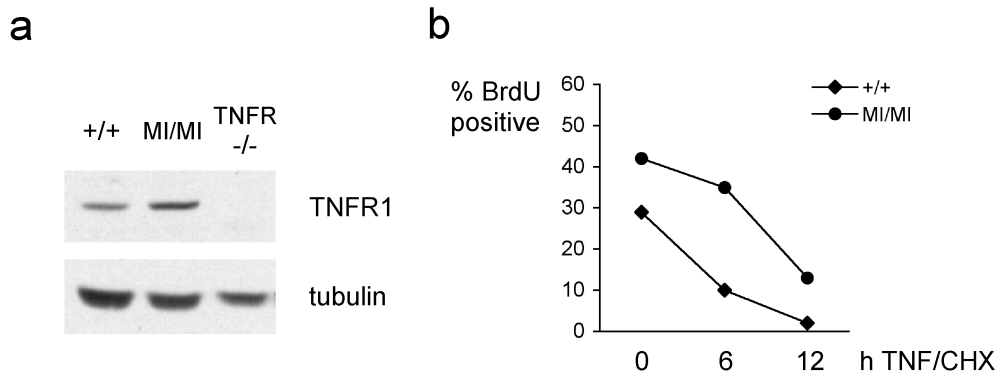
Figure14. Normal expression of TNFR1 and continuing proliferation of TNF-resistant $Rb^{MI/MI}$ cells
(a) TNFR1 protein levels. Whole cell lysates from wild-type, $Rb^{MI/MI}$ cells and $TNFR^{-/-}$ cells were resolved by SDS page, and TNFR1 and tubulin were detected by immunoblotting. (b) Time course of TNF-induced changes in the proliferative index of wild-type and $Rb^{MI/MI}$ cells. Cells were treated with hTNF/CHX for the indicated times and pulse-labeled with BrdU during the last hour. The percentage of BrdU-positive cells was determined by flow cytometry.

2.2.2.1   Preparation of biotin-labeled cRNA as hybridization probe

From total cellular RNA, double stranded cDNA was synthesized in a reverse transcription reaction (Figure 15). The use of oligo-dT-primers that hybridize with the distinctive poly A-signal of mRNA ensured the selective synthesis of expressed sequences. In addition, the T7 promoter sequence was contained in the oligo-dT-primers and was thus added to each cDNA sequence. The in this way generated cDNA pool served as the template for the synthesis of biotin-labeled cRNA. The T7 promoter allowed the *in vitro* translation of cDNA by T7 RNA polymerase. In this step, cRNA was amplified in a linear way and labeled through the incorporation of biotinylated ribonucleotides. The resulting pool of biotin-labeled cRNA (biotin-cRNA) quantitatively represented the cellular mRNA content at the time of sample collection.

For hybridization, biotinylated molecules were fragmented to a more uniform size ranging between approximately 40 to 200 base pairs. This helps to minimize differences in hybridization kinetics between diverse RNA molecules that would result in their over-or underrepresentation on the DNA array. The quality and size

distribution of RNA and cRNA samples was analyzed by gel electrophesis (Figure 16). RNA and biotin-labeled cRNA samples were resolved on ethidium bromide-stained agarose gels and visualized under UV light. In total RNA (Figure 16a), ribosomal RNAs (28 S and 18 S rRNA) are visible as distinct bands due to their relative abundance in the cell. The visual absence of rRNA degradation is an indicator for high quality of the preparation. Biotin-cRNAs show a size distribution ranging from ca. 500 bp to 1.5 kB, which is typical for mRNA representing cRNA (Figure 16b, lanes 1-3). Fragmentation resulted in a homogeneous size distribution from ca. 50 to 200 bp (Figure 16b, lanes 4-6).

2.2.2.2   Analysis of DNA microarray hybridization data

For each condition (untreated, hTNF-treated, mTNF-treated), total cellular RNA samples were collected from three independent experiments. Biotin-labeled cRNA from each sample was incubated with a separate oligonucleotide microarray. Following hybridization of biotin-labeled cRNA with DNA oligos on the microarray, unbound cRNA was washed away and biotin-cRNAs bound to the chip were stained with a streptavidin-conjugated fluorescent dye. Finally, excess dye was washed away and the chip was analyzed with a fluorescent microarray scanner. The amount of light emitted from each spot on the array is determined by the number of oligonucleotide bound cRNA molecules at this location and is thus proportional to the abundance of the corresponding mRNA in the sample. Therefore, the fluorescence intensity values for all spots can therefore be translated into expression values for each gene represented on the array. Since scanned images of different chips vary in their overall brightness the comparison of expression levels across different samples (and thus, separate chips) requires normalization of signal intensities. Data was normalized against an array with median overall intensity using DNA-Chip Analyzer (dChip) software (Li and Hung Wong 2001; Li and Wong 2001).

Upon normalization, the data was compared via a statistical analysis that calculates the significance of changes in gene expression based on the standard deviation in data from repeated measurements. This analysis was performed using software (SAM, significance analysis of microarrays, (Tusher *et al.* 2001) that calculates two statistical parameters for each gene: the "relative difference in expression" (*d*) between two states (*e.g.* untreated and treated), which is based on the

Starting RNA samples   total RNA

5'- TTTTTTTTTT AAAAA - 3'

Primer hybridization   3'-T T T T T −■■■- 5'
                              oligo(dT)-primer

5'- TTTTTTTTTT AAAAA - 3'
                3'-T T T T T −■■■- 5'

Reverse transcription
First strand cDNA synthesis

5'- TTTTTTTTTT AAAAA - 3'
3'- ⊥⊥⊥⊥⊥⊥⊥⊥⊥⊥ TTTTT −■■■- 5'

Second strand synthesis

5'- ⊤⊤⊤⊤⊤⊤⊤⊤⊤⊤ AAAAA−■■■- 3'
3'- ⊥⊥⊥⊥⊥⊥⊥⊥⊥⊥ TTTTT −■■■- 5'

Cleanup of
double-stranded cDNA   biotinylated
                                        ribonucleotides U C
Amplification and
biotin-labeling of antisense cRNA

3'- ⊥⊥⊥⊥⊥⊥⊥⊥⊥⊥ UUUUU - 5'

3'- ⊥⊥⊥⊥⊥⊥⊥⊥⊥⊥ UUUUU - 5'

3'- ⊥⊥⊥⊥⊥⊥⊥⊥⊥⊥ UUUUU - 5'

Cleanup of
biotin-labeled cRNA

Fragmentation and hybridization onto
gene expression microarrays

TTTTTT DNA   ⊤⊤⊤⊤⊤⊤ RNA   ■■■ T7 promoter   ●— biotin

Figure 15. Flow chart for the preparation of biotin-labeled cRNA as hybridization probes for GeneChip® gene expression arrays (modified from Affymetrix GeneChip® Expression Analysis Technical Manual)
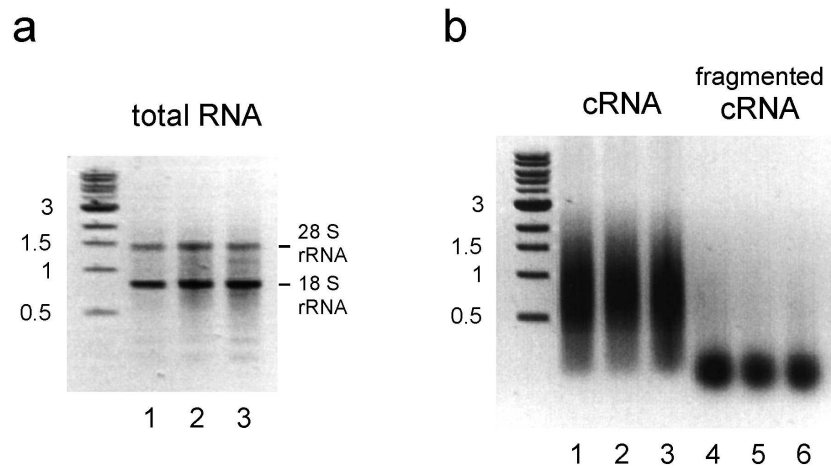
Figure 16. Size distribution of cellular RNA and biotin-labeled cRNA

(a) Total RNA (1 µg) isolated from untreated (lane 1), hTNF/CHX-treated (lane 2) and mTNF/CHX-treated (lane 3) $Rb^{MI/MI}$ cells was resolved on an 1 % ethidium bromide-stained agarose gel and visualized under UV light. (b) Biotin-labeled cRNA (cRNA) derived from the samples shown in (a) was visualized on an ethidium bromide-stained gel before (lanes 1-3) and after (lanes 4-6) fragmentation. DNA length standard (1 kB ladder) was loaded as reference; 0.5; 1; 1.5 and 3 kB bands are labeled.

ratio of average change in expression to standard deviation in the data for an individual gene, and the "expected relative difference in expression" (d_E), which is the average of multiple d values, which are calculated for random permutations of the data for the same gene. If there is no significant change in gene expression, permutation of the data does not change the d value, so that d_E is equal to d. If the observed d value differs from the expected value by more than a given threshold, the change in gene expression is called significant.

To identify all significant changes in gene expression, the experimentally observed d values of all genes are plotted versus the expected d_E values in a scatter plot. Genes with a positive change in expression (upregulated genes) are represented by points above the $d=d_E$ line, downregulated genes are represented by points below this line. Depending on the threshold Δ after which a change in expression is called significant the SAM software calculates the false discovery rate (FDR), which is the percentage of genes identified by chance. By adjusting Δ, the number of estimated false positive genes was reduced to less than one.

The results of the SAM analysis for TNF-treated $Rb^{MI/MI}$ fibroblasts are summarized in Figure 17. The comparison of human TNF-treated cells with murine TNF-treated cells yielded no significantly induced or repressed genes (Figure 17a). In the scatter plot of observed versus expected d values, all genes are represented by points on or very close to the $d=d_E$ line (FDR < 1 for $\Delta = 0.5$). By contrast, the comparison of untreated cells with either human-TNF treated cells (Figure 17b) or murine TNF-treated cells (not shown) yielded a set of 67 known genes that showed a significant and at least 1.25 fold change in expression (FDR < 1 for $\Delta = 2.4$). Most of them (64) were upregulated in TNF-treated samples. Among these were 18 apoptosis-related genes (Table 1). Seven out of the nine most highly ranked apoptosis-related genes (score $\geq$ 10) were previously reported to be induced by TNF, indicating the validity of the assay (Table 1). In summary, while a number of known TNF-regulated genes were induced in response to TNF, no Rb-dependent changes in gene expression could be observed in TNF treated $Rb^{MI/MI}$ fibroblasts.

a

relative changes in gene expression
[hTNF-treated vs. mTNF-treated]

significant: 0
$\Delta = 0.5$
median false significant < 1

b

relative changes in gene expression
[untreated vs. hTNF-treated]

significant: 94
$\Delta = 2.4$
median false significant < 1
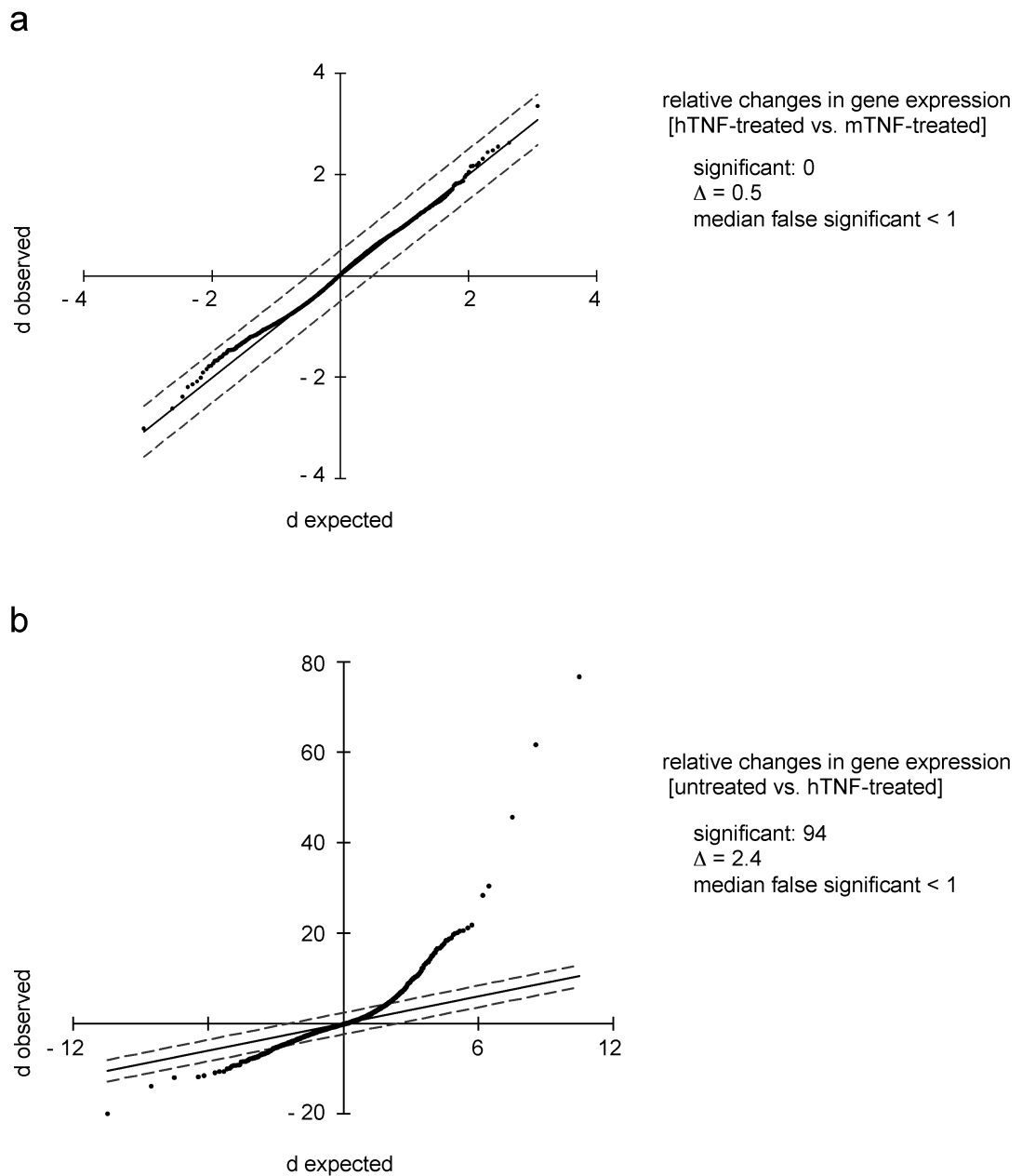
Figure 17. Significance analysis of DNA microarray hybridization data

(a) Relative changes in gene expression between hTNF-treated and mTNF-treated $Rb^{MI/MI}$ cells. No significant changes in gene expression are identified by the SAM analysis; all genes are represented by points on or very close to the $d=d_E$ line (FDR < 1 for $\Delta = 0.5$).

(b) Relative changes in gene expression between untreated and hTNF-treated $Rb^{MI/MI}$ cells. For $\Delta = 2.4$, a significant change in gene expression is identified for 94 genes (FDR <1 for $\Delta = 2.4$). Most of them are represented by points above the $d=d_E$ line, indicating a positive change in expression level. Data was analyzed using the SAM algorithm for a two-class, unpaired response.

Gene	Gene name	Score	Fold change
A20	tumor necrosis factor-α-induced protein 3	61.7	1.6
Rel B	v-rel oncogene related protein B	30.4	1.4
NF-κB2/p100	nuclear factor of κ gene enhancer in B-cells 2	20.5	1.3
Caspase-11	caspase-11	18.3	1.4
TNFaip2	tumor necrosis factor-α-induced protein 2	16.3	1.4
Tnfrsf6	TNF receptor superfamily member 6	16.3	1.4
IκB-α	NF-κB inhibitor α	15.5	1.4
TNF-α	tumor necrosis factor α	13.6	1.3
NF-κB1/p105	nuclear factor of κ gene enhancer in B-cells 1	10.2	1.3
Birc2/Miap2	baculoviral IAP repeat-containing 2/murine IAP 2	9.6	1.3
Fos	FBJ osteosarcoma oncogene	8.8	1.5
Tank	TRAF family member-associated NF-κB activator	8.8	1.3
Ttp	zinc finger protein 36/tristetraproline	8.4	1.3
Gadd45-β	growth arrest and DNA damage-inducible 45 β	7.8	1.3
IL-6	interleukin 6	7.5	1.9
Bid	BH3 interacting domain death agonist	7.3	1.4
Phlda1	T-cell death associated gene	7.1	1.4
JunB	Jun-B oncogene	6.9	1.3

Table 1. List of genes induced upon TNF treatment in $Rb^{MI/MI}$ cells. Genes are ordered by their score assigned by significance analysis (SAM). Genes that have previously been identified as NF-κB targets are printed bold. "Fold change" refers to the fold change in expression level compared to untreated control cells.

2.2.3 Analysis of mitochondria-mediated apoptosis in TNF-treated wild-type and *Rb$^{MI/MI}$* cells

The gene expression analysis described above had confirmed efficient NF-κB activation by human TNF in *Rb$^{MI/MI}$* fibroblasts (Table 1). Together with NF-κB, JNK/AP-1 is activated in response to TNF by a receptor-proximal signaling complex via the TRAF2 adaptor protein; and has been reported to modulate the TNF-induced apoptosis response (Varfolomeev and Ashkenazi 2004). To test, if JNK activation occurs differentially in hTNF-treated wild-type and *Rb$^{MI/MI}$* cells, phosphorylation of the JNK substrate c-jun was analyzed by immunoblotting with a phospho-specific antibody directed against phosphorylated serine 63 of c-jun (Figure 18a). Cells were lysed by adding hot SDS sample buffer directly to the tissue culture dish to eliminate phosphatase activity in the lysate. C-jun phosphorylation occurred to the same extent and with the same time-course in both wild-type and *Rb$^{MI/MI}$* cells. Phospho-c-jun was detectable as early as 15 min after treatment and was maintained for at least one hour (Figure 18a). Thus, the TNFR1 DISC-mediated activation of both the NF-κB and the Jun/AP1 transcription factor pathway was unaffected in TNF-treated *Rb$^{MI/MI}$* cells.

The Bcl-2 homolog Mcl-1 has been identified as an early control point of cell death pathways and degradation of Mcl-1 has been shown to be a pre-requisite for TNF-induced apoptosis (Danial and Korsmeyer 2004). Therefore, it was determined if Mcl-1 is efficiently degraded in *Rb$^{MI/MI}$* cells (Figure 18b). Mcl-1 degradation was observed in both wild-type and *Rb $^{MI/MI}$* cells within the same time frame (Figure 18b). These data suggest that Mcl-1 degradation was not prevented by Rb-MI and thus could not account for the absence of TNF-induced apoptosis in *Rb$^{MI/MI}$* cells.

Analysis of caspase-3 processing by immunoblot had indicated differential caspase-3 activation in wild-type and *Rb$^{MI/MI}$* cells in response to human and mouse TNF. Caspase processing, however, does not necessarily correlate with effector caspase activity *in vivo*, because cleaved caspases-3 and -7 can be subject to inhibition by IAPs (Salvesen and Duckett 2002; Shi 2002). Therefore, an enzymatic activity assay was performed to confirm differential effector caspase activation in TNF-treated wild-type and *Rb$^{MI/MI}$* fibroblasts. DEVDase activity was measured in extracts from untreated control cells and TNF-treated cells (Figure 19a) using the fluorogenic caspase substrate Ac-DEVD-AMC. In wild-type cells, both human and mouse TNF

a

b
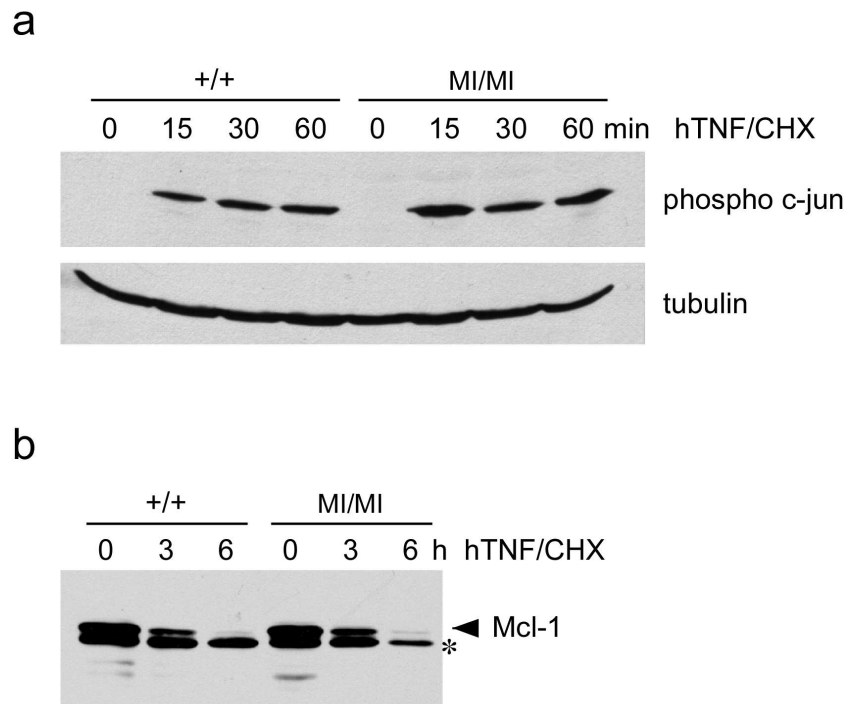
Figure 18. Normal c-jun phosphorylation and Mcl-1 cleavage in hTNF-treated $Rb^{MI/MI}$ cells
(a) Human TNF induces c-jun phosphorylation in wild-type and $Rb^{MI/MI}$ cells. Equal numbers of cells were treated with 10 ng/ml human TNF (hTNF) plus cycloheximide (CHX) for the indicated times and lysed in hot SDS sample buffer. Lysates were resolved by SDS-PAGE and phosphorylated c-jun was detected by immunoblotting. Tubulin was detected to confirm equal loading. (b) Human TNF- induced Mcl-1 degradation. Wild-type and $Rb^{MI/MI}$ cells were treated with hTNF/CHX for the indicated times. Equal amounts of protein from whole cell lysates were resolved by SDS-Page and Mcl-1 was detected by immunoblotting. ∗ indicates a cross-reactive band

induced DEVDase activity, while in $Rb^{MI/MI}$ cells only mouse TNF caused a significant increase in DEVDase activity (Figure 19a). These results confirm that caspase-3 type effector caspases are rapidly and efficiently activated in hTNF-treated and mTNF-treated wild-type cells as well as mTNF-treated $Rb^{MI/MI}$ cells, but not hTNF-treated in $Rb^{MI/MI}$ cells.

Effector caspase activation in the TNFR apoptosis pathway can be achieved via direct cleavage of caspase-3 (-6, -7) by caspase-8, or in a proteolytic cascade initiated by active caspase-9, which is itself activated by apoptosome-mediated oligomerization (Srinivasula *et al.* 1998; Rodriguez and Lazebnik 1999). Apoptosome formation is triggered by the release of cytochrome c from mitochondria, which can be induced by death receptors via caspase-8-mediated generation of truncated BID (Li *et al.* 1998; Luo *et al.* 1998). Truncated BID (tBID) translocates to the mitochondria

membrane and is thought to initiate cytochrome c release by promoting oligomerization of BAX or BAK (Desagher *et al.* 1999; Wei *et al.* 2001). In addition to cytochrome c, other pro-apoptotic factors like Omi/Hrta2 and Smac/Diablo are released from mitochondria (Kuwana and Newmeyer 2003). To test if the mitochondrial apoptosis pathway is impaired in $Rb^{MI/MI}$ cells, TNF-induced release of cytochrome c and Smac was analyzed by immunoblotting of cytosolic cell extracts (Figure 19b). In wild-type cells, both human and mouse TNF induced release of cytochrome c and Smac into the cytosol. In $Rb^{MI/MI}$ cells, only mTNF/CHX treatment caused cytochrome c and Smac release from mitochondria (Figure 19b). This result showed that the defect in the apoptosis response of hTNF-treated $Rb^{MI/MI}$ cells occurs at the level of or upstream of mitochondria.

To test, if tBid is generated in $Rb^{MI/MI}$ cells, lysates from TNF-treated cells were analyzed for the presence of cleaved Bid (Figure 19c). A Bid cleavage fragment of the expected size could be detected in lysates from hTNF-treated wild-type cells and mTNF-treated wild-type and $Rb^{MI/MI}$ cells, but not in $Rb^{MI/MI}$ cells treated with human TNF. Thus, the cleavage of Bid in TNF-treated wild-type and $Rb^{MI/MI}$ cells correlated with the release of pro-apoptotic factors from the mitochondria (Figure 19b, c), effector caspase activation (Figure 19a) and cell death (Chau *et al.* 2002) and Figure 22). This observation suggested impaired tBid generation as a possible cause for the apoptosis-resistance of $Rb^{MI/MI}$ cells.

2.2.4 *In vitro* analysis of cytochrome c release

To confirm the correlation between tBid generation and cytochrome c release in wild-type and $Rb^{MI/MI}$ 3T3 cells, the capacity of cytosolic extracts derived from TNF-treated cells to release cytochrome c was analyzed in an in vitro assay (outlined in Figure 20). Freshly isolated mouse liver mitochondria were incubated with cytosolic extracts and subsequently pelleted by centrifugation. The release of cytochrome c into the supernatant was detected by immunoblot analysis of supernatant and pellet fractions (Figure 21). Cytosolic extracts from hTNF-treated, but not untreated wild-type cells caused the complete release of cytochrome c from mitochondria into the supernatant after at least 3 hours of TNF/CHX treatment (Figure 21a, lanes +/+ 3, 5).

a

b

c
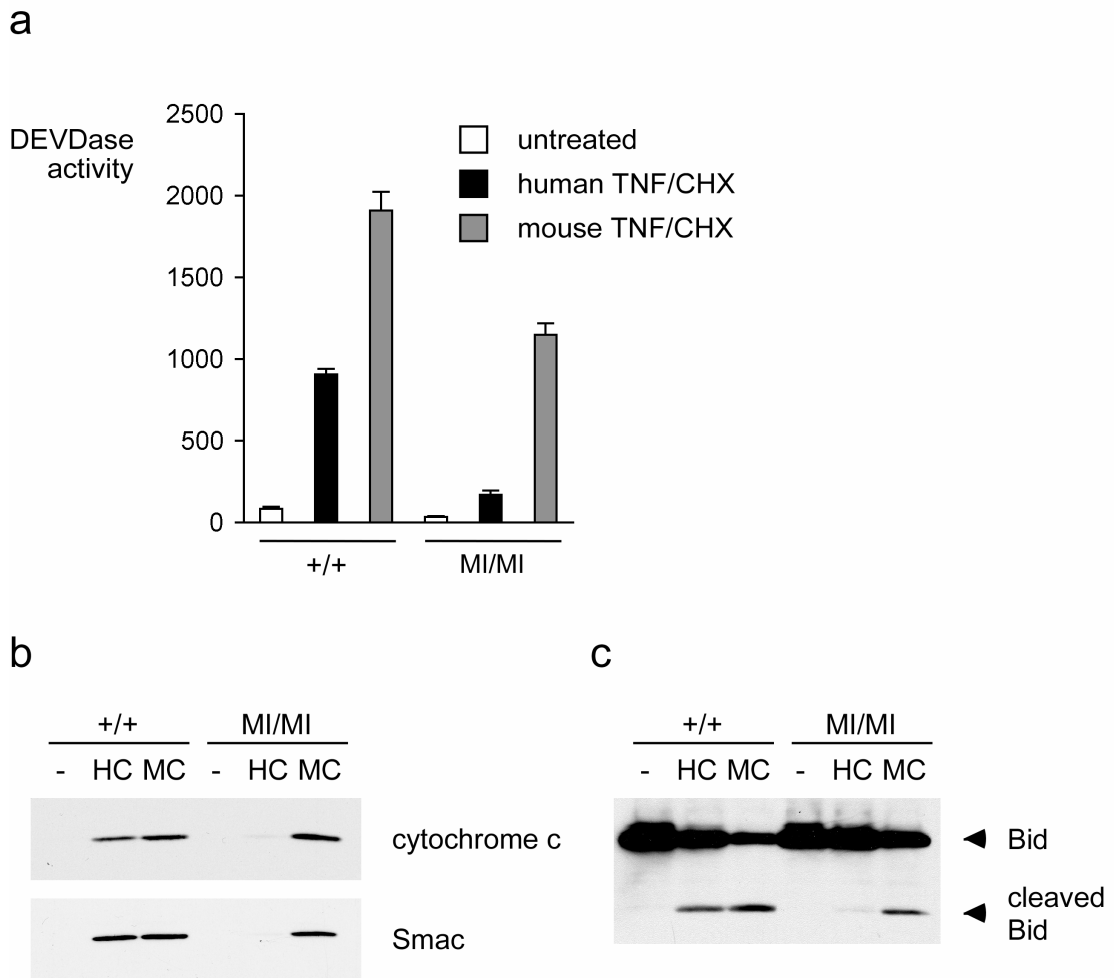
Figure 19. Differential response of wild-type and $Rb^{MI/MI}$ cells to human and mouse TNF

(a) Mouse but not human TNF induces DEVDase activity in $Rb^{MI/MI}$ cells. Wild-type and $Rb^{MI/MI}$ cells were treated with hTNF/CHX for 4 h. Equal amounts of protein from whole cell lysates were incubated with the fluorogenic caspase substrate Ac-DEVD-AMC for 30 min and fluorescence intensity was measured in triplicate samples. (b) Mouse but not human TNF induces release of cytochrome c and Smac from mitochondria in $Rb^{MI/MI}$ cells. Wild-type and $Rb^{MI/MI}$ cells were treated with hTNF/CHX for 5 h. Equal amounts of protein from cytosolic extracts were resolved by SDS-Page and cytochrome c and Smac were detected by immunoblotting. (c) Mouse but not human TNF induces cleavage of Bid in $Rb^{MI/MI}$ cells. Wild-type and $Rb^{MI/MI}$ cells were treated as in (b). Equal amounts of protein from whole cell lysates were resolved by SDS-Page and Bid was detected by immunoblotting.
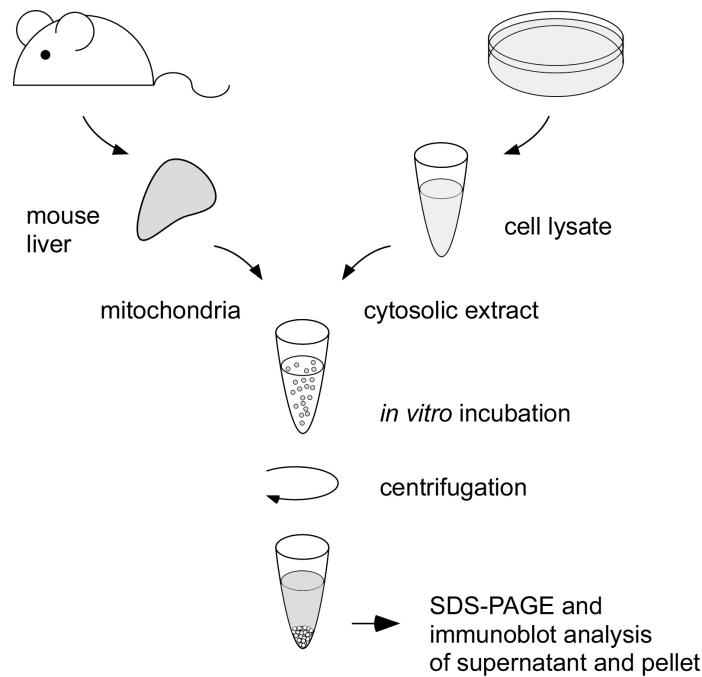
Figure 20. Outline of an *in vitro* cytochrome c release assay.
Mitochondria were isolated from mouse liver and incubated with cytosolic extracts prepared from cultured cells. Following incubation, mitochondria and cytosol were separated and each fraction was analyzed for the presence of cytochrome c.

In contrast, cytochrome c remained in the mitochondrial fraction after incubation with extracts from TNF-treated $Rb^{MI/MI}$ cells. The addition of recombinant truncated Bid ,termed NC-Bid (Kuwana *et al.* 2002), to the reaction was sufficient to induce cytochrome c release in the presence of $Rb^{MI/MI}$ cell extracts (Figure 21b, MI/MI lanes), consistent with the notion that the lack of tBid causes the absence of cytochrome c release in $Rb^{MI/MI}$ cells.

Moreover, titration of the cytochrome c release capacity of NC-Bid in the presence of extracts from hTNF-treated $Rb^{MI/MI}$ cells and untreated wild-type cells showed that there is no specific inhibitory activity in $Rb^{MI/MI}$ cells (Figure 21b, MI/MI vs. +/+ lanes). Finally, extracts from TNF-treated wild-type cells were able to efficiently induce cytochrome c release from mitochondria isolated from $Rb^{MI/MI}$ mice (Figure 21c, MI/MI mito), excluding the possibility that a mitochondrial defect prevents cytochrome c release in TNF-treated $Rb^{MI/MI}$ cells. Taken together, these results confirm the notion that in $Rb^{MI/MI}$ cells cytochrome c is not released in response to hTNF, because no truncated Bid is generated.

a

		+/+				MI/MI				
B	0	1	3	5	0	1	3	5	h hTNF/CHX

sup ──────────────── cytochrome c

pellet ──────────────── cytochrome c

b

	+/+		MI		MI/MI					+/+					
	-	+	-	+	+					-					
					5	10	20	50	100	5	10	20	50	100	nM NC-Bid

sup ──────────────── cytochrome c

pellet ──────────────── cytochrome c

c

	+/+ mito			MI/MI mito			
	0	3	6	0	3	6	h hTNF/CHX

sup ──────────────── cytochrome c

pellet ──────────────── cytochrome c
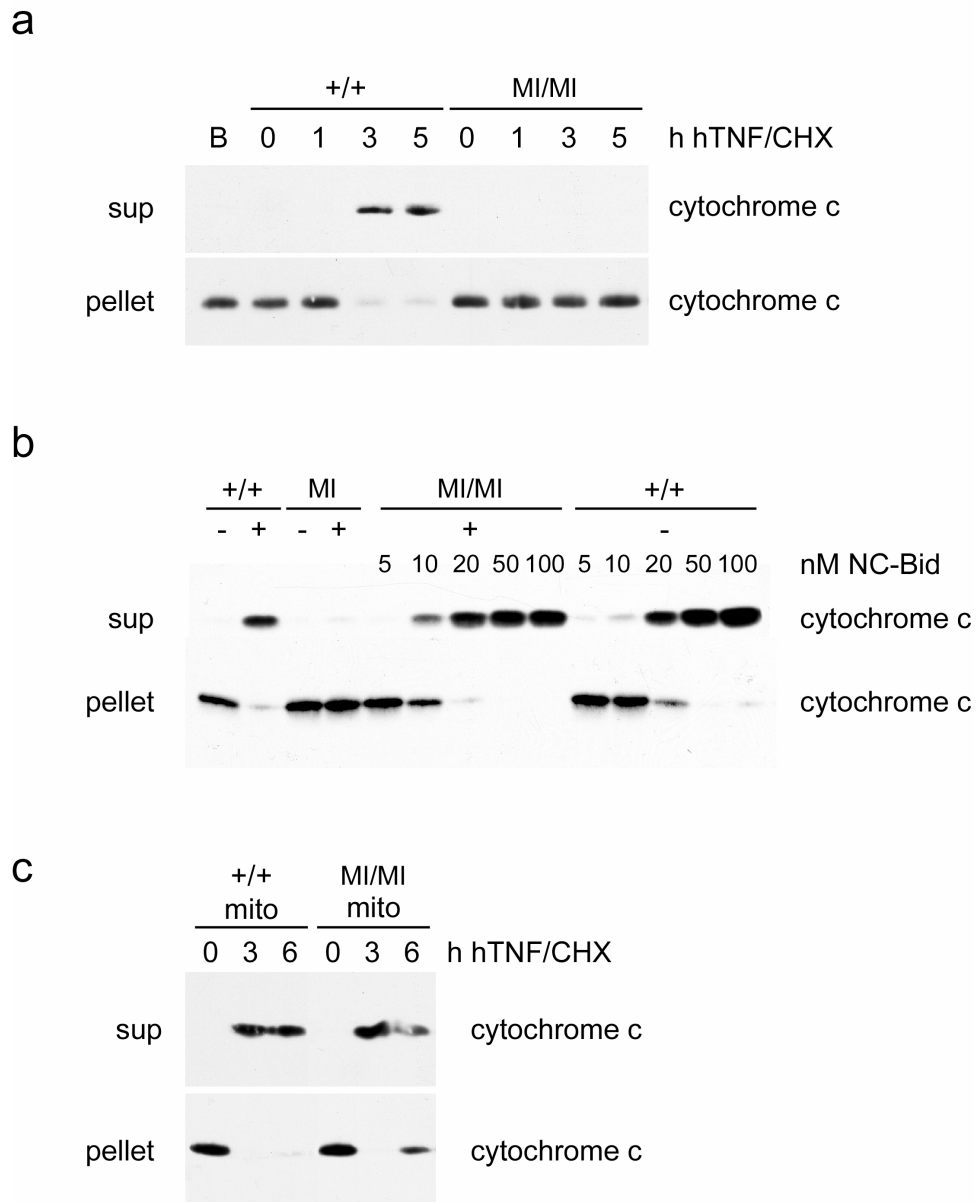
Figure 21. *In vitro* analysis of cytochrome c release

(a) Cytosolic extracts from hTNF-α-treated wild-type but not *Rb$^{MI/MI}$* cells induce cytochrome c release from mitochondria *in vitro*. Wild-type and *Rb$^{MI/MI}$* cells were treated with hTNF/CHX for the indicated times. Cytosolic extracts were prepared and incubated with mouse liver mitochondria for 45 min. Mitochondria were pelleted by centrifugation and supernatants and pellets analyzed for cytochrome c by immunoblotting. B, buffer (b) Recombinant truncated Bid (NC-Bid) can restore cytochrome c release activity in cytosolic extracts from hTNF-treated *Rb$^{MI/MI}$* cells. Wild-type and *Rb$^{MI/MI}$* cells were treated with hTNF/CHX for 3 h in the presence of the indicated concentrations of NC-Bid and analyzed for cytochrome c releasing activity as in (a). (c) Mitochondria from *Rb$^{MI/MI}$* mice release cytochrome c in the presence of cytosolic extracts from hTNF-α-treated wild-type cells. Wild-type cells were treated with hTNF/CHX for the indicated times. Cytosolic extracts were incubated with mitochondria isolated from wild-type (+/+ mito) or *Rb$^{MI/MI}$* (MI/MI mito) mice. Cytochrome c release was analyzed as in (a).

2.2.5   TNF dosage effects in *Rb^{MI/MI}* cells

The analysis of mTNF-treated *Rb^{MI/MI}* cells had shown that *Rb^{MI/MI}* cells are principally capable of cleaving Bid to induce mitochondria permeabilization (Figure 18b, c). Titration of TNF over a wide range of concentrations indicated that apoptosis could be triggered in *Rb^{MI/MI}* cells by high concentrations of TNF (Figure 22a). While *Rb^{MI/MI}* cells were resistant to 10 ng/ml hTNF, a ten-fold higher dose induced cell death in almost 60% of *Rb^{MI/MI}* cells compared to nearly 80% in wild-type cells (Figure 22a). This observation suggests that TNF concentration, sensed via the number of ligated TNF receptors per cell, can qualitatively alter the cellular response to TNF.

Upon ligand binding, TNF receptors are internalized by vesicle-mediated endocytosis. Interestingly, the TNF-induced internalization of TNFR1 was recently shown to be a pre-requisite for the induction of apoptosis by TNF (Schneider-Brachert *et al.* 2004). Altered membrane dynamics at low temperatures allow binding of TNF to its receptor, but prevent receptor internalization, thus leading to the accumulation of ligand-receptor complexes on the cell surface. When TNF-receptor triggering was synchronized by this pre-loading of TNF receptors, the dose response curve for TNF-induced death at 37°C was shifted to lower concentrations in both wild-type and *Rb^{MI/MI}* cells (Figure 22b): for wild-type cells the death curve now already nearly reached a plateau at 10 ng/ml hTNF. In *Rb^{MI/MI}* cells, ca. 30 ng/ml hTNF were enough to induce about 75% of the cell death level seen in wild-type cells after synchronized triggering of pre-loaded receptors. Consistently, synchronized TNFR activation induced effector caspase activity in both wild-type and *Rb^{MI/MI}* cells (Figure 22c), while *Rb^{MI/MI}* cell extracts had been devoid of caspase activity after treatment with low doses of hTNF (Figure 19a). Activation of caspase-3 by synchronized TNFR triggering could also be detected in both wild-type and *Rb^{MI/MI}* cells by substrate affinity labeling. To this end, cell lysates were incubated with biotin-z-VAD-fmk *in vitro*. Active caspase-3 irreversibly binds to biotin-z-VAD-fmk and can be precipitated with streptavidin-conjugated sepharose and detected by immunoblotting (Figure 19d). Both assays indicated that effector caspase activation in *Rb^{MI/MI}* cells by synchronized TNFR-triggering did not reach wild-type levels.
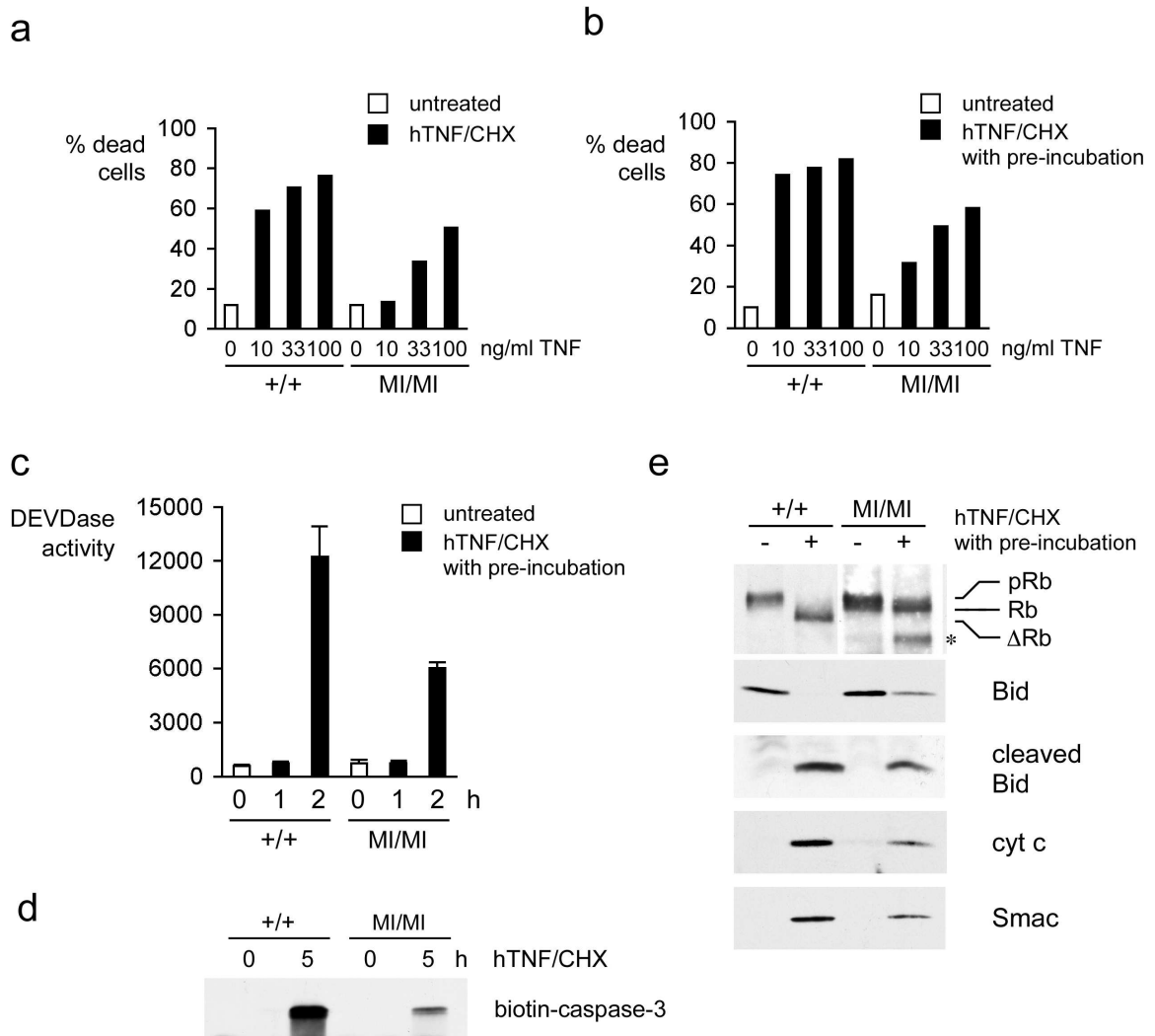
Figure 22. Mitochondria-mediated apoptosis is induced by synchronized activation of TNF receptors in $Rb^{MI/MI}$ cells

(a) Protection from cell death is dose dependent in $Rb^{MI/MI}$ cells. Wild-type and $Rb^{MI/MI}$ cells were treated with the indicated doses of hTNF/CHX for 24 h and cell death was quantified by analysis of PI uptake. (b) Synchronized TNF receptor triggering shifts TNF dose response curve. Cells were first incubated with the indicated doses of hTNF/CHX at 4°C for 90 min, then shifted to 37°C for 24 h. Cell death was analyzed as in (a). (c, d) Synchronized TNF receptor triggering induces caspase activation in $Rb^{MI/MI}$ cells (c) Wild-type and $Rb^{MI/MI}$ cells were pre-incubated with 33 ng/ml hTNF/CHX at 4°C for 90 min, then shifted to 37°C for the indicated times. Caspase activity was measured with the fluorogenic substrate assay described in Figure 5. (d) Wild-type and $Rb^{MI/MI}$ cells were first incubated with 33 ng/ml hTNF/ CHX at 4°C for 90 min, then shifted to 37°C for 5 h. Lysates were incubated with biotin-z-VAD-fmk and biotin-labeled active caspase-3 was precipitated with streptavidin-conjugated sepharose and detected by immunoblotting. (e) Synchronized TNF receptor triggering induces mitochondria-dependent apoptosis in the presence of Rb-MI. Cells were treated as in (d). Rb was immunoprecipitated from whole cell lysates and detected by immunoblotting. Whole cell lysates were analyzed for Bid; cytosolic extracts were analyzed for cytochrome c (cyt c) and Smac. ∗ indicates an Rb fragment resulting from an unknown cleavage event.

Analysis of $Rb^{MI/MI}$ cell lysates after high dose or synchronized TNF treatment confirmed that death was induced via the mitochondria apoptosis pathway (Figure 22d): truncated Bid was detected and Smac and cytochrome c appeared in the cytosolic fraction. Importantly, after the same treatment, intact Rb-MI protein could be detected after immunoprecipitation from whole cell lysate (Figure 22d). The observation that apoptosis under this condition proceeded slower in $Rb^{MI/MI}$ cells than in wild-type cells (Figure 19 and 22) is consistent with the notion that induction of apoptosis in $Rb^{MI/MI}$ cells after high dose or synchronized TNF treatment was not due to degradation of Rb-MI, but proceeded despite an inhibitory effect of Rb-MI.

Taken together, these results suggested that the mitochondria apoptosis pathway, which is induced by hTNF in wild-type fibroblasts, is intact in $Rb^{MI/MI}$ cells and can induce cell death. However, the threshold for activation of the mitochondria pathway in response to TNF was considerably higher in $Rb^{MI/MI}$ cells than in wild-type cells. Thus, apoptosis of $Rb^{MI/MI}$ cells required a stronger death stimulus. In the case of TNF signaling, signal strength is apparently determined by the number of TNF receptors triggered simultaneously on one cell. The crucial point for activation of the mitochondrial apoptosis pathway in $Rb^{MI/MI}$ cells seemed to be the induction of caspase-8 mediated Bid cleavage.

To test, if caspase-8 activity was impaired in Rb-MI cells, IETDase activity was measured in hTNF-treated $Rb^{MI/MI}$ cell extracts using the fluorogenic substrate Ac-IETD-AFC (Figure 23). Indeed, human TNF induced IETDase activity in wild-type, but not in $Rb^{MI/MI}$ cells (Figure 23a). In contrast, mouse TNF induced IETDase activity in cells of both genotypes. When cells were treated with high doses of TNF following a 4°C pre-incubation, hTNF-induced IETDase activity was observed in both wild-type and $Rb^{MI/MI}$ cells (Figure 23b). Thus, induction of IETDase activity correlated with the generation of tBid and induction of caspase-3 activity (Figure 18b), suggesting that insufficient caspase-8 activation in hTNF treated $Rb^{MI/MI}$ cells prevents tBid-induced activation of the mitochondria apoptosis pathway. Analysis of caspase-8 activation via affinity labeling proved unfeasible, most likely because the concentration of active caspase-8 molecules was below the detection limit of the assay.
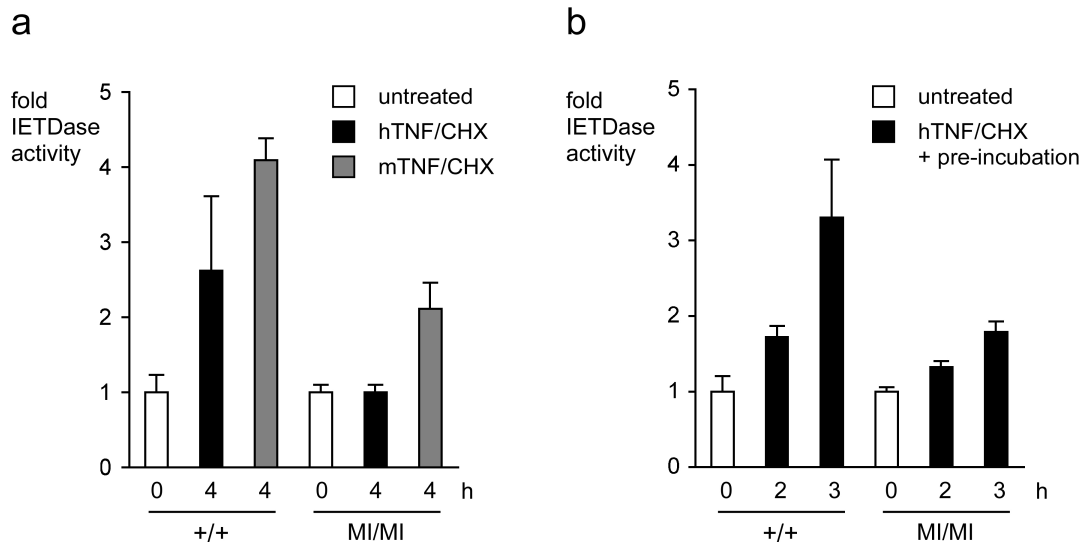
Figure 23. IETDase activity in TNF-treated wild-type and $Rb^{MI/MI}$ cells

(a) IETDase activity in TNF-treated wild-type and $Rb^{MI/MI}$ cells. Cells were incubated with 10 ng/ml hTNF plus CHX. For each time point, equal amounts of protein from whole cell lysates were incubated with the fluorogenic caspase-8 substrate Ac-IETD-AFC for 30 min and fluorescence intensity was measured. The fold increase in IETDase activity was determined compared to untreated control cells. (b) Synchronized TNF receptor triggering induces caspase-8 activation in $Rb^{MI/MI}$ cells. Wild-type and $Rb^{MI/MI}$ cells were first incubated with 33 ng/ml hTNF plus CHX at 4°C for 90 min, then shifted to 37°C for the indicated times. For each time point, the fold increase in IETDase activity was determined as in (a)

2.2.6   Effect of caspase inhibition on TNF response in wild-type and $Rb^{MI/MI}$ cells

To complement the results of the *in vitro* caspase activity assays, the effect of peptide caspase inhibitors on TNF-induced cell death *in vivo* was analyzed. Synthetic peptide substrates function as irreversible inhibitors of caspase enzymes if they are modified with a fluoromethylketone (fmk) group. The fmk group forms a covalent bond with the reactive cysteine in the active site of the caspase, thereby inactivating the enzyme. Members of the caspase family differ in their substrate preferences due to their different affinity to specific tetra-peptide sequences (Thornberry *et al.* 2000). Therefore, selected tetrapeptide substrates act as more or less specific inhibitors of caspase family members (Stennicke and Salvesen 1999) and can be used to assess the contribution of different caspases to an apoptotic response. The effect of caspase-8 inhibitor (z-IETD-fmk), caspase-2 inhibitor (z-VDVAD-fmk) and the broad-spectrum

caspase inhibitor z-VAD-fmk (zVAD) on TNF-induced cell death is shown in Figure 24. All three inhibitors reduced the levels of hTNF-induced death on wild-type cells (Figure 24a, +/+). zVAD had the most pronounced effect, which is consistent with its ability to inhibit caspase-8, -9 and -3. zVAD is a poor inhibitor of caspase-2 in vivo (Troy and Shelanski 2003). The combined application of caspase-2 inhibitor and zVAD could reduce cell death levels more than zVAD alone, suggesting a contributing role for caspase-2 in TNF-induced cell death in these cells.

Surprisingly, caspase-8 inhibitor and z-VAD-fmk both sensitized $Rb^{MI/MI}$ cells to apoptosis induced by human TNF (Figure 24a, MI/MI). Caspase-2 inhibitor had no effect alone, but seemed to increase cell death synergistically with zVAD. Taken together, these results indicate that both caspase-8 and caspase-2 are involved in the apoptosis response to TNF in wild-type cells. Under conditions of caspase-8 inhibition, cell death in response to hTNF unexpectedly occurs in $Rb^{MI/MI}$ cells. Treatment of cells with high dose of TNF following 4°C pre-incubation, did not change the effect of caspase-8 inhibitor and zVAD in wild-type cells (Figure 24b +/+). Since $Rb^{MI/MI}$ cells are sensitive to high doses of hTNF, addition of caspase-8 inhibitor or zVAD did not significantly increase cell death under these conditions (Figure 24b, MI/MI).

To see, if $Rb^{MI/MI}$ cells, sensitized to hTNF/CHX treatment under conditions of caspase-8 inhibition, die in the presence of intact Rb-MI protein Rb-protein levels after hTNF/CHX and zVAD treatment were analyzed (Figure 24c). Rb-MI was stable after hTNF/CHX treatment, irrespective of the addition of zVAD (Figure 24c, MI/MI). Surprisingly, addition of zVAD could not prevent hTNF-induced cleavage of wild-type Rb, but rather enhanced its degradation (Figure 24c, +/+). This result is in contrast to the ability of zVAD to prevent Rb cleavage *in vitro* (Tan and Wang 1998), and indicates that in addition to effector caspases other proteases are activated by TNF *in vivo*, which, at least under conditions of caspase inhibition, are responsible for the elimination of Rb. As a control for the caspase inhibitory effect of zVAD, levels of cleaved Parp and Bid were analyzed in parallel. TNF-induced cleavage of Parp and Bid in wild-type cells was efficiently inhibited by zVAD (Figure 24c, +/+).
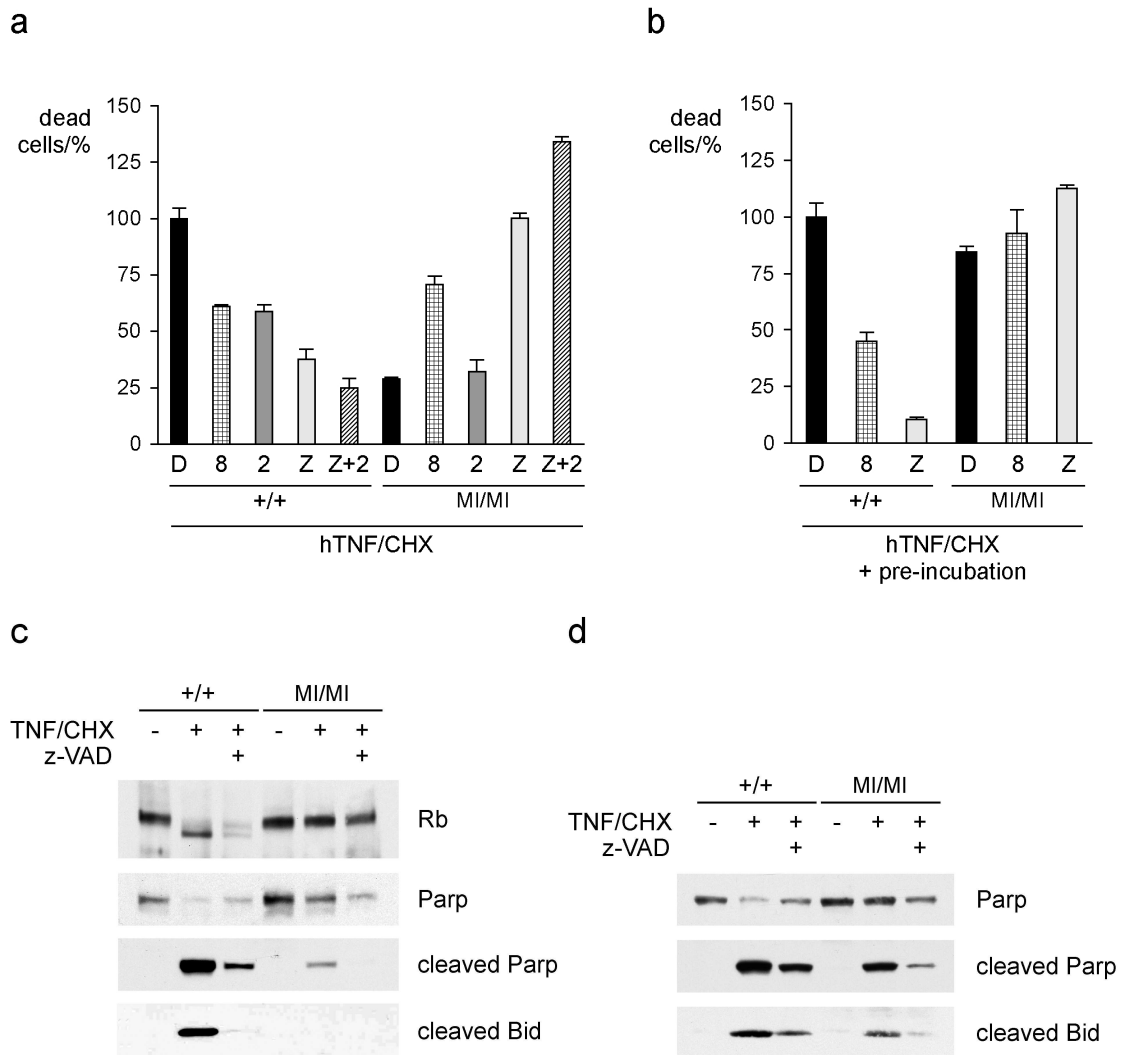
Figure 24. Effect of caspase inhibitors on TNF–induced apoptosis

(a) Caspase inhibition has diverse effect on TNF-induced cell death in wild-type and $Rb^{MI/MI}$ cells. Cells were incubated with 10 ng/ml hTNF plus CHX and the indicated caspase inhibitors (D, DMSO control; 8, z-IETD-fmk; 2, z-VDVAD-fmk; Z, z-VAD-fmk) for 16 h and cell death was quantified by flow cytometry analysis of propidium iodide (PI) uptake. (b) Synchronization of TNF receptor activation does not change the effect of caspase inhibition on TNF-induced cell death. Wild-type and $Rb^{MI/MI}$ cells were first incubated with 33 ng/ml hTNF plus CHX and the indicated caspase inhibitors at 4°C for 90 min, then shifted to 37C for 16 h. Cell death was analyzed as in (a). (c) Caspase inhibition prevents TNF-induced cleavage of Parp and Bid but not Rb degradation. Wild-type and $Rb^{MI/MI}$ cells were incubated as indicated with 10 ng/ml hTNF plus CHX with or without z-VAD-fmk for 5 h. Rb was immunoprecipitated from whole cell lysates and detected by immunoblotting. Whole cell lysates were analyzed for Parp and Bid. (d) Cleavage of Parp and Bid after synchronized TNFR activation are inhibited by z-VAD-fmk. Wild-type and $Rb^{MI/MI}$ cells were first incubated with 33 ng/ml hTNF plus CHX with or without z-VAD-fmk at 4°C for 90 min, and then shifted to 37°C for 5 h. Whole cell lysates were analyzed for Parp and Bid.

Moreover, the absence of Parp and Bid cleavage in TNF/ZVAD treated $Rb^{MI/MI}$ cells (Figure 24c, MIMI) suggests that these cells do not die by mitochondria-dependent apoptosis. After treatment with apoptosis-inducing doses of TNF following pre-incubation, zVAD prevented cleavage of Parp and Bid in $Rb^{MI/MI}$ cells as well as in wild-type cells (Figure 24 d). This inhibitory effect was not as complete as after low doses of TNF, most likely because caspase activity reached much higher levels. Again, $Rb^{MI/MI}$ cells died after the combined treatment with hTNF/CHX and zVAD, while Parp and Bid cleavage were inhibited under these conditions (Figure 24d, last lane). Taken together, these results confirm the importance of caspase-8 activity for TNF induced apoptosis in wild-type and $Rb^{MI/MI}$ cells. Under conditions of caspase inhibition, an alternative cell death pathway is activated in $Rb^{MI/MI}$ cells.

3   Discussion

Cellular proliferation and death are subject to intricate regulation at several levels. The commitment of a cell for replication, differentiation or apoptosis is the integrated response to multiple signals, which are received from the cells environment or are generated within the cell itself. One important mode of regulating the process of apoptosis is transcriptional and post-translational control of pro- and anti-apoptotic proteins by cell death and survival signaling pathways. In addition, recent evidence suggests that the apoptotic core machinery - the proteolytic caspase activation cascade - can be inherently controlled by the cleavage of effector caspase substrates (Chau and Wang 2003). The expression of caspase-cleavage resistant variants of certain key caspase substrates, including RIP, IKK and the Retinoblastoma protein, has been shown to protect cells from efficient caspase activation during death receptor-induced apoptosis (Lin *et al.* 1999; Tang *et al.* 2001; Chau *et al.* 2002), suggesting that cleavage of these substrates regulates an important positive feedback loop in this pathway (described in Figure 25).

A role for RB in the inhibition of apoptosis was first suggested by the phenotype of Rb-deficient mice and is now supported by many lines of evidence (Harbour 2000; Chau and Wang 2003). Thus, the Rb protein has an intriguing dual role in the control of cellular proliferation, as an inhibitor of both cell growth and death. While the pathway of RB-mediated cell cycle regulation has been resolved, the mechanism of apoptosis suppression by RB is not fully understood. There is ample evidence that Rb suppresses apoptosis during embryonic development by controlling E2F1-regulated apoptotic gene expression (Tsai *et al.* 1998; Guo *et al.* 2001; Moroni *et al.* 2001; Muller *et al.* 2001; Simpson *et al.* 2001). In contrast, the role of E2F-dependent suppression of apoptosis genes by Rb in developmentally mature cells remained unclear. Moreover, the fundamental question, whether the apoptosis suppressing activity of RB generally depends on the regulation of gene expression or if RB can act through a transcription-independent mechanism to inhibit apoptosis, has not been resolved. Finally, it remains to be elucidated if and how the growth and apoptosis suppressing activities of RB can be separately regulated.
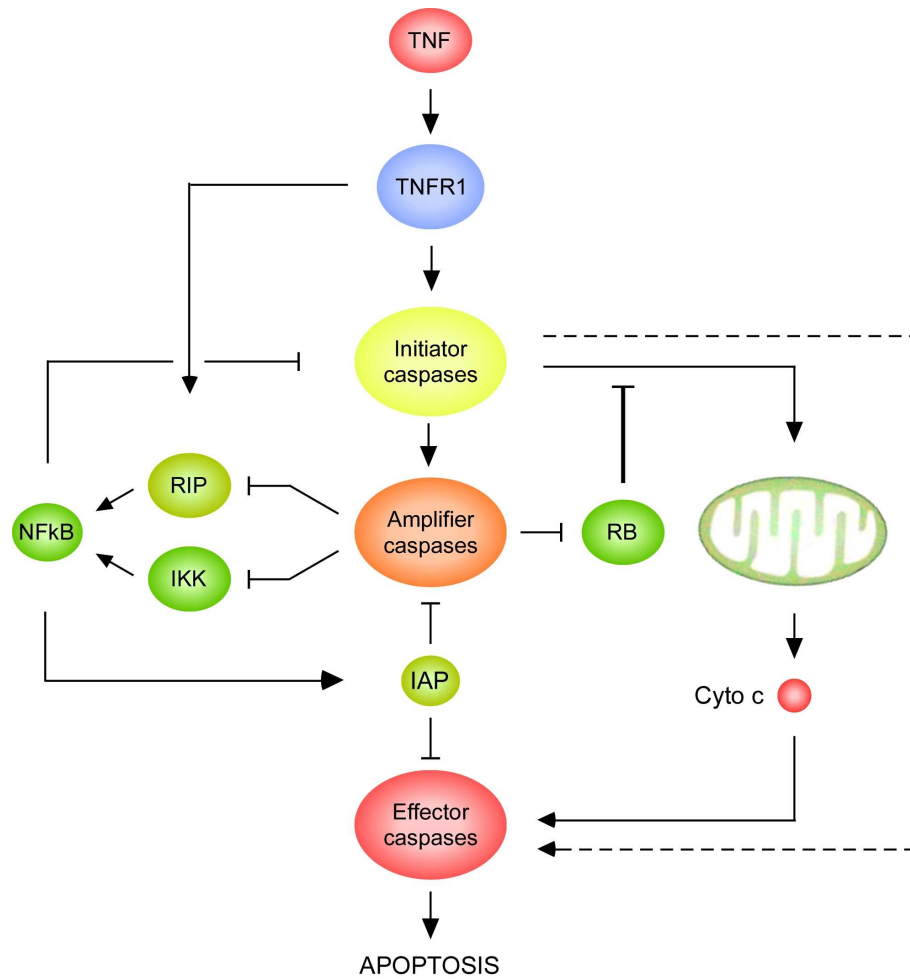
Figure 25. Caspase-mediated amplification of a death receptor-generated apoptosis signal

The activation of RIP and IKK by TNFR1 first activates an NF-κB-dependent survival pathway, which promotes the expression of anti-apoptotic proteins like IAPs. RB inhibits mitochondria permeabilization by an unknown mechanism. Receptor-activated initiator caspases activate amplifier caspases whose function is to inactivate regulatory proteins, such as RIP, IKK and RB. Inactivation of these key substrates by caspase cleavage leads to amplification of caspase activity and eventually to apoptotic cell death.

3.1 Rb-MI-dependent suppression of apoptosis in $Rb^{MI/MI}$ fibroblasts

In this study the mechanism of apoptosis suppression by caspase-resistant Rb (Rb-MI) was investigated in fibroblasts derived from $Rb^{MI/MI}$ "knock-in" mice. In these cells, mutation of the conserved C-terminal caspase cleavage site prevented Rb-MI degradation in response to TNFR1 activation and specifically protected cells from TFNR1-induced apoptosis, indicating that Rb degradation is required for TNFR1 to activate apoptosis (Chau *et al.* 2002) and this work). Interestingly, Rb-MI was not protected from degradation after simultaneous activation of TNFR1 and TNFR2 and the loss of Rb-MI correlated with normal sensitivity to apoptosis in response to this stimulus. This phenotype provided an internal control for the identification of Rb-MI-dependent changes in the apoptosis response of $Rb^{MI/MI}$ cells.

Significantly, in this model system, the growth suppressing activity of RB could be separated from the suppression of apoptosis: while cell cycle progression was unaffected in $Rb^{MI/MI}$ fibroblasts, the presence of Rb-MI protected these cells from TNFR1-induced cell death. Thus, Rb-MI can at the same time be inactive as an inhibitor of cell cycle progression and active as an inhibitor of apoptosis, suggesting that these are independent activities, which may be regulated by distinct mechanisms. Further indication for a separate regulation of RB's apoptosis suppressing function is provided by the spectrum of mutations in the RB pathway that are found in human malignancies. Genes involved in the RB-dependent growth suppression pathway, such as *p16(INK4a)* and *cyclin D1* are frequently mutated in human cancers, while mutations in *RB* itself are rare (Sherr 1996). Intriguingly, in some tumors RB is expressed at a very high level and is at the same time inactivated by constitutive hyperphosphorylation. This suggests that the presence of RB confers a selective advantage during tumor development, if its growth suppressing function is turned of. This advantage may be the suppression of apoptosis, which might be selectively retained via site-specific phosphorylation.

Assuming a separation of apoptosis and cell cycle regulation by RB, two possible mechanisms can be distinguished through which RB could carry out its opposing functions independently 1) RB might be able to specifically suppress cell cycle genes or apoptosis related genes via differential action on specific promoters; or alternatively, 2) apoptosis suppression by RB might be independent from

transcriptional regulation. To distinguish between these possibilities, a microarray analysis of TNF-treated $Rb^{MI/MI}$ cells was conducted. Changes in the expression of apoptosis-related genes were compared after stimulation of TNFR1 by human TNF (associated with intact Rb-MI and cell survival) and stimulation of TNFR1 and 2 by murine TNF (leading to degradation of Rb-MI and cell death). This comprehensive analysis of TNF-induced changes in gene expression gave no indication for the suppression of pro-apoptotic genes by Rb-MI. The same set of apoptosis-related genes was induced by TNF in cells that maintained active Rb-MI, and in those in which Rb-MI was inactivated upon TNF treatment (Figure 17). This result suggests, that Rb-dependent changes in gene expression cannot account for the protection of $Rb^{MI/MI}$ cells from TNF-induced apoptosis.

3.2 Post-transcriptional suppression of mitochondrial apoptosis by Rb-MI

The normal gene expression profile of TNF-resistant $Rb^{MI/MI}$ cells indicated that RB can function as a post-transcriptional regulator of apoptosis. To identify possible execution points for the anti-apoptotic activity of Rb-MI, a stepwise analysis of TNF-induced activation of the mitochondrial apoptosis pathway was conducted in $Rb^{MI/MI}$ cells. The analysis of caspase-3 processing and caspase-3 type protease activity showed that $Rb^{MI/MI}$ cells were deficient in effector caspase activation after TNFR1 stimulation by human TNF (hTNF). This defect correlated with the absence of mitochondria permeabilization, since neither cytochrome c nor Smac could be detected in the cytosol of hTNF-treated $Rb^{MI/MI}$ cells. Thus, in these cells, TNFR1-induced activation of effector caspases depended on cytochrome c release from the mitochondria and apoptosome-formation. The requirement for mitochondria permeabilization in death receptor induced apoptosis has been reported previously for a number of cell types classified as "type II cells" based on this phenotype (Scaffidi *et al.* 1998). Mitochondria-mediated caspase activation by death receptors is achieved via cleavage of Bid by caspase-8 (Li *et al.* 1998; Luo *et al.* 1998). The resulting truncated Bid, known as tBid, translocates to the mitochondrial membrane where it initiates changes in membrane permeability via interaction with BAX or BAK (Desagher *et al.* 1999; Wei *et al.* 2001).

In correlation with the absence of cytochrome c and Smac release from mitochondria, no tBid could be detected in hTNF-treated $Rb^{MI/MI}$ cells. Consistently,

cytosolic extracts from these cells were devoid of cytochrome c releasing activity in an *in vitro* assay. Complementation of non-release-inducing extracts from hTNF-treated *Rb^{MI/MI}* cells with recombinant cleaved Bid was sufficient to confer normal cytochrome c release activity, indicating that the susceptibility to BH3 protein-induced changes in membrane permeability is not altered in *Rb^{MI/MI}* cells. Thus, the expression of Rb-MI does not seem to affect the ratio of BAX/BAK proteins and BCL-2 proteins. Moreover, the capability of recombinant cleaved Bid to induce cytochrome c release from mitochondria isolated from *Rb^{MI/MI}* mice, confirmed that the defect in the TNF response of *Rb^{MI/MI}* cells does not lie within the mitochondria. Taken together, these results are consistent with the notion that impaired tBid generation was responsible for cytochrome c release deficiency and absence of mitochondria-mediated apoptosis in hTNF-treated *Rb^{MI/MI}* cells.

Impaired tBid generation, in turn, may be the result from insufficient caspase-8 activation. Indeed, in an enzymatic assay, caspase-8 like protease activity could be detected in hTNF-treated wild-type, but not *Rb^{MI/MI}* cells. However, even in wild-type cells, levels of active caspase-8 were too low to be detected by *in vivo* affinity labeling, which prevented a direct comparison of caspase-8 activity in wild-type and *Rb^{MI/MI}* cells. Thus, the possibility of impaired caspase-8 activation in *Rb^{MI/MI}* cells awaits further proof. Interestingly, *Rb^{MI/MI}* cells remain sensitive to DNA damage-induced apoptosis, although the Rb-MI protein is maintained in this condition (Chau *et al.* 2002). This suggests that Rb-MI does not generally block the mitochondrial apoptosis pathway. Rather, the inhibition of mitochondria-dependent apoptosis seems to be a signal dependent effect, impeding, for instance, the TNFR1 signaling pathway.

Taken together, the results of the present study are consistent with the notion that Rb-MI inhibits an early, signal-specific step in mitochondria-mediated caspase activation. It had previously been shown that simultaneous stimulation of both TNFR1 and TNFR2 by murine TNF (mTNF) induced cleavage and degradation of the Rb-MI protein and death of *Rb^{MI/MI}* cells (Chau *et al.* 2002). In this work, previous observations could be extended to support the notion that after degradation of Rb or Rb-MI, death of both wild-type and *Rb^{MI/MI}* cells is mediated by activation of the mitochondria apoptosis pathway. Stimulation of both TNFR1 and TNFR2 by mTNF induced cleavage of Bid, the release of cytochrome c and Smac from the mitochondria, and caspase activity. Thus, the inhibition of the mitochondria apoptosis pathway in *Rb^{MI/MI}* cells is relieved by the loss of Rb-MI (Table 2). This observation

	+/+			MI/MI		
	Rb	tBid	death	Rb-MI	tBid	death
hTNF low	-	+	+	+	-	-
hTNF high	-	+	+	+	+	+
hTNF low + zVAD	-	-	-	+	-	+
hTNF high + zVAD	ND (-)	-	-	ND (+)	-	+
mTNF	-	+	+	-	+	+

Table 2. Summary of the effects of different TNF treatment conditions in wild-type and $Rb^{MI/MI}$ fibroblasts (-, degraded/not observed; +, intact/observed, ND, not determined)

confirms that the inhibition depends on the presence of Rb-MI and thus rules out the possibility that genetic changes were selected during the establishment of immortalized 3T3 $Rb^{MI/MI}$ cell lines that prevent activation of mitochondrial apoptosis by TNF.

Which segment of the mitochondria apoptosis pathway is affected by Rb-MI could be further defined by the observation that the resistance of $Rb^{MI/MI}$ cells to TNFR1-induced apoptosis is not absolute, but depends on the strength of the stimulus, *i.e.* the dose and application scheme of TNF. Accumulation and simultaneous activation of pre-loaded TNFR1 receptor complexes was shown to activate the mitochondria apoptosis pathway in $Rb^{MI/MI}$ cells (Table 2, hTNF high). This occurred without cleavage or degradation of Rb-MI. Thus, even the signal-dependent inhibition of TNFR1-induced apoptosis in $Rb^{MI/MI}$ cells can be overcome without eliminating Rb-MI. In addition, TNFR1-induced activation of NF-κB and Jun/AP-1 signaling pathways was unimpaired in $Rb^{MI/MI}$ cells. These results indicate that the initial signal transduction by activated TNFR1 is not impaired in $Rb^{MI/MI}$ cells. TNFR1 is principally capable of inducing mitochondria-mediated apoptosis $Rb^{MI/MI}$ cells, but the threshold for mitochondria-dependent caspase activation in response to TNF is higher than in wild-type cells.

Taken together, the results from this study place the Rb-MI sensitive step of TNF-induced apoptosis between the formation of a TNF receptor signaling complex and caspase-8 mediated cleavage of the BH3-only protein Bid (Figure 26). Rb-MI seems to constitute a roadblock in the pathway for TNFR1-induced apoptosis

activation that can be removed by either inactivating Rb-MI – as during combined TNFR1 and TNFR2 signaling – or bypassing Rb-MI – as during synchronized TNFR1 triggering - (Table 2).

3.2.1   Role of nucleo-cytoplasmic signaling during TNF-induced apoptosis

While survival gene expression has been shown to have a major impact on death receptor induced cells death, the regulation of death receptor induced apoptosis by nuclear signaling events that are independent from the regulation of gene expression may be unexpected. How Rb-MI in particular can interfere with the initiation of the mitochondria apoptosis pathway by the TNF receptor is not obvious. However, recent studies of apoptosis induction by TNFR1 revealed a multi-step pathway that can be subject to manifold modulation: caspase-8 activation by TNFR1 does not occur at the plasma membrane-associated DISC, but in a cytoplasmic complex, termed complex II (Micheau and Tschopp 2003). This complex forms only after a TRADD-based complex dissociates from the receptor and recruits FADD in the cytoplasm. FADD in turn recruits pro-caspase-8 to the complex, thus initiating caspase activation.

Moreover, TNF-induced apoptosis induction has recently been shown to require internalization of ligand-bound TNFR1 (Schneider-Brachert *et al.* 2004). The same study indicated that caspase-8 and FADD associate with the receptor within a few minutes (Schneider-Brachert *et al.* 2004). Since this interaction was not detected by two similar studies (Harper *et al.* 2003; Micheau and Tschopp 2003) it is presumably transient or instable and may thus be insufficient for caspase-8 activation. The internalized TNF receptor is sorted into vesicles and eventually targeted for degradation in lysosomes (Schneider-Brachert *et al.* 2004). Thus, caspase-8 activation in a cytoplasmic complex, separated from the receptor might prevent caspase-activating complexes from sharing the fate of receptors targeted for degradation.

In summary, the activation of caspase-8 is uncoupled from receptor activation in a both spatial and temporal sense. Caspase activation and apoptosis are optional downstream events that seem to require post-translational modifications of death domain adaptor proteins (Micheau and Tschopp 2003). Thus, several steps required for TNF-induced caspase-8 activation might be subject to regulation by Rb-MI. For example, Rb-MI might sequester adaptor proteins like FADD in the nucleus, thereby

limiting their availability for complex formation and impeding the recruitment of caspase-8 to an activating signaling complex. Interestingly, both FADD and TRADD have been shown to shuttle between nucleus and cytosol (Morgan *et al.* 2002; Gomez-Angelats and Cidlowski 2003; Screaton *et al.* 2003). Other steps that may be subject to control by Rb-MI are the sorting of internalized TNFR1 complexes into vesicles and the dissociation of adaptor proteins from the receptor (Figure 26). Rb-MI may inhibit enzymes responsible for post-translational modification of adaptor proteins involved in these processes, thereby regulating their localization or modulating their activity. Alternatively, Rb-MI might prevent interaction of active caspase-8 with Bid by controlling Bid localization or accessibility. Full-length BID has recently been reported to be associated with endosomal compartments in non-apoptotic cells, suggesting a non-random distribution of the protein (Heinrich *et al.* 2004). Consistent with a transcription-independent function, RB has been shown to interact with a plethora of different cellular proteins (Morris and Dyson 2001) and to regulate the activity of several kinases that are involved in apoptosis regulation, such as c-Abl (Wang 2000; Chau *et al.* 2004).

In summary, the detailed analysis of apoptosis suppression in $Rb^{MI/MI}$ fibroblast revealed a previously unrecognized function of RB as a post-transcriptional regulator of caspase activation and apoptosis. The data suggest that in $Rb^{MI/MI}$ cells, mitochondria permeabilization during TNF-induced apoptosis signaling requires accumulation of caspase-8 activity or tBid levels, which is inhibited by Rb-MI. Presumably, once the critical level of caspase-8 activity or cleaved Bid is reached, the presence of Rb-MI does no longer interfere with the progression of apoptosis. This notion is consistent with the observation that $Rb^{MI/MI}$ cells do not activate mitochondrial apoptosis in response to TNF as readily as wild-type cells, but are capable of activating this pathway in response to high levels of TNFR1 activity. The precise mechanism by which Rb interferes with caspase-8 function during TNF signaling remains to be elucidated.
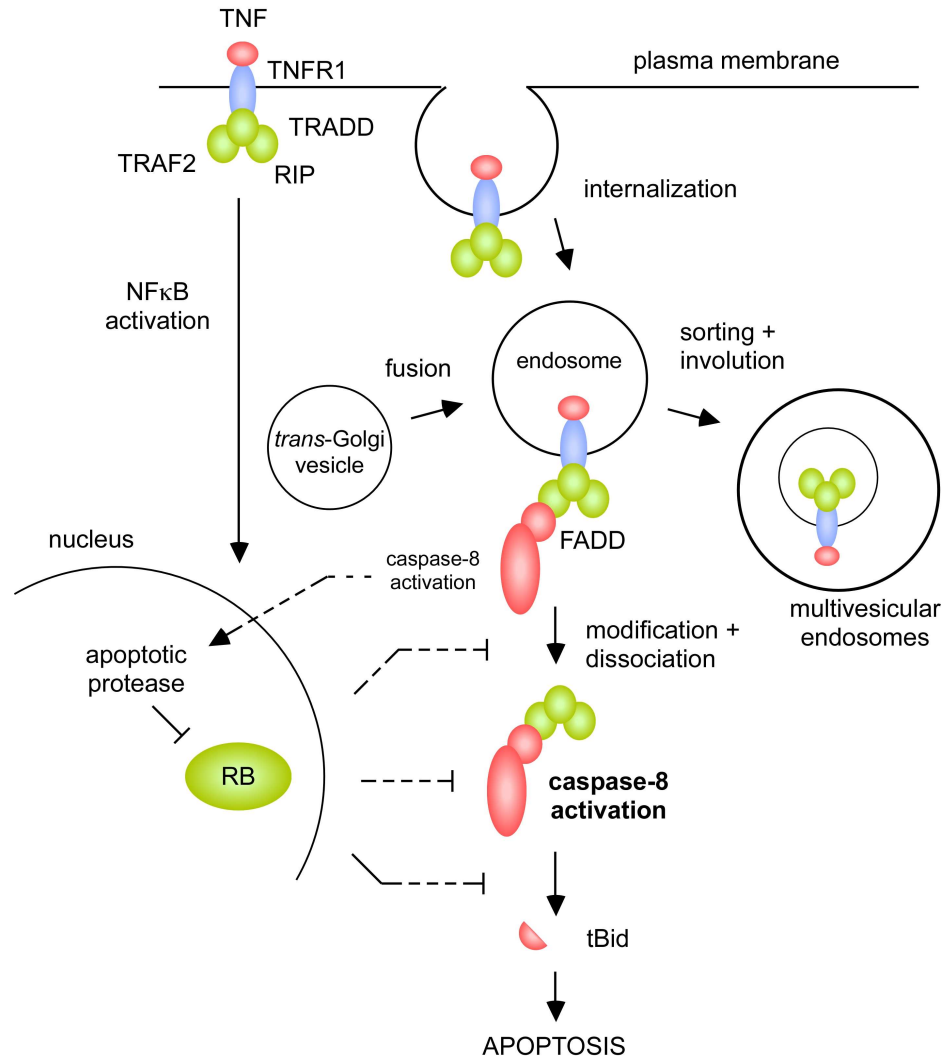
Figure 26. TNFR1 activation of apoptosis is a multi-step process that requires internalization of ligand-receptor complexes. RB presumably suppresses TNF-induced apoptosis by inhibiting one of several steps leading to TNFR1-induced caspase-8 activation and Bid cleavage.

3.2.2 Caspase-independent cell death in TNF treated *Rb*$^{MI/MI}$ fibroblasts

Consistent with the pivotal role of caspase-8 for TNFR1-induced apoptosis, TNF-induced cell death of wild-type cells was sensitive to inhibition of caspase-8 and broad spectrum caspase inhibition by synthetic caspase inhibitors. Unexpectedly, inhibition of caspases sensitized *Rb*$^{MI/MI}$ fibroblasts to TNFR1-induced cell death (Table 2). The absence of Bid cleavage during this response suggested that under conditions of caspase inhibition an alternative cell death pathway is triggered in TNF-treated

$Rb^{MI/MI}$ cells. Caspase activity has been shown to counteract the activation of non-apoptosis cell death pathways (Lemaire *et al.* 1998; Los *et al.* 2002). Accordingly, inhibition of caspase activity promotes caspase-independent cell death pathways like necrosis or apoptosis-like programmed cell death. Surprisingly, the activation of a caspase-independent pathway was specific to $Rb^{MI/MI}$ cells, since in wild-type cells, the inhibition of caspases protected cells from death. Moreover, the activation of a caspase-independent death pathway in response to hTNF, apparent by death in the absence of Bid cleavage, correlated with the presence of Rb-MI (Table 2).

In summary, preliminary data suggest that Rb-MI may facilitate the activation of a caspase-independent cell death pathway and that this effect might be linked to the suppression of caspase-activity by Rb-MI. Further studies will be needed to shed light on this aspect of Rb-MI function.

3.3 Constitutively active RB variants have contrasting effects on the apoptotic response to different stimuli

For the cellular response to TNF, the suppression of apoptosis could be separated from the growth suppressing activity of Rb (this work). On the other hand, the observation that cells arrested in G1/S are less sensitive to cell death in response to several stimuli (Meikrantz and Schlegel 1995) and the regulation of pro-apoptotic genes by the E2F family of transcription factors (Muller *et al.* 2001) suggested that Rb-E2F-dependent cell cycle arrest may be associated with a reduced sensitivity to apoptosis. Consistently, RB had been reported to promote cell cycle arrest and inhibit apoptosis in response to DNA damage (Knudsen *et al.* 2000). Thus, the question remained whether apoptosis and growth suppression by Rb are generally independent activities in developmentally mature cells and how both functions affect the apoptotic response to different death stimuli. To shed light on this question, Rb variants with constitutive growth suppressor function, resistance to caspases cleavage, or both, were analyzed in this work for their capacity to protect cells from different apoptotic stimuli.

3.3.1 Effect of PSM-RB induced growth arrest on apoptosis

The induction of cell cycle arrest by growth-suppressing RB variants had contrasting effects on cellular apoptosis responses (summarized in Figure 27). Cells arrested in G1 by CDK phosphorylation-resistant RB variants (PSM-RB and PSM-RB-MI) did not activate effector caspases as efficiently as proliferating cells in response to the DNA damaging agent doxorubicin (Figure 27a). PSM-RB expression inhibited the activation of caspase-3, but, although E2F binding sites are present in the caspase-3 promoter (Muller *et al.* 2001), PSM-RB did not interfere with pro-caspase-3 production. Thus, PSM-RB-dependent inhibition of caspase activation may be achieved either through the repression of other E2F-regulated apoptotic proteins, or alternatively, by a transcription-independent mechanism. The expression of WT-RB and RB-MI did not cause G1 arrest and did not affect doxorubicin-induced caspase activation. However, inhibition of doxorubicin-induced caspase activation was observed in serum-starved Rat-16 cells. These results are in agreement with the conclusion that G1 arrest, triggered by phosphorylation-resistant RB or growth factor deprivation is protective against DNA-damage-induced apoptosis.

Despite the activation of caspases, doxorubicin-induced DNA damage did not induce acute cell death in Rat-16 cells, but caused the loss of clonogenic survival by the induction of permanent growth arrest. The reduction of clonogenic survival was unaffected by prior induction of PSM-RB variants, showing that RB-dependent growth arrest did not prevent the establishment of irreversible growth arrest by DNA damage. Similar to DNA damage, broad-spectrum kinase inhibition by staurosporine has been shown to induce either growth arrest or apoptosis through the mitochondria-dependent intrinsic pathway (Li *et al.* 2000). Staurosporine-induced G1 arrest was shown to depend on Rb activity (Schnier *et al.* 1996; Orr *et al.* 1998; Chen *et al.* 2000), implying that the induction of G1 arrest by PSM-RB variants might render cells less susceptible to staurosporine-induced cell death. However, the induction of

a

PSM-RB
PSM-RB-MI

⊖

Doxorubicin

⊕ → Caspases

⊕ → Growth arrest

⊖

b

PSM-RB
PSM-RB-MI

?

Staurosporine

⊕ → Caspases
Other proteases → Death

⊖ ?

c

PSM-RB
PSM-RB-MI

⊕

Stalled Replication Fork

⊕

TNF/CHX

⊕ → Caspases → Death

Other
pathways → Death

⊖
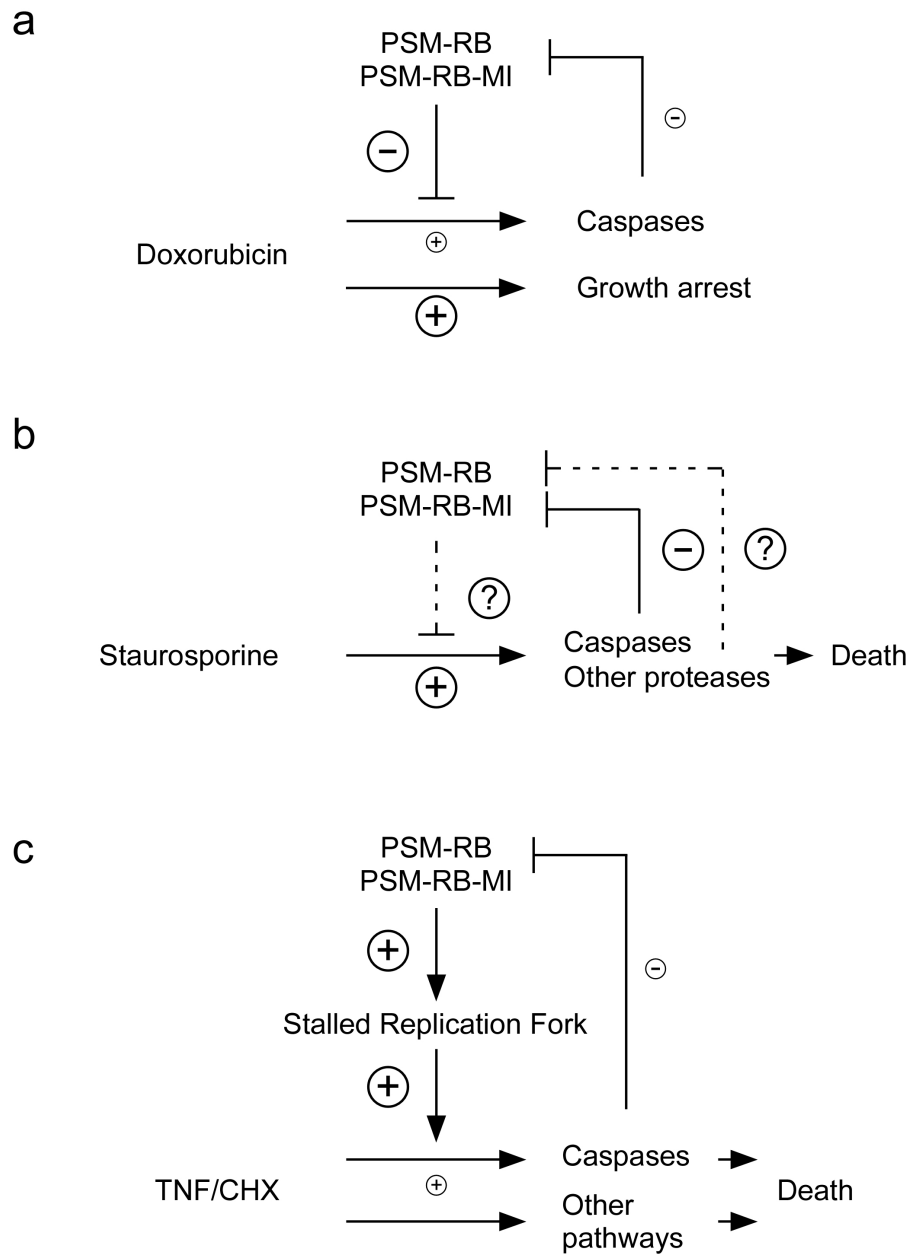
Figure 25. Constitutively active RB variants have contrasting effects on different cellular stress responses.
(a) Doxorubicin primarily induces growth arrest, but also causes caspase activation in Rat-16 cells. PSM-RB and PSM-RB-MI inhibit doxorubicin-induced caspase activation. (b) Staurosporine induces rapid apoptosis in Rat-16 cells, irrespective of PSM-RB induced growth arrest. PSM-RB and PSM-RB-MI are efficiently degraded during staurosporine-induced apoptosis. (c) Overproduction of PSM-RB and PSM-MI-RB augments TNF-induced apoptosis in Rat-16 cells, possibly by causing a replication stress response.

PSM-RB-induced growth arrest did not protect Rat-16 cells from staurosporine-induced apoptosis (Figure 27b). In contrast to its effect on the DNA damage response, growth arrest induced by PSM-RB variants did not prevent caspase activation in response to staurosporine. These observations suggest that the cellular susceptibility to apoptosis does not generally depend on the cells capacity to establish growth arrest.

3.3.2 Cell-cycle independent effects on apoptosis by overexpression of RB variants

TNF can induce TNFR1-dependent apoptosis (Micheau and Tschopp 2003; Schneider-Brachert *et al.* 2004) and caspase-independent necrotic death, mediated by oxidative stress (Los *et al.* 2002; Cauwels *et al.* 2003). In Rat-16 cells, TNF/CHX treatment resulted in necrotic cell death, which was not prevented by PSM-RB induced growth arrest. Surprisingly, induced expression of PSM-RB variants sensitized Rat-16 cells to TNF-induced caspase activation and apoptosis (Figure 27c). Unlike the inhibition of DNA-damage induced caspase activation, the sensitizing effect of PSM-RB expression occurred prior to the induction of G1/S arrest. Consistently, the PSM mutation was not required for sensitization. Interestingly, synchronization of Rat-16 cells in quiescence by serum starvation also enhanced TNF-induced apoptosis, which was probably an effect of survival factor limitation.

Induction of PSM-RB variants had no additive effect on the apoptosis sensitivity of serum-starved cells, indicating, that RB-dependent suppression of survival gene expression might be responsible for the sensitization to TNF-induced apoptosis. Alternatively, interference with replication fork movement, a function previously described for PSM-RB (Sever-Chroneos *et al.* 2001), might cause a replication stress response that enhanced the susceptibility to a second stress signal (Figure 27c). This notion was supported by the observation that aphidicolin-induced S-phase arrest augmented TNF-induced apoptotic DNA fragmentation in Rat-16 cells, which is consistent with a previous report that aphidicolin sensitized L929 fibrosarcoma cells to TNF-induced apoptosis (Gera *et al.* 1993). In either case, sensitization to TNF-induced apoptosis by RB may be an effect that is unique to the non-physiological conditions of induced RB expression and may thus not reflect an *in vivo* function of RB.

In contrast to observations in many other cell types, neither doxorubicin nor TNF caused significant RB degradation in Rat-16 cells. A minor fraction of wild-type and PSM-RB proteins was cleaved at the C-terminal caspase site during doxorubicin treatment, but overall levels of all RB variants were nearly unaffected, which is consistent with the induction of growth arrest and the absence of apoptosis under these conditions. Accordingly, mutation of the caspase cleavage site did not alter the effect of RB variants on the cells response to doxorubicin. Likewise, caspase-resistant RB variants had no specific effect on the TNF response in Rat-16 cells: the extent of sensitization to TNF induced apoptosis was comparable between PSM-RB and PSM-RB-MI variants.

The absence of RB degradation during DNA damage and TNF stimulation did not reflect a general incapacity of Rat-16 cells to degrade RB. This was evident by the rapid caspase cleavage and degradation of PSM-RB variants in response to staurosporine, which correlated with high levels of caspase activity and apoptosis. Mutation of the C-terminal cleavage site did not protect from staurosporine-induced apoptosis and was not sufficient to prevent PSM-RB degradation under these conditions. Cleavage of RB at additional sites has been previously observed during etoposide and TNF-induced apoptosis (Fattman *et al.* 2001; Chau *et al.* 2002). These signal-specific differences in RB degradation may be due to a context-dependent activation of a different spectrum of apoptotic proteases. The MI mutation has previously been shown to preserve Rb, but offer no protection during DNA damage-induced apoptosis (Chau *et al.* 2002). Thus, C-terminal caspase cleavage is not required during staurosporine-induced apoptosis, either, because of equivalent cleavage at other sites, or because RB cleavage is a bystander effect in staurosporine and DNA damage-induced apoptosis pathways. Taken together, these results show that RB-dependent cell cycle arrest is not generally associated with resistance against apoptosis. In Rat-16 cell, PSM-RB induced G1/S arrest could inhibit DNA damage-induced caspase activation, but did not affect caspase activation in response to staurosporine. RB expression sensitized Rat-16 cells to TNF-induced apoptosis independent from the induction of cell cycle arrest, this was possibly an effect of unphysiologically high RB expression levels after RB induction in these cells.

4   Summary

The retinoblastoma tumor suppressor protein (RB) is a critical regulator of cell proliferation capable of inhibiting both cell cycle progression and apoptosis. While the pathway of RB-mediated cell cycle regulation has been resolved, the mechanism of apoptosis suppression by Rb remained largely elusive. RB is inactivated by CDK-dependent phosphorylation in response to mitogenic signals and by caspase-dependent degradation during apoptotic cell death. Phosphorylation-resistant PSM-RB *(phosphorylation site-mutated RB)* is a strong inhibitor of proliferation, while caspase-resistant RB-MI *(RB mutated at ICE site)* can protect cells from apoptosis.

In the present work, the regulation apoptosis by RB was analyzed in two experimental systems: (I.) in Rat fibroblast cell lines harboring inducible expression of inactivation-resistant RB variants (phosphorylation resistant PSM-RB, caspase-resistant RB-MI and PSM-RB-MI, in which both mutations were combined); (II.) in fibroblasts derived from transgenic $Rb^{MI/MI}$ mice expressing caspase-resistant Rb-MI. Inducible expression of RB and inactivation-resistant RB variants in Rat fibroblasts had diverse effects on the cellular response to different cell death stimuli. RB-induced cell cycle arrest had an anti-apoptotic effect on DNA damage response, but did not affect staurosporine-induced apoptosis, indicating that RB-induced G1 arrest is not generally associated with apoptosis-resistance. RB expression sensitized Rat-16 cells to TNF-induced apoptosis independent from the induction of cell cycle arrest, possibly as an effect of unphysiologically high RB expression levels after RB induction in these cells. These results indicate signal-specific differences in apoptosis regulation by RB. For TNF-induced apoptosis of mouse fibroblasts the apoptosis suppressing activity of Rb-MI could be separated from its growth suppressing activity, which implies an independent regulation of RB's two major functions. DNA Microarray analysis of TNF-induced gene expression in $Rb^{MI/MI}$ cells gave no indication for the suppression of pro-apoptotic gene expression by Rb-MI. This observation implies that RB can function as a post-transcriptional regulator of apoptosis. The detailed analysis of the TNF-induced mitochondrial apoptosis pathway in $Rb^{MI/MI}$ cells suggested that Rb-MI inhibits cleavage of the BH3-only protein Bid by inhibiting either caspase-8 activation or interaction of caspase-8 and Bid. These results revealed a previously unrecognized role of RB as a post-transcriptional regulator of caspase activation and apoptosis.

Zusammenfassung

Dem Retinoblastoma Tumor Suppressor Protein (RB) kommt eine zentrale Rolle bei der Regulation zellulärer Proliferation zu, da es sowohl Zellteilung als auch Zelltod durch Apoptose inhibieren kann. Während der Signalweg der RB-vermittelten Zellzyklus-Regulation erforscht ist, blieb der Mechanismus zur Unterdrückung von Apoptose durch RB weitgehend ungeklärt. RB wird unter Einfluss von Wachstumsfaktoren durch CDK-abhängige Phosphorylierung inaktiviert und im Verlauf von Apoptose von Caspasen proteolytisch gespalten. Phosphorylierungs-resistentes PSM-RB *(phosphorylation site-mutated RB)* hemmt die Zellteilung; Caspase-resistentes RB-MI (*RB mutated at ICE site*) kann Zellen vor TNF-induzierter Apoptose schützen.

In dieser Arbeit wurde die Regulation von Apoptose durch RB in zwei experimentellen Systemen analysiert:

I. in Ratten-Fibroblasten-Zellen mit induzierbarer Expression inaktivierungsresistenter RB-Varianten (PSM-RB, RB-MI und PSM-RB-MI, in dem beide Mutationen kombiniert wurden);

II. in Fibroblasten-Zellen, die aus transgenen $Rb^{MI/MI}$-Mäusen isoliert wurden, welche Caspase-resistentes Rb-MI exprimieren.

Die induzierte Expression von RB und inaktivierungsresistenten RB-Varianten in Ratten-Fibroblasten-Zellen hatte einen unterschiedlichen Einfluss auf die zellulären Reaktionen auf verschiedene Apoptose-Stimuli. RB-induzierter Zellzyklus-Arrest hatte einen anti-apoptotischen Effekt auf die zelluläre Antwort auf DNA-Schäden, aber keinen Einfluss auf Staurosporin-induzierte Apoptose, was darauf schließen lässt, dass RB-induzierter G1-Arrest nicht grundsätzlich mit einer erhöhten Apoptose-Resistenz verbunden ist. Die induzierte Expression von RB und RB-Varianten erhöhte die Sensitivität der Ratten-Fibroblasten-Zellen für TNF-induzierte Apoptose, dieser Effekt ist möglicherweise auf die nach RB-Induktion unphysiologisch hohe RB-Konzentration in den Zellen zurückzuführen. Diese Ergebnisse weisen auf signal-spezifische Unterschiede in der RB-abhängigen Apoptose-Regulation hin.

Für TNF-stimulierte Apoptose in Maus-Fibroblasten konnte eine Trennung der anti-apoptotischen Aktivität des Rb-MI-Proteins von seiner wachstumshemmenden Aktivität nachgewiesen werden, was auf unabhängige Regulation der beiden Hauptfunktionen von RB schließen lässt. Eine DNA-Mikroarray-Analyse TNF-

induzierter Genexpression in $Rb^{MI/MI}$-Zellen ergab keinen Hinweis auf eine negative Regulation pro-apoptotischer Gene durch Rb-MI. Diese Beobachtung lies vermuten, dass RB Apoptose auf post-transkriptionaler Ebene regulieren kann. Die detaillierte Analyse des TNF-induzierten mitochondrialen Apoptose-Signalwegs in $Rb^{MI/MI}$-Zellen deutete darauf hin, dass Rb-MI die proteolytische Spaltung des BH3-Proteins Bid verhindert, entweder durch Inhibierung der Aktivierung von Caspase-8 oder durch Verhinderung der Interaktion von Caspase-8 und Bid. Diese Ergebnisse identifizierten einen zuvor unbekannten, post-transkriptionalen Mechanismus für die negative Regulation von Caspase-Aktivierung und Apoptose durch RB.

5 Materials and Methods

5.1 Abbreviations and Symbols

5.1.1 Abbreviations

APS	ammonium persulfate
aa	amino acid
ATP	adenosine 5'-triphosphate
bp	base pairs
β-ME	β-mercaptoethanol
BrdU	bromodeoxyuridine
BSA	bovine serum albumin
dH_2O/ddH_2O	distilled/double distilled water
cDNA	complementary DNA
CHAPS	3-[(3-cholamidopropyl)-dimethylammonio]-1-propanesulfonate
DEPC	diethylpyrocarbonate
DOX	doxorubicine
DNA	deoxyribonucleic acid
DNase	deoxyribonuclease
dATP	deoxyadenosine 5'-triphosphate
dGTP	deoxyguanosine 5'-triphosphate
dNTP	deoxynuclueotide 5'-triphosphate
DMEM	Dulbecco's modified Eagle's medium
DMSO	dimethylsulfoxide
DTT	1,4-dithiothreitol
ECL	enhanced chemoluminiscence
E. coli	*Escherichia coli*
EDTA	ethylenediaminetetraacetate
EGTA	ethyleneglycol-bis-(β-aminomethylether)-tetraacetate
FACS	fluorescence-activated cell sorting
FITC	fluorescein
FBS	fetal bovine serum
f.c.	final concentration
fmk	fluoromethylketone
HEPES	N-2-hydroxyethylpiperazine-N'-2-ethanesulfonic acid
Hyg	hygromycin
HRP	horseradish peroxidase
IB	immunoblotting
IP	immunoprecipitation
IGF-1	insulin-like growth factor 1

IVT	*in vitro* transcription
kDa	kilodalton
LB	Luria Bertani
M	molar
MCS	multiple cloning site
MES	morpholineethanesulfonic acid
MWCO	molecular weight cut off
OD	optical density
PA	polyacrylamide
PAGE	polyacrylamide-gel electrophoresis
PBS	phosphate-buffered saline
PCR	polymerase chain reaction
pH	negative decadic logarithm of H^+ ion concentration
PIPES	piperazine-1,4-bis-(2-ethanesulfonic acid)
PFA	paraformaldehyde
PMSF	phenylmethylsulfonylfluorid
PVDF	polyvinylidenfluorid
RIPA	radio-immuno-precipitation assay
RNA	ribonucleic acid
RNase	ribonuclease
rRNA	ribosomal RNA
RT	room temperature
SAPE	Streptavidin phycoerythrin
S	Svedberg
SDS	sodium dodecyl sulfate
STS	staurosporine
TE	Tris-EDTA
TBE	Tris-borate-EDTA
TBS	Tris-buffered saline
TEMED	N,N,N',N'-tetramethylethylendiamine
TET	tetracycline
TNF	tumor necrosis factor α
Tris	tris-(hydroxymethyl)-aminomethane
rpm	revolutions per minute
U	enzyme activity unit
UV	ultraviolett
vol	volume
v/v	volume per volume
w/v	weight per volume
z-	benzyloxycarbonyl-

5.1.2   Amino acid symbols

A	Ala	Alanine
C	Cys	Cysteine
D	Asp	Aspartic acid
E	Glu	Glutamic acid
F	Phe	Phenylalanine
G	Gly	Glycine
H	His	Histidine
I	Ile	Isoleucine
K	Lys	Lysine
L	Leu	Leucine
M	Met	Methionine
N	Asn	Asparagine
P	Pro	Proline
Q	Gln	Glutamine
R	Arg	Arginine
S	Ser	Serine
T	Thr	Threonine
V	Val	Valine
W	Trp	Tryptophan
Y	Tyr	Tyrosine

5.1.3   Prefixes for measurement units

k	kilo-	10^3
m	milli-	10^{-3}
μ	micro-	10^{-6}
n	nano-	10^{-9}
p	pico-	10^{-12}

5.2   Materials

5.2.1   Bacteria strains

E. coli XL-1 Blue (Stratagene)

5.2.2   Bacterial culture media and solutions

Ampicillin stock solution:	50 mg/ml	ampicillin in dH_2O
	sterile filtered, stored at -20°C	

LB medium:	1% w/v	Bacto tryptone
	0.5% w/v	Bacto yeast extract
	170 mM	NaCl

LB plates: LB medium + 1.5% agarose

5.2.3   Plasmids and Plasmid constructs

pTK-Hyg (BD Bioscience)

pTRE (BD Bioscience)

pTRE-based expression plasmids, obtained by subcloning of the following sequences into the pTRE vector via the BamH1 restriction site:

> pTRE-WT-RB: human RB cDNA
>
> pTRE-RB-MI: RB-MI, described in (Chau *et al.* 2002)
>
> pTRE-PSM-RB: PSM-RB, described in (Knudsen and Wang 1997)
>
> pTRE-PSM-RB-MI: PSM-RB-MI, which was generated by subcloning a sequence containing the RB-MI mutation into pTRE-PSM-RB.

5.2.4   Cell culture media and solutions

DMEM, high glucose, formulated with sodium pyruvate and L-glutamine (HyCult)

FBS, heat inactivated (HyCult)

G418, Hygromycin, Penicillin/streptomycin (Gibco)

IGF-1 (Sigma)

TET-free FBS, heat inactivated (HyCult)

Trypsin-EDTA solution (Gibco)

5.2.5 Buffers and solutions

5.2.5.1 Cell lysis and fractionation buffers

HEPES buffer:	10 mM	HEPES-KOH, pH 7.5
	10 mM	KCl
	1.5 mM	$MgCl_2$
	1 mM	EDTA
	1 mM	EGTA

HEPES saline:	10 mM	HEPES-KOH, pH 7.5
	150 mM	NaCl

Hypotonic lysis buffer:	20 mM	HEPES-KOH, pH 7.2
	10 mM	KCl
	1.5 mM	$MgCl_2$
	1 mM	EDTA
	1 mM	EGTA

Mannitol/sucrose buffer I:	210 mM	mannitol
	70 mM	sucrose
	10 mM	HEPES, pH 7.5
	1 mM	EDTA
	0.45 %	BSA

Mannitol/sucrose buffer II:	210 mM	mannitol
	70 mM	sucrose
	10 mM	HEPES, pH 7.5
	0.5 mM	EDTA
	+ protease inhibitors	

Mannitol/sucrose buffer III:	210 mM	mannitol
	70 mM	sucrose
	10 mM	HEPES-KOH, pH 7.4
	5 mM	Na_2HPO_4
	4 mM	$MgCl_2$
	0.5 mM	EGTA
	1 mM	DTT
	+ protease inhibitors	

Nuclear extract buffer:	20 mM	HEPES-KOH, pH 7.2
	420 mM	NaCl
	25 %	glycerol
	1.5 mM	$MgCl_2$
	0.2 mM	EDTA

PIPES/CHAPS buffer	20 mM	PIPES, pH 7.2,
	0.1 %	CHAPS
	100 mM	NaCl
	10 %	sucrose
	2 mM	EDTA
	5 mM	DTT

RIPA buffer:	50 mM	Tris-HCl, pH 7.4
	150 mM	NaCl
	1 %	NP-40 (Igepal)
	0.25 %	sodium deoxycholate
	0.1 %	SDS
	0.5 mM	EDTA
	1 mM	EGTA
	1 mM	DTT
	+ protease inhibitors	

5.2.5.2 Plasmid DNA isolation buffers

Solution A (re-suspension):	50 mM	Tris-HCl, pH 7.5
	10 mM	EDTA
	100 µg/ml	RNase A

Solution B (lysis):	0.2 M	NaOH
	1 %	SDS

Solution C (neutralization):	1.32 M	potassium acetate, pH 4.8

Column wash solution:	80 mM	potassium acetate
	8.3 mM	Tris-HCl, pH 7.5
	40 µM	EDTA
	55 %	ethanol

5.2.5.3 Miscellaneous buffers and solutions

Acrylamide/bisacrylamide 30:1

Chloroform/isoamylalcohol 24:1

Ethidiumbromide 10 mg/ml

Phenol/chloroform/isoamylalcohol 25:24:1

DNA loading dye:	10 mM	Tris-HCL, pH 8.0
	100 mM	EDTA
	60 %	sucrose
	0.05 %	bromphenol blue
IFA buffer (FACS)	1 x	HEPES-KOH
	4 %	FBS
	0.1 %	NaN_3
KCL buffer:	125 mM	KCl, pH 7.4
	10 mM	HEPES-KOH
	5 mM	Na_2HPO_4
	4 mM	$MgCl_2$
	0.5 mM	EGTA
PBS:	137 mM	NaCl
	2.7 mM	KCl
	43 mM	Na_2HPO_4 x 7 H_2O, pH 7.4
	1.4 mM	KH_2PO_4
4 % PFA/PBS	stored at -20	
TE buffer:	10 mM	Tris-HCl, pH 7.5
	1 mM	EDTA, pH 8
TAE buffer:	40 mM	Tris-acetate, pH 8
	1 mM	EDTA

5.2.5.4 SDS-PAGE and Immunoblotting solutions

Immunoblot transfer buffer:	48 mM	Tris-HCl, pH 8.4
	39 mM	glycine
	10-20 % v/v	methanol
	0.04 % w/v	SDS

| Resolving gel buffer (4x): | 1.5 M | Tris-HCl, pH 8.8 |
| | 0.4 % w/v | SDS |

| Stacking gel buffer (4x): | 0.5 M | Tris-HCl, pH 6.8 |
| | 0.4 % w/v | SDS |

Running buffer:	25 mM	Tris-HCl, pH 8.3
	190 mM	glycine
	0.1 % w/v	SDS

SDS sample buffer (6x):	0.35 M	Tris-HCl, pH 6.8
	30 % v/v	glycerol
	10 % w/v	SDS
	0.6 M	DTT
	0.012 % w/v	bromphenol blue
	stored at -20	

| TBS: | 20 mM | Tris-HCl, pH 7.5 |
| | 150 mM | NaCl |

| TBST: | TBS + 0,1 % | Tween20 |

5.2.5.5 Buffers and solutions for microarray gene expression analysis

DEPC-dH$_2$O   treatment with 0.1 mg/ml DEPC overnight, inactivation of DEPC by autoclaving (20 min)

Hybridization buffer:	100 mM	MES, pH 6.5
	1 M	[Na$^+$]
	20 mM	EDTA
	0.01 %	Tween 20
	sterile filtered, stored in the dark at 4°C	

20 x SSPE:	3 M	NaCl
	0.2 M	NaH2PO4
	0.02 M	EDTA

SAPE stain solution:	1 x	MES buffer
	2 mg/ml	Acetylated BSA
	10 µg/ml	SAPE
	stored in the dark at 4°C	

Stain buffer:	100 mM MES	
	0.1 M Na$^+$	
	0.05 %	Tween20
	filtered to 0.2 µm filter, stored in the dark at 4°C	

Non-stringent wash buffer:	6 x	SSPE
	0.01 %	Tween2
	filtered to 0.2 µm filter	

Stringent wash buffer:	100 mM	MES
	0.1 M	Na$^+$
	0.01 %	Tween20
	filtered to 0.2 µm filter, stored in the dark at 4°C	

5.2.5.6 Restriction digest buffers:

NEB1: 10 mM bis-Tris-propane-HCl, 10 mM MgCl$_2$, 1 mM DTT, pH 7.0

NEB2: 10 mM Tris-HCl, 10 mM MgCl$_2$, 50 mM NaCl, 1 mM DTT, pH 7.9

NEB3: 50 mM Tris-HCl, 10 mM MgCl$_2$, 100 mM NaCl, 1 mM DTT, pH 7.9

NEB4: 20 mM Tris-acetate, 10 mM Mg acetate, 50 mM K acetate, 1 mM DTT, pH 7.9

5.2.5.7 Other enzymatic reaction buffers

DNA ligase buffer (NEB): 50 mM Tris-HCl, 10 mM MgCl$_2$, 10 mM DTT, 1 mM ATP, 25 µg/ml BSA, pH 7.5

PCR buffer for KOD hot start DNA polymerase (Novagen)

5.2.6 Antibodies

5.2.6.1 Primary antibodies (given are standard dilutions for IB)

anti-Bid goat polyclonal (Biovision), 1:1000

anti-BrdU mouse monoclonal, FITC-conjugated (BD Biosciences)

anti-caspase-3 rabbit polyclonal

(kind gift from Yuri Lazebnik, Cold Spring Harbour Laboratories), 1:500

anti-caspase-8 AR-17 rabbit polyclonal

(kind gift from Guy Salvesen, Burnham Institute, La Jolla), 1:10 000

anti-cleaved caspase-3 rabbit polyclonal (Cell Signaling), 1:1000

anti-cytochrome c mouse monoclonal (Pharmingen), 1:1000

anti-Mcl-1 rabbit polyclonal (Santa Cruz), 1:1000

anti-Parp rabbit polyclonal (Cell Signaling), 1:1000

anti-phospho-c-jun rabbit polyclonal (Cell Signaling), 1:500

anti-Rb rabbit polyclonal,

raised against the C terminus (residues 768 – 928) of RB, 1:2000

anti-SMAC/DIABLO (Chemicon), 1:500

anti-TNFR1 (Santa Cruz), 1:250

anti-TNFR1 agonistic (HyCult), 0.625 µg/ µl for receptor activation *in vivo*

anti-TNFR2 agonistic (HyCult), 2.5 µg/ µl for receptor activation *in vivo*

anti-tubulin goat polyclonal (Santa Cruz), 1:250

5.2.6.2 Secondary antibodies

AlexaRed-anti-rabbit (Molecular Probes), 1:500

HRP-donkey anti-rabbit (Pierce),1:5000

HRP-goat anti-mouse (Pierce), 1:5000

HRP-rabbit anti-goat (Pierce),1:5000

5.2.7 Caspase substrates and inhibitors

Ac-IETD-AFC (Calbiochem)

Ac-DEVD-AMC (Molecular Probes)

z-VAD(OMe)-fmk, z-IE(OMe)TD(OMe)-fmk, z-VD(OMe)VAD(OMe)-fmk

(R&D systems)

5.2.8   Enzymes

E. coli DNA Ligase (Invitrogen)

E. coli DNA polymerase I (Invitrogen)

E. coli RNase H (Invitrogen)

KOD hot start DNA polymerase (Novagen)

RNase A (Invitrogen)

SuperScript II reverse transcriptase (Invitrogen)

T4 DNA polymerase (Invitrogen)

Restriction enzymes were obtained from NEB.

5.2.9   Miscellaneous reagents and materials

Acetylated BSA solution, 50 mg/ml (Invitrogen)

Bradford Protein assay (BioRad)

DC-Protein assay (BioRad)

DNA molecular weight standards: 1 kB ladder (NEB), 100 bp ladder (NEB)

Doxorubicine (Sigma)

dNTP stock solution, 10 mM (Invitrogen)

ECL reagents (Pierce)

Enzo BioArray™ RNA transcript labeling kit (Affymetrix)

GeneChip eukaryotic hybridization control kit, containing control cRNA and

      control oligo B2 (Affymetrix)

GeneChip T7-oligo(dT) promoter primer, HPLC purified (Affymetrix),

(5'-GGCCAGTGAATTGTAATACGACTCACTATAGGGAGGCGG-(dT)$_{24}$-3')

Herring sperm DNA (Promega)

Protease inhibitor cocktail (Roche)

Protein molecular weight standard: Precision plus pre-stained protein molecular

                      weight standard (BioRad)

PVDF membranes (Millipore)

QIAquick PCR purification kit (QIAGEN)

Recombinant human and mouse TNF-α (Peprotech)

RNeasy Mini RNA purification kit (QIAGEN)

R-phycoerythrin streptavidin (Molecular Probes)

Staurosporine (Calbiochem)

SuperScript II system for cDNA synthesis (Invitrogen)

Tetracycline (Sigma)

Tris-Glycine pre-cast gels (Invitrogen)

TRIzol reagent (Invitrogen)

All other chemicals were obtained *p.a.* from Sigma or Fluka.

5.3 Methods

5.3.1 Transformation of *E. coli*

Frozen stocks of *E. coli* cells were thawed on ice and incubated for 20 min with purified plasmid DNA. Cells were transfected by heat shock at 42°C for 45 sec. Cells were cooled on ice and directly plated onto LB agar plates containing 20 mg/ml ampicillin.

5.3.2 Preparation of plasmid DNA from *E. coli*

5.3.2.1 Miniprep

1-3 ml aliquots of LB containing 50 µg/ml ampicillin (Amp-LB) were inoculated with individual *E. coli* colonies and grown at 37°C overnight with constant agitation. Cells were harvested by centrifugation for 1-2 min at 10 000 x g and resuspended in 200 µl solution A. Cells were lyzed by addition of 200 µl solution B and inverting the tube 4-5 times. 200 µl of solution C were added and mixed by inverting the tube 4-5 times to neutralize the pH. Lysates were cleared by centrifugation at 10 000 x g for 5 – 15 min and processed using Wizard Miniprep columns (Promega) and a vacuum manifold. 1 ml Wizard miniprep resin (Promega) was pipetted into each minicolumn. Cleared bacterial lysates were passed through the minicolumns by applying a vacuum to the manifold. Columns were washed with 2 ml of column wash solution and dried by drawing a vacuum for 30 s after the solution had passed the column. Minicolumns were then transferred to a microcentrifuge tube and centrifuged at 10 000 x g for 2 min to remove residual wash solution. Columns were transferred to clean microcentrifuge tubes and DNA was eluted by incubation with 50 µl dH2O or TE buffer for 1 min and centrifugation at 10 000 x g for 20 sec.

5.3.2.2 Midiprep

Starter cultures of 3-5 ml Amp-LB were inoculated with individual *E. coli* colonies and grown at 37°C for 7-9 h with constant agitation. 100 ml Amp-LB containing were inoculated from the starter culture (1:500) and incubated at 37°C for 12-16h with constant agitation. Cells were harvested by centrifugation at 6000 x g, 4°C for 15 min. The pellet was resuspended in 4-5 ml solution A and lysed by addition of 4-5 ml solution B. After addition of 4-5 ml solution C, the lysate was incubated for 10 min at RT and passed through a QIAGEN Midi column that had been equilibrated with buffer QBT (QIAGEN). Columns were washed with 10 ml buffer QC (QIAGEN) and eluted with 5 ml buffer QF (QIAGEN). DNA was purified by ethanol precipitation.

5.3.3 Spectrophotometric quantification of nucleic acids

The DNA or RNA concentration of a solution was determined by measuring the solution's absorbance at 260 nm and calculating the concentration using the convention that one absorbance unit (OD_{260}) equals a concentration of 50 µg/ml double-stranded DNA and 40 µg/ml single stranded RNA.

5.3.4 Enzymatic manipulation of DNA

5.3.4.1 Restriction digest of DNA

Restriction digest of DNA was performed in a volume of 30-50 µl. A standard reaction contained:

> DNA (0.1-1µg/µl)
>
> 1 x restriction buffer 1-4 (NEB)
>
> 1-10 U restriction enzyme per µg DNA

Reactions were incubated 1-3 h at 37°C for most enzymes.

5.3.4.2 Dephosphorylation of DNA ends

The 5' phosphate group of DNA ends were removed to prevent re-ligation of linearized vectors. A standard reaction (30-50 µl) contained:

> 50-100 ng/µl DNA
>
> 1 x AP buffer (NEB)
>
> 1 U bovine intestinal alkaline phosphatase (CIP) per pmol DNA

Alternatively, CIP was added directly to the restriction digest reaction. Reactions were incubated for 1 h at 37°C.

5.3.4.3 Ligation of DNA ends

A standard reaction (10 µl) contained:

Vector and insert DNA in a molar ratio of 1:3 (together ca. 1µM DNA)

1 x Ligase buffer (NEB)

10 U T4 Ligase (NEB)

Reactions were incubated 5 h to overnight at RT.

5.3.4.4 Standard PCR amplification of DNA fragments

A standard reaction contained:

1 x PCR buffer (Novagen)

0.2 mM   dNTPs

1 mM $MgSO_4$

5 – 50 ng   template DNA

0.3 µM   5' primer

0.3 µM   3' primer

1 U   KOD hot start DNA polymerase (Novagen)

KOD DNA polymerase was activated by heating for 2 min at 94°C and reactions incubated for 30 cycles of

1 min at 94°C

1 min at 52°C

1.5 min at 72°C

5.3.5 Isolation, purification and characterization of nucleic acids

5.3.5.1 Agarose gel electrophoresis

Depending on size, DNA or RNA was separated by electrophoresis on 0.8 -1 % agarose/TAE gels containing 2 µl ethidium bromide stock solution. Samples were diluted in DNA loading dye and gels were run in 1 x TAE buffer. Nucleic acids were detected under UV light.

5.3.5.2 Ethanol precipitation

For precipitation of DNA, 2 vol ethanol and 0.1 vol 3 M sodium acetate (pH 5.2) were added to the DNA solution and the mixture was incubated at -20 for 1 h to overnight. The precipitate was pelleted by centrifugation for 15 min at 10 000 x g. The DNA pellet was washed twice with 70 % ethanol, dried and resuspended in TE or dH2O.

5.3.5.3 Phenol/chloroform extraction

To remove protein contamination from DNA solutions, an equal volume of phenol/chloroform/isoamylalcohol was added and dispersed by shaking the tube. Phases were separated by centrifugation for 10 min at 10 000 x g and the upper phase was transferred to a clean tube. An equal volume of chloroform/isoamylalcohol was added, the solution mixed and phases again separated by centrifugation. From the upper phase DNA was isolated via ethanol precipitation.

5.3.5.4 Isolation of DNA fragments from agarose gels

DNA fragments were excised from agarose gels under UV light with a clean scalpel. Agarose slices were weight and 3 vol of buffer QG (QIAGEN)/1 vol gel were added.

After 10 min incubation at 50°C, 1 gel vol isopropanol was added and the mixture applied to a QIAquick column and centrifuged for 1 min. DNA was washed with buffer PE (QIAGEN) and eluted with ddH$_2$O or TE buffer.

5.3.6 Construction of Rat-16 cell lines

The pTRE-based WT-RB, PSM-RB, MI-RB and PSM-MI-RB expression plasmids were co-transfected with a pTK-Hyg plasmid in a molar ratio of 20:1 into Rat 16 cells, which were engineered to express the TET-VP16 fusion protein and provide tight regulation of TET-regulated gene expression. These cells were kindly provided by E. S. Knudsen (University of Cincinnati). Transfection was carried out when cells had reached 40-60 % confluence using Fugene transfection agent, according to the manufacturers protocol. Selection was started 48 h post transfection by the addition of hygromycin (200 µg/ml) to the culture media. After 10 days in selection media, 48 single colonies from each transfection were picked using 4-5 µl trypsin-EDTA and a micropipette. Colonies were transferred to individual wells of 24 well plates and grown in selection media. After 16 days, cells were transferred to 6 well plates and grown to confluence. Clones were finally split and analyzed for RB expression by immunoblotting after 24 h culture in TET-free media. For each plasmid, several clones expressing wild-type or mutant RB were isolated and clones with comparable expression levels were selected for the present study.

5.3.7 Cell culture

Rat-16 cell lines harboring inducible expression of WT or mutant RB were cultured in DMEM containing 10 % FBS, G418 (400 µg/ml), tetracycline (1 µg/ml), glutamine, penicillin and streptomycin. To induce RB expression, cells were washed three times in PBS and once in TET-free media and were then switched to TET-free media. Murine wild-type and $Rb^{MI/MI}$ fibroblasts were cultured in DMEM containing 10 % FBS, glutamine, penicillin/streptomycin and 5 x 10^{-4} % β-ME. All cells were maintained at 37°C in 5 % CO_2 in a standard cell culture incubator.

5.3.7.1 Synchronization of cells in early S phase:

For synchronization in early S phase cells were incubated in DMEM containing the following supplements:

> 0.1 % FBS for 72 h
>
> 10 % FBS for 16 h
>
> APH 2 µg/ml for 10 h

5.3.8 Clonogenic survival assay

Cells were cultured for 24 h in the presence (uninduced) or absence (induced) of TET and subsequently treated with 2 µM doxorubicin for 24 h in the presence or absence of TET. Cells were washed and equal numbers of cells were seeded in 96 well plates in TET-containing media. After 7 days cells were stained with 0.1 % crystal violet in methanol and washed with PBS. From each well the dye was extracted with acetic acid and absorbance read at 500 nm. Untreated cells (100 % survival) were used to calculate the percentage of surviving docorubicin treated cells.

5.3.9 Flow cytometry

Flow cytometry analysis was performed using a BD FACS apparatus (BD Biosciences) and CellQuest acquisition and analysis software (BD Biosciences). Data was alternatively analyzed using FlowJow FACS analysis software.

5.3.9.1 PI uptake assay for loss of membrane integrity

For labeling of dead or necrotic cells, cells were trypsinized, collected in PBS and sedimented by centrifugation at 1 000 rpm for 5 min. Cells were re-suspended in 500 ml PBS containing 1 µg/ml propidium iodide (PI) per sample. Samples were filtered

and incubated 10 min at RT before analysis by flow cytometry. FSC (forward scatter) and FL2-H (PI peak height) channels were recorded counting 10 000 events. For each treatment condition, triplicate samples were analyzed from which the average percentage of PI positive cells was calculated.

5.3.9.2   Cell cycle distribution and subG1 DNA content analysis

For cell cycle profile and subG1 DNA content analysis, cells were trypsinized, fixed in 70% ethanol overnight and stained with propidium iodide (20 µg/ml) in PBS plus RNase (40 µg/ml) for 30 min at RT in the dark. Samples were filtered and analyzed by flow cytometry recording FL2-A (PI peak area) and FL2-W (PI peak width) channels. Debris and cell clusters were excluded through a gate based on the FL2-A vs. FL2-W plot and 10 000 gated events were counted.

5.3.9.3   BrdU incorporation analysis

Cells were pulse labeled with BrdU (30 µg/ml), trypsinized and fixed in 70% ethanol overnight. Fixed cells were pelleted, resuspended in 2N HCL containing 0.2 mg/ml freshly dissolved pepsin and incubated 30 min at room temperature. Samples were neutralized with 3 ml 0.1 M sodium tetraborate, pH 8.5 and cells were washed once with IFA buffer, once with IFA, 0.5% Tween 20 and stained with a FITC-conjugated anti-BrdU antibody (diluted 1:5 in IFA) for 30 min at RT in the dark. Cells were washed once with 3 ml IFA, 0.5% Tween 20 and incubated with RNase and propidium iodide for 10 min at RT in the dark. Samples were filtered and analyzed by flow cytometry recording FL1-H (FITC peak height), FL2-A (PI peak area) and FL2-W (PI peak width) channels. Life cells were gated based on the FL2-A vs. FL2-W plot and 10 000 gated events were counted.

5.3.10   Immunofluorescence microscopy

Cells were fixed with 4 % PFA/PBS and permeabilized with 0.1 % Triton X-100. Unspecific binding sites were blocked with 0.1 % normal goat serum (NGS)/PBS. RB was detected using a polyclonal antibody raised against the C-terminus (residues 768 – 928) of RB, 1: 500 and AlexaRed goat anti-rabbit 1:500, both diluted in0.1 % normal goat serum (NGS)/PBS.

5.3.11 DNA microarray analysis of gene expression

The entire procedure was performed following the manufacturers suggestions (GeneChip® Expression Analysis Technical Manual, Affymetrix). All glassware was baked and dH2O was treated with DEPC to inactivate RNases.

5.3.11.1 Isolation of total cellular RNA

Cells were washed in PBS, scraped of the culture dish and sedimented by centrifugation. The pellet was resuspended in at least 0.5 ml TRIzol reagent (Invitrogen) per confluent culture dish and incubated 5 min at RT. 0.2 vol chloroform were added, the tube was shaken for 15 seconds and incubated for 2-3 min at RT. The phases were separated by centrifugation (12 000 rpm in a conventional microcentrifuge, 15 min) at 4°C. To the upper phase, 0.5 vol isopropanol were added, the mix incubated for 10 min at RT and centrifuged (12 000 rpm, 10 min, at 4°C) to precipitated RNA. The pellet was resuspended and washed once with 75 % ethanol and pelleted again by centrifugation (7 500 rpm, 5 min, 4°C). Dried pellets were resuspended in DEPC-treated dH20 or formamide. RNA was purified using the RNeasy Mini Kit spin columns (QIAGEN) according to the manufacturers instructions. RNA yield was quantified by spectrophotometric analysis. Between 5 and 10 µg high-quality total RNA was used as a template for cDNA synthesis.

5.3.11.2 Synthesis of double-stranded cDNA

cDNA synthesis was carried out using the GeneChip T7 oligo(dT) promoter primer kit (Affymetrix) and SuperScript II reverse transcriptase (Invitrogen). The reaction contained for the first strand synthesis:

T7-oligo(dT) primer	100 pmol
RNA	5 -10 µg
1x cDNA buffer	
dNTPs	500 µM each
SuperScript II	200 U (added only before the last step)

For primer hybridization, reactions were incubated at 70°C for 10 min, allowed to cool on ice and incubated at 42°C for 2 min for temperature adjustment. At this point, reverse transcriptase was added and the first strand synthesis reaction incubated at 42°C for 1 h.

For second strand synthesis, the following was added to the first strand synthesis tube (given are resulting final concentrations):

dNTPs	200 µM
E. coli DNA Ligase	10 U
E. coli DNA Polymerase I	40 U
E. coli RNase H	2 U

The second strand synthesis reaction was incubated at 16°C for 2 h. After addition of 10 U T4 DNA polymerase the reaction was returned to 16 °C for 5 min before the reaction was stopped with 0.5 M EDTA. Cleanup of double stranded cDNA was performed via a standard phenol/chloroform extraction followed by ethanol precipitation using 0.5 vol of 7.5 M NH4OAc, 2.5 vol absolute ethanol (-20°C) and 1 µl glycogen as a carrier. Precipitated cDNA was washed 2x with 80 % ethanol (-20°C). The air-dried pellet was resuspended in 12 µl RNase-free dH2O.

5.3.11.3 Synthesis of biotin-labeled cRNA

Biotin-cRNA synthesis was performed through *in vitro* transcription using the Enzo BioArray RNA transcript labeling Kit (Affymetrix).

The reaction contained:

> double stranded cDNA template
>
> 1 x Biotin-labeled ribonucleotide mix
>
> 1 x HY reaction buffer
>
> 1 x DTT stock
>
> 1 x RNase inhibitor mix
>
> 1 x Enzo T7 polymerase

and was incubated at 37°C for 6 h. The obtained cRNA was purified using the RNeasy Mini Kit spin columns (QIAGEN) according to the manufacturers instructions. Cleanup of biotin-labeled cRNA was performed using specific spin columns for GeneChip sample cleanup (Affymetrix) according to the manufacturers instructions and fragmented by incubation with fragmentation buffer (Affymetrix) at 94°C for 35 min. Undiluted, fragmented biotin-cRNA was stored at -20°C until hybridization.

5.3.11.4 Target hybridization

A hybridization cocktail for a single microarray contained:

Fragmented biotin-c RNA	5 µg (0.05 µg/µl f. c.)
control oligonucleotide B2	50 pM
eukaryotic hybridization controls	
(*bioB, bioC, bioD, cre*)	1.5, 5, 25 and 100 pm, respectively
herring sperm DNA	0.1 mg/ml
acetylated BSA	0.5 mg/ml
1 x hybridization buffer	

The hybridization cocktail was heated to 99°C for 5 min and equilibrated to 45°C for 5 min and the probe array was pre-incubated with 1 x hybridization buffer at 45°C for 10 min, before the hybridization cocktail was incubated with a MGU74A murine genome probe array at 45°C in a rotisserie oven for 16 h.

5.3.11.5 Probe array wash and stain

MGU74A probe arrays were washed and stained using a microarray fluidics wash and stain station following the following protocol:

10 cycles of 2 mixes/cycle with non-stringent wash buffer at 25°C

4 cycles of 15 mixes/cycle with stringent wash buffer at 50 °C

Staining for 30 min in SAPE solution at 25°C

10 cycles of 4 mixes/cycle with non-stringent wash buffer at 25°C

5.3.11.6 Probe array scan

Probe arrays were scanned with a microarray scanner controlled by Affymetrix Microarray Suite software. Each complete probe array image was stored in a separate data file. The image was analyzed for probe intensities by the Affymetrix Microarray Suite software. Results were reported in tabular and graphical formats; the array images allowed a quality analysis of hybridization and scan, *e.g.* the absence of blank spots or scratches, the labeling of all control oligos and a homogeneous distribution of signal intensities.

5.3.11.7 Statistical analysis of gene expression data

Normalization of gene expression values was performed using dChip software (Li and Hung Wong 2001; Li and Wong 2001). Intensity values were normalized against a probe array with medium average intensity. Significant changes in gene expression were identified using Significance analysis of Microarrays (SAM) software (Tusher *et*

al. 2001). Details of the SAM procedure are given in "SAM - User guide and technical document", available at http://www-stat.stanford.edu/˜tibs/SAM. Data was analyzed using the SAM algorithm for a two-class, unpaired response.

5.3.12 Preparation of cell lysates

Whole cell lysates were generally prepared on ice using RIPA buffer and sonication. Lysates were clarified by centrifugation (13 000 rpm, 15 min) at 4°C and protein concentration was determined using the DC-Protein assay (BioRad).

5.3.13 Isolation of fractionated cell extracts

Cells were resuspended in hypotonic lysis buffer and incubated 15 in on ice. To break up the cells they were passed 5 times through 22.5 gauge needle or sheared with 5 – 10 strokes with a loose (type B) pestle. Trypan blue staining was performed to check for outer membrane disruption. Nuclei and heavy membranes were pelleted by centrifugation (13 000 rpm, 15 min, 4°C). The supernatant was collected as cytosolic fraction. The pellet (nuclear and heavy membrane fraction) was washed 1x with hypotonic lysis buffer, resuspended in nuclear extract buffer and lysed by sonication. Extracts were cleared by centrifugation (13 000 rpm, 15 min, 4°C).

5.3.14 Isolation of mitochondria/heavy membrane fraction from mouse liver

The entire procedure (modified from Eskes et al., 1998, Cowling et al. 2002) was carried out on ice and in refrigerated centrifuges.

One third to one half of a freshly isolated mouse liver was rinsed in PBS and homogenized with 15 strokes of a loose fitting (B type) pestle in 30 ml mannitol/sucrose buffer I. The homogenate was centrifuged for 6 min at 13 000 g. The pellet was dissolved in 20-30 ml mannitol/sucrose buffer I and centrifuged for 3 min at1 400 g. The supernatant was centrifuged for 3 min at 13 000 g to pellet the heavy membrane fraction containing mitochondria. This fraction was resuspended in mannitol/sucrose buffer II and centrifuged for 3 min at 13 000 g. The pellet was resuspended in mannitol/sucrose buffer II and used within 1 h of preparation. An

aliquot of the preparation was lysed in RIPA and protein concentration was determined using the DC-Protein Assay (BioRad).

5.3.15 Determination of protein concentration

Detergent compatible (DC)-Protein Assays (modified Lowry assay) or Protein Assays (modified Bradford assay) (BioRad) were performed in microtiter plates according to the manufacturers instructions. Samples were diluted 1:10 and reactions were set up in triplicate. For each reaction, absorbance at 595 nm (Protein Assay) or 750 nm (DC-Protein Assay) was determined and the O.D. curve for serial dilutions (0.125 mg – 1 mg) of a BSA standard solution was used to calculate protein concentrations.

5.3.16 Caspase activity assay

Cells were lysed in PIPES/CHAPS buffer and clarified by centrifugation. Protein concentration was determined using the Protein Assay (BioRad) and 50 µg of total protein was incubated with 50 µM Acetyl-DEVD-7-amino-4-methylcoumarin (Ac-DEVD-AMC) or Acetyl-IETD-7-amino-4-trifluoromethylcoumarin (Ac-IETD-AFC) for 15-30 min at 37° C. Fluorometric detection of AMC and AFC was performed in triplicates by excitation at 360 nm/emission at 460 nm (AMC) and excitation at 405 nm/emission at 500 nm (AFC).

5.3.17 Immunoblotting

Usually, 50-100 µg of total protein were resolved by SDS-PAGE and transferred onto PVDF membranes. Membranes were blocked for at least 30 min in 5 % nonfat dry milk/TBST and incubated with primary antibodies diluted in 5 % nonfat dry milk/TBST (see paragraph 5.2.6 for dilution ratios) for 1 h (at RT) to overnight (at 4°C). Membranes were washed 3-4 times for 10 min with TBST and incubated with HRP-conjugated secondary antibodies diluted in 5 % nonfat dry milk/TBST for 1-3 h at RT. After washing (3 x 10 min TBST), membranes were incubated with enhanced chemoluminiscence (ECL) reagent for 1-5 min and incubated with an autoradiographic film. Films were automatically developed.

5.3.18 Immunoprecipitation

For immunoprecipitation of Rb, whole cell lysates were prepared by sonication in RIPA buffer. Lysates were cleared by centrifugation for 20 min at 10 000 x g. 1-2 mg of total lysate were used per sample. Sample volume was adjusted to 900 ml with RIPA buffer. 100 ml RIPA buffer containing 2-3 ml antibody and 40 ml protein A/G sepharose beads (50 % slurry in PBS) were added per sample and samples were incubated overnight at 4°C with constant rotation. Sepharose beads were pelleted by centrifugation and washed 1 x with RIPA + 0.5 M NaCl, 1 x with RIPA + 0.25 M NaCl, 2 x with RIPA and 1 x with PBS. Washed beads were boiled in SDS sample buffer for 15 min and pelleted by centrifugation. Supernatants were resolved on a 6-8 % SDS-PA gel.

5.3.19 Analysis of *in vivo* cytochrome c release by cell fractionation

Cells were trypsinized, washed in PSB, resuspended in mannitol/sucrose buffer on ice and broken up by passage through a 22.5 gauge needle (ca. 15 times). Efficient rupture of plasma membranes was confirmed by trypan blue staining. Heavy membrane fractions (containing mitochondria) were pelleted by centrifugation (10 min, 13 000 rpm) at 4°C. 100 µg of the supernatants was resolved on a 14% SDS-PA gel. Proteins were transferred on PVDF membranes in SDS free transfer buffer (20% methanol) for 1-1.5 h at 80-100 V and cytochrome c was detected by immunoblotting.

5.3.20 *In vitro* cytochrome c release assay

Freshly isolated liver mitochondria (ca. 1 µg/µl) were combined with cytosolic extracts from untreated or TNF-treated wild-type or $Rb^{MI/MI}$ cells diluted in KCL buffer. Reactions were incubated for 45 min at 37°C under gentle agitation. Mitochondria were pelleted by centrifugation for 15 min at 10 000 x g at 4°C. One quart to one third of supernatants and pellets were separately analyzed for cytochrome c release by immunoblotting as described above. Supernatants were diluted with sample buffer directly, pellets were first resuspended in RIPA buffer, lysed by sonication and cleared by centrifugation for 10 min at 10 000 x g at 4°C.

6 References

Acehan, D., Jiang, X., Morgan, D. G., Heuser, J. E., Wang, X. and Akey, C. W. (2002). "Three-dimensional structure of the apoptosome: implications for assembly, procaspase-9 binding, and activation." *Mol Cell* 9(2): 423-32.

Adams, J. M. and Cory, S. (2001). "Life-or-death decisions by the Bcl-2 protein family." *Trends Biochem Sci* 26(1): 61-6.

Alnemri, E. S., Livingston, D. J., Nicholson, D. W., Salvesen, G., Thornberry, N. A., Wong, W. W. and Yuan, J. (1996). "Human ICE/CED-3 protease nomenclature." *Cell* 87(2): 171.

Ashkenazi, A. and Dixit, V. M. (1998). "Death receptors: signaling and modulation." *Science* 281(5381): 1305-8.

Boatright, K. M. and Salvesen, G. S. (2003). "Mechanisms of caspase activation." *Curr Opin Cell Biol* 15(6): 725-31.

Bonner, W. M., Wu, R. S., Panusz, H. T. and Muneses, C. (1988). "Kinetics of accumulation and depletion of soluble newly synthesized histone in the reciprocal regulation of histone and DNA synthesis." *Biochemistry* 27(17): 6542-50.

Boutillier, A. L., Trinh, E. and Loeffler, J. P. (2000). "Caspase-dependent cleavage of the retinoblastoma protein is an early step in neuronal apoptosis." *Oncogene* 19(18): 2171-2178.

Bremner, R., Cohen, B. L., Sopta, M., Hamel, P. A., Ingles, C. J., Gallie, B. L. and Phillips, R. A. (1995). "Direct transcriptional repression by pRB and its reversal by specific cyclins." *Mol Cell Biol* 15(6): 3256-65.

References

Budihardjo, I., Oliver, H., Lutter, M., Luo, X. and Wang, X. (1999). "Biochemical pathways of caspase activation during apoptosis." *Annu Rev Cell Dev Biol* 15: 269-90.

Cauwels, A., Janssen, B., Waeytens, A., Cuvelier, C. and Brouckaert, P. (2003). "Caspase inhibition causes hyperacute tumor necrosis factor-induced shock via oxidative stress and phospholipase A2." *Nat Immunol* 4(4): 387-93.

Chang, D. W., Xing, Z., Pan, Y., Algeciras-Schimnich, A., Barnhart, B. C., Yaish-Ohad, S., Peter, M. E. and Yang, X. (2002). "c-FLIP(L) is a dual function regulator for caspase-8 activation and CD95-mediated apoptosis." *Embo J* 21(14): 3704-14.

Chau, B. N., Borges, H. L., Chen, T. T., Masselli, A., Hunton, I. C. and Wang, J. Y. (2002). "Signal-dependent protection from apoptosis in mice expressing caspase-resistant Rb." *Nat Cell Biol* 4(10): 757-65.

Chau, B. N., Chen, T. T., Wan, Y. Y., DeGregori, J. and Wang, J. Y. (2004). "Tumor necrosis factor alpha-induced apoptosis requires p73 and c-ABL activation downstream of RB degradation." *Mol Cell Biol* 24(10): 4438-47.

Chau, B. N. and Wang, J. Y. (2003). "Coordinated regulation of life and death by RB." *Nat Rev Cancer* 3(2): 130-8.

Chen, X., Lowe, M., Herliczek, T., Hall, M. J., Danes, C., Lawrence, D. A. and Keyomarsi, K. (2000). "Protection of normal proliferating cells against chemotherapy by staurosporine-mediated, selective, and reversible G(1) arrest." *J Natl Cancer Inst* 92(24): 1999-2008.

Cheng, E. H., Wei, M. C., Weiler, S., Flavell, R. A., Mak, T. W., Lindsten, T. and Korsmeyer, S. J. (2001). "BCL-2, BCL-X(L) sequester BH3 domain-only molecules preventing BAX- and BAK-mediated mitochondrial apoptosis." *Mol Cell* 8(3): 705-11.

Chipuk, J. E., Kuwana, T., Bouchier-Hayes, L., Droin, N. M., Newmeyer, D. D., Schuler, M. and Green, D. R. (2004). "Direct activation of Bax by p53 mediates mitochondrial membrane permeabilization and apoptosis." *Science* 303(5660): 1010-4.

Clarke, A. R., Maandag, E. R., van Roon, M., van der Lugt, N. M., van der Valk, M., Hooper, M. L., Berns, A. and te Riele, H. (1992). "Requirement for a functional Rb-1 gene in murine development." *Nature* 359(6393): 328-30.

Clem, R. J. (2001). "Baculoviruses and apoptosis: the good, the bad, and the ugly." *Cell Death Differ* 8(2): 137-43.

Danial, N. N. and Korsmeyer, S. J. (2004). "Cell death: critical control points." *Cell* 116(2): 205-19.

Darnell, G. A., Antalis, T. M., Johnstone, R. W., Stringer, B. W., Ogbourne, S. M., Harrich, D. and Suhrbier, A. (2003). "Inhibition of retinoblastoma protein degradation by interaction with the serpin plasminogen activator inhibitor 2 via a novel consensus motif." *Mol Cell Biol* 23(18): 6520-32.

Denecker, G., Vercammen, D., Steemans, M., Vanden Berghe, T., Brouckaert, G., Van Loo, G., Zhivotovsky, B., Fiers, W., Grooten, J., Declercq, W. and Vandenabeele, P. (2001). "Death receptor-induced apoptotic and necrotic cell death: differential role of caspases and mitochondria." *Cell Death Differ* 8(8): 829-40.

Desagher, S., Osen-Sand, A., Nichols, A., Eskes, R., Montessuit, S., Lauper, S., Maundrell, K., Antonsson, B. and Martinou, J. C. (1999). "Bid-induced conformational change of Bax is responsible for mitochondrial cytochrome c release during apoptosis." *J Cell Biol* 144(5): 891-901.

References

Deveraux, Q. L., Roy, N., Stennicke, H. R., Van Arsdale, T., Zhou, Q., Srinivasula, S. M., Alnemri, E. S., Salvesen, G. S. and Reed, J. C. (1998). "IAPs block apoptotic events induced by caspase-8 and cytochrome c by direct inhibition of distinct caspases." *Embo J* 17(8): 2215-23.

Du, C., Fang, M., Li, Y., Li, L. and Wang, X. (2000). "Smac, a mitochondrial protein that promotes cytochrome c-dependent caspase activation by eliminating IAP inhibition." *Cell* 102(1): 33-42.

Earnshaw, W. C., Martins, L. M. and Kaufmann, S. H. (1999). "Mammalian caspases: structure, activation, substrates, and functions during apoptosis." *Annu Rev Biochem* 68: 383-424.

Eskes, R., Desagher, S., Antonsson, B. and Martinou, J. C. (2000). "Bid induces the oligomerization and insertion of Bax into the outer mitochondrial membrane." *Mol Cell Biol* 20(3): 929-35.

Fattman, C. L., Delach, S. M., Dou, Q. P. and Johnson, D. E. (2001). "Sequential two-step cleavage of the retinoblastoma protein by caspase- 3/-7 during etoposide-induced apoptosis." *Oncogene* 20(23): 2918-26.

Ferguson, K. L. and Slack, R. S. (2001). "The Rb pathway in neurogenesis." *Neuroreport* 12(9): A55-62.

Gera, J. F., Fady, C., Gardner, A., Jacoby, F. J., Briskin, K. B. and Lichtenstein, A. (1993). "Inhibition of DNA repair with aphidicolin enhances sensitivity of targets to tumor necrosis factor." *J Immunol* 151(7): 3746-57.

Goldstein, J. C., Waterhouse, N. J., Juin, P., Evan, G. I. and Green, D. R. (2000). "The coordinate release of cytochrome c during apoptosis is rapid, complete and kinetically invariant." *Nat Cell Biol* 2(3): 156-62.

Gomez-Angelats, M. and Cidlowski, J. A. (2003). "Molecular evidence for the nuclear localization of FADD." *Cell Death Differ* 10(7): 791-7.

References

Green, D. R. and Reed, J. C. (1998). "Mitochondria and apoptosis." *Science* 281(5381): 1309-12.

Guo, Z., Yikang, S., Yoshida, H., Mak, T. W. and Zacksenhaus, E. (2001). "Inactivation of the retinoblastoma tumor suppressor induces apoptosis protease-activating factor-1 dependent and independent apoptotic pathways during embryogenesis." *Cancer Res* 61(23): 8395-400.

Harbour, J. W. a. D., D. C. (2000). "Rb function in cell-cycle regulation and apoptosis." *Nature Cell Biol.* 2(4): E65-E76.

Harper, N., Hughes, M., MacFarlane, M. and Cohen, G. M. (2003). "Fas-associated death domain protein and caspase-8 are not recruited to the tumor necrosis factor receptor 1 signaling complex during tumor necrosis factor-induced apoptosis." *J Biol Chem* 278(28): 25534-41.

Hegde, R., Srinivasula, S. M., Zhang, Z., Wassell, R., Mukattash, R., Cilenti, L., DuBois, G., Lazebnik, Y., Zervos, A. S., Fernandes-Alnemri, T. and Alnemri, E. S. (2002). "Identification of Omi/HtrA2 as a mitochondrial apoptotic serine protease that disrupts inhibitor of apoptosis protein-caspase interaction." *J Biol Chem* 277(1): 432-8.

Heinrich, M., Neumeyer, J., Jakob, M., Hallas, C., Tchikov, V., Winoto-Morbach, S., Wickel, M., Schneider-Brachert, W., Trauzold, A., Hethke, A. and Schutze, S. (2004). "Cathepsin D links TNF-induced acid sphingomyelinase to Bid-mediated caspase-9 and -3 activation." *Cell Death Differ* 11(5): 550-63.

Huang, D. C. and Strasser, A. (2000). "BH3-Only proteins-essential initiators of apoptotic cell death." *Cell* 103(6): 839-42.

Humphreys, D. T. and Wilson, M. R. (1999). "Modes of L929 cell death induced by TNF-alpha and other cytotoxic agents." *Cytokine* 11(10): 773-82.

Igney, F. H. and Krammer, P. H. (2002). "Death and anti-death: tumour resistance to apoptosis." *Nat Rev Cancer* 2(4): 277-88.

References

Jacks, T., Fazeli, A., Schmitt, E. M., Bronson, R. T., Goodell, M. A. and Weinberg, R. A. (1992). "Effects of an Rb mutation in the mouse." *Nature* 359(6393): 295-300.

Karin, M. (1998). "The NF-kappa B activation pathway: its regulation and role in inflammation and cell survival." *Cancer J Sci Am* 4 Suppl 1: S92-9.

Kerr, J. F., Wyllie, A. H. and Currie, A. R. (1972). "Apoptosis: a basic biological phenomenon with wide-ranging implications in tissue kinetics." *Br J Cancer* 26(4): 239-57.

Kischkel, F. C., Hellbardt, S., Behrmann, I., Germer, M., Pawlita, M., Krammer, P. H. and Peter, M. E. (1995). "Cytotoxicity-dependent APO-1 (Fas/CD95)-associated proteins form a death-inducing signaling complex (DISC) with the receptor." *Embo J* 14(22): 5579-88.

Knudsen, E. S., Buckmaster, C., Chen, T. T., Feramisco, J. R. and Wang, J. Y. (1998). "Inhibition of DNA synthesis by RB: effects on G1/S transition and S-phase progression." *Genes Dev* 12(15): 2278-92.

Knudsen, E. S. and Wang, J. Y. (1996). "Differential regulation of retinoblastoma protein function by specific Cdk phosphorylation sites." *J Biol Chem* 271(14): 8313-20.

Knudsen, E. S. and Wang, J. Y. (1997). "Dual mechanisms for the inhibition of E2F binding to RB by cyclin-dependent kinase-mediated RB phosphorylation." *Mol Cell Biol* 17(10): 5771-83.

Knudsen, K. E., Booth, D., Naderi, S., Sever-Chroneos, Z., Fribourg, A. F., Hunton, I. C., Feramisco, J. R., Wang, J. Y. and Knudsen, E. S. (2000). "RB-dependent S-phase response to DNA damage." *Mol Cell Biol* 20(20): 7751-63.

Knudson, A. G., Jr. (1971). "Mutation and cancer: statistical study of retinoblastoma." *Proc Natl Acad Sci U S A* 68(4): 820-3.

References

Konishi, A., Shimizu, S., Hirota, J., Takao, T., Fan, Y., Matsuoka, Y., Zhang, L., Yoneda, Y., Fujii, Y., Skoultchi, A. I. and Tsujimoto, Y. (2003). "Involvement of histone H1.2 in apoptosis induced by DNA double-strand breaks." *Cell* 114(6): 673-88.

Krueger, A., Baumann, S., Krammer, P. H. and Kirchhoff, S. (2001). "FLICE-inhibitory proteins: regulators of death receptor-mediated apoptosis." *Mol Cell Biol* 21(24): 8247-54.

Kuwana, T., Bouchier-Hayes, L., Chipuk, J. E., Bonzon, C., Sullivan, B. A., Green, D. R. and Newmeyer, D. D. (2005). "BH3 domains of BH3-only proteins differentially regulate Bax-mediated mitochondrial membrane permeabilization both directly and indirectly." *Mol Cell* 17(4): 525-35.

Kuwana, T., Mackey, M. R., Perkins, G., Ellisman, M. H., Latterich, M., Schneiter, R., Green, D. R. and Newmeyer, D. D. (2002). "Bid, Bax, and lipids cooperate to form supramolecular openings in the outer mitochondrial membrane." *Cell* 111(3): 331-42.

Kuwana, T. and Newmeyer, D. D. (2003). "Bcl-2-family proteins and the role of mitochondria in apoptosis." *Curr Opin Cell Biol* 15(6): 691-9.

Lassus, P., Opitz-Araya, X. and Lazebnik, Y. (2002). "Requirement for caspase-2 in stress-induced apoptosis before mitochondrial permeabilization." *Science* 297(5585): 1352-4.

Lee, E. Y., Chang, C. Y., Hu, N., Wang, Y. C., Lai, C. C., Herrup, K., Lee, W. H. and Bradley, A. (1992). "Mice deficient for Rb are nonviable and show defects in neurogenesis and haematopoiesis." *Nature* 359(6393): 288-94.

Lee, J. O., Russo, A. A. and Pavletich, N. P. (1998). "Structure of the retinoblastoma tumour-suppressor pocket domain bound to a peptide from HPV E7." *Nature* 391(6670): 859-65.

References

Lemaire, C., Andreau, K., Souvannavong, V. and Adam, A. (1998). "Inhibition of caspase activity induces a switch from apoptosis to necrosis." *FEBS Lett* 425(2): 266-70.

Li, C. and Hung Wong, W. (2001). "Model-based analysis of oligonucleotide arrays: model validation, design issues and standard error application." *Genome Biol* 2(8): RESEARCH0032.

Li, C. and Wong, W. H. (2001). "Model-based analysis of oligonucleotide arrays: expression index computation and outlier detection." *Proc Natl Acad Sci U S A* 98(1): 31-6.

Li, H., Zhu, H., Xu, C. J. and Yuan, J. (1998). "Cleavage of BID by caspase 8 mediates the mitochondrial damage in the Fas pathway of apoptosis." *Cell* 94(4): 491-501.

Li, K., Li, Y., Shelton, J. M., Richardson, J. A., Spencer, E., Chen, Z. J., Wang, X. and Williams, R. S. (2000). "Cytochrome c deficiency causes embryonic lethality and attenuates stress-induced apoptosis." *Cell* 101(4): 389-99.

Lin, Y., Choksi, S., Shen, H. M., Yang, Q. F., Hur, G. M., Kim, Y. S., Tran, J. H., Nedospasov, S. A. and Liu, Z. G. (2004). "Tumor necrosis factor-induced nonapoptotic cell death requires receptor-interacting protein-mediated cellular reactive oxygen species accumulation." *J Biol Chem* 279(11): 10822-8.

Lin, Y., Devin, A., Rodriguez, Y. and Liu, Z. G. (1999). "Cleavage of the death domain kinase RIP by caspase-8 prompts TNF-induced apoptosis." *Genes Dev* 13(19): 2514-26.

Lindsten, T., Ross, A. J., King, A., Zong, W. X., Rathmell, J. C., Shiels, H. A., Ulrich, E., Waymire, K. G., Mahar, P., Frauwirth, K., Chen, Y., Wei, M., Eng, V. M., Adelman, D. M., Simon, M. C., Ma, A., Golden, J. A., Evan, G., Korsmeyer, S. J., MacGregor, G. R. and Thompson, C. B. (2000). "The combined functions of proapoptotic Bcl-2 family members bak and bax are essential for normal development of multiple tissues." *Mol Cell* 6(6): 1389-99.

Lipinski, M. M. and Jacks, T. (1999). "The retinoblastoma gene family in differentiation and development." *Oncogene* 18(55): 7873-82.

Liu, Z. G. (2003). "Adding facets to TNF signaling. The JNK angle." *Mol Cell* 12(4): 795-6.

Liu, Z. G., Hsu, H., Goeddel, D. V. and Karin, M. (1996). "Dissection of TNF receptor 1 effector functions: JNK activation is not linked to apoptosis while NF-kappaB activation prevents cell death." *Cell* 87(3): 565-76.

Los, M., Mozoluk, M., Ferrari, D., Stepczynska, A., Stroh, C., Renz, A., Herceg, Z., Wang, Z. Q. and Schulze-Osthoff, K. (2002). "Activation and caspase-mediated inhibition of PARP: a molecular switch between fibroblast necrosis and apoptosis in death receptor signaling." *Mol Biol Cell* 13(3): 978-88.

Luo, X., Budihardjo, I., Zou, H., Slaughter, C. and Wang, X. (1998). "Bid, a Bcl2 interacting protein, mediates cytochrome c release from mitochondria in response to activation of cell surface death receptors." *Cell* 94(4): 481-90.

Macleod, K. F., Hu, Y. and Jacks, T. (1996). "Loss of Rb activates both p53-dependent and independent cell death pathways in the developing mouse nervous system." *Embo J* 15(22): 6178-88.

Martinou, J. C. and Green, D. R. (2001). "Breaking the mitochondrial barrier." *Nat Rev Mol Cell Biol* 2(1): 63-7.

McDonnell, T. J., Deane, N., Platt, F. M., Nunez, G., Jaeger, U., McKearn, J. P. and Korsmeyer, S. J. (1989). "bcl-2-immunoglobulin transgenic mice demonstrate extended B cell survival and follicular lymphoproliferation." *Cell* 57(1): 79-88.

Medema, J. P., Scaffidi, C., Kischkel, F. C., Shevchenko, A., Mann, M., Krammer, P. H. and Peter, M. E. (1997). "FLICE is activated by association with the CD95 death-inducing signaling complex (DISC)." *Embo J* 16(10): 2794-804.

References

Meikrantz, W. and Schlegel, R. (1995). "Apoptosis and the cell cycle." *J Cell Biochem* 58(2): 160-74.

Micheau, O., Thome, M., Schneider, P., Holler, N., Tschopp, J., Nicholson, D. W., Briand, C. and Grutter, M. G. (2002). "The long form of FLIP is an activator of caspase-8 at the Fas death-inducing signaling complex." *J Biol Chem* 277(47): 45162-71.

Micheau, O. and Tschopp, J. (2003). "Induction of TNF receptor I-mediated apoptosis via two sequential signaling complexes." *Cell* 114(2): 181-90.

Mittnacht, S. (1998). "Control of pRB phosphorylation." *Curr Opin Genet Dev* 8(1): 21-7.

Morgan, D. O., Fisher, R. P., Espinoza, F. H., Farrell, A., Nourse, J., Chamberlin, H. and Jin, P. (1998). "Control of eukaryotic cell cycle progression by phosphorylation of cyclin-dependent kinases." *Cancer J Sci Am* 4 Suppl 1: S77-83.

Morgan, M., Thorburn, J., Pandolfi, P. P. and Thorburn, A. (2002). "Nuclear and cytoplasmic shuttling of TRADD induces apoptosis via different mechanisms." *J Cell Biol* 157(6): 975-84.

Moroni, M. C., Hickman, E. S., Denchi, E. L., Caprara, G., Colli, E., Cecconi, F., Muller, H. and Helin, K. (2001). "Apaf-1 is a transcriptional target for E2F and p53." *Nat Cell Biol* 3(6): 552-8.

Morris, E. J. and Dyson, N. J. (2001). "Retinoblastoma protein partners." *Adv Cancer Res* 82: 1-54.

Muller, H., Bracken, A. P., Vernell, R., Moroni, M. C., Christians, F., Grassilli, E., Prosperini, E., Vigo, E., Oliner, J. D. and Helin, K. (2001). "E2Fs regulate the expression of genes involved in differentiation, development, proliferation, and apoptosis." *Genes Dev* 15(3): 267-85.

References

Nagata, S. (1997). "Apoptosis by death factor." *Cell* 88(3): 355-65.

Nakano, K. and Vousden, K. H. (2001). "PUMA, a novel proapoptotic gene, is induced by p53." *Mol Cell* 7(3): 683-94.

Nevins, J. R., Leone, G., DeGregori, J. and Jakoi, L. (1997). "Role of the Rb/E2F pathway in cell growth control." *J Cell Physiol* 173(2): 233-6.

Nielsen, S. J., Schneider, R., Bauer, U. M., Bannister, A. J., Morrison, A., O'Carroll, D., Firestein, R., Cleary, M., Jenuwein, T., Herrera, R. E. and Kouzarides, T. (2001). "Rb targets histone H3 methylation and HP1 to promoters." *Nature* 412(6846): 561-5.

Oda, E., Ohki, R., Murasawa, H., Nemoto, J., Shibue, T., Yamashita, T., Tokino, T., Taniguchi, T. and Tanaka, N. (2000). "Noxa, a BH3-only member of the Bcl-2 family and candidate mediator of p53-induced apoptosis." *Science* 288(5468): 1053-8.

Orr, M. S., Reinhold, W., Yu, L., Schreiber-Agus, N. and O'Connor, P. M. (1998). "An important role for the retinoblastoma protein in staurosporine-induced G1 arrest in murine embryonic fibroblasts." *J Biol Chem* 273(7): 3803-7.

Osborne, B. A., Smith, S. W., McLaughlin, K. A., Grimm, L., Kallinch, T., Liu, Z. and Schwartz, L. M. (1996). "Genes that regulate apoptosis in the mouse thymus." *J Cell Biochem* 60(1): 18-22.

Panaretakis, T., Pokrovskaja, K., Shoshan, M. C. and Grander, D. (2002). "Activation of Bak, Bax, and BH3-only proteins in the apoptotic response to doxorubicin." *J Biol Chem* 277(46): 44317-26.

Riedl, S. J., Renatus, M., Schwarzenbacher, R., Zhou, Q., Sun, C., Fesik, S. W., Liddington, R. C. and Salvesen, G. S. (2001). "Structural basis for the inhibition of caspase-3 by XIAP." *Cell* 104(5): 791-800.

References

Riedl, S. J. and Shi, Y. (2004). "Molecular mechanisms of caspase regulation during apoptosis." *Nat Rev Mol Cell Biol* 5(11): 897-907.

Robertson, K. D., Ait-Si-Ali, S., Yokochi, T., Wade, P. A., Jones, P. L. and Wolffe, A. P. (2000). "DNMT1 forms a complex with Rb, E2F1 and HDAC1 and represses transcription from E2F-responsive promoters." *Nat Genet* 25(3): 338-42.

Rodriguez, J. and Lazebnik, Y. (1999). "Caspase-9 and APAF-1 form an active holoenzyme." *Genes Dev* 13(24): 3179-84.

Roy, N., Deveraux, Q. L., Takahashi, R., Salvesen, G. S. and Reed, J. C. (1997). "The c-IAP-1 and c-IAP-2 proteins are direct inhibitors of specific caspases." *Embo J* 16(23): 6914-25.

Ruiz-Vela, A., Opferman, J. T., Cheng, E. H. and Korsmeyer, S. J. (2005). "Proapoptotic BAX and BAK control multiple initiator caspases." *EMBO Rep* 6(4): 379-385.

Salvesen, G. S. and Dixit, V. M. (1997). "Caspases: intracellular signaling by proteolysis." *Cell* 91(4): 443-6.

Salvesen, G. S. and Duckett, C. S. (2002). "IAP proteins: blocking the road to death's door." *Nat Rev Mol Cell Biol* 3(6): 401-10.

Scaffidi, C., Fulda, S., Srinivasan, A., Friesen, C., Li, F., Tomaselli, K. J., Debatin, K. M., Krammer, P. H. and Peter, M. E. (1998). "Two CD95 (APO-1/Fas) signaling pathways." *Embo J* 17(6): 1675-87.

Schneider-Brachert, W., Tchikov, V., Neumeyer, J., Jakob, M., Winoto-Morbach, S., Held-Feindt, J., Heinrich, M., Merkel, O., Ehrenschwender, M., Adam, D., Mentlein, R., Kabelitz, D. and Schutze, S. (2004). "Compartmentalization of TNF receptor 1 signaling: internalized TNF receptosomes as death signaling vesicles." *Immunity* 21(3): 415-28.

References

Schnier, J. B., Nishi, K., Goodrich, D. W. and Bradbury, E. M. (1996). "G1 arrest and down-regulation of cyclin E/cyclin-dependent kinase 2 by the protein kinase inhibitor staurosporine are dependent on the retinoblastoma protein in the bladder carcinoma cell line 5637." *Proc Natl Acad Sci U S A* 93(12): 5941-6.

Scorrano, L., Oakes, S. A., Opferman, J. T., Cheng, E. H., Sorcinelli, M. D., Pozzan, T. and Korsmeyer, S. J. (2003). "BAX and BAK regulation of endoplasmic reticulum Ca2+: a control point for apoptosis." *Science* 300(5616): 135-9.

Scott, F. L., Denault, J. B., Riedl, S. J., Shin, H., Renatus, M. and Salvesen, G. S. (2005). "XIAP inhibits caspase-3 and -7 using two binding sites: evolutionarily conserved mechanism of IAPs." *Embo J* 24(3): 645-55.

Screaton, R. A., Kiessling, S., Sansom, O. J., Millar, C. B., Maddison, K., Bird, A., Clarke, A. R. and Frisch, S. M. (2003). "Fas-associated death domain protein interacts with methyl-CpG binding domain protein 4: a potential link between genome surveillance and apoptosis." *Proc Natl Acad Sci U S A* 100(9): 5211-6.

Sever-Chroneos, Z., Angus, S. P., Fribourg, A. F., Wan, H., Todorov, I., Knudsen, K. E. and Knudsen, E. S. (2001). "Retinoblastoma tumor suppressor protein signals through inhibition of cyclin-dependent kinase 2 activity to disrupt PCNA function in S phase." *Mol Cell Biol* 21(12): 4032-45.

Sherr, C. J. (1996). "Cancer cell cycles." *Science* 274(5293): 1672-7.

Shi, Y. (2002). "Mechanisms of caspase activation and inhibition during apoptosis." *Mol Cell* 9(3): 459-70.

Shiozaki, E. N., Chai, J., Rigotti, D. J., Riedl, S. J., Li, P., Srinivasula, S. M., Alnemri, E. S., Fairman, R. and Shi, Y. (2003). "Mechanism of XIAP-mediated inhibition of caspase-9." *Mol Cell* 11(2): 519-27.

Simpson, M. T., MacLaurin, J. G., Xu, D., Ferguson, K. L., Vanderluit, J. L., Davoli, M. A., Roy, S., Nicholson, D. W., Robertson, G. S., Park, D. S. and Slack, R. S. (2001). "Caspase 3 deficiency rescues peripheral nervous system defect in retinoblastoma nullizygous mice." *J Neurosci* 21(18): 7089-98.

Smith, C. A., Farrah, T. and Goodwin, R. G. (1994). "The TNF receptor superfamily of cellular and viral proteins: activation, costimulation, and death." *Cell* 76(6): 959-62.

Spadari, S., Focher, F., Sala, F., Ciarrocchi, G., Koch, G., Falaschi, A. and Pedrali-Noy, G. (1985). "Control of cell division by aphidicolin without adverse effects upon resting cells." *Arzneimittelforschung* 35(7): 1108-16.

Srinivasula, S. M., Ahmad, M., Fernandes-Alnemri, T. and Alnemri, E. S. (1998). "Autoactivation of procaspase-9 by Apaf-1-mediated oligomerization." *Mol Cell* 1(7): 949-57.

Srinivasula, S. M., Hegde, R., Saleh, A., Datta, P., Shiozaki, E., Chai, J., Lee, R. A., Robbins, P. D., Fernandes-Alnemri, T., Shi, Y. and Alnemri, E. S. (2001). "A conserved XIAP-interaction motif in caspase-9 and Smac/DIABLO regulates caspase activity and apoptosis." *Nature* 410(6824): 112-6.

Stennicke, H. R. and Salvesen, G. S. (1999). "Caspases: preparation and characterization." *Methods* 17(4): 313-9.

Suzuki, Y., Imai, Y., Nakayama, H., Takahashi, K., Takio, K. and Takahashi, R. (2001). "A serine protease, HtrA2, is released from the mitochondria and interacts with XIAP, inducing cell death." *Mol Cell* 8(3): 613-21.

Suzuki, Y., Nakabayashi, Y., Nakata, K., Reed, J. C. and Takahashi, R. (2001). "X-linked inhibitor of apoptosis protein (XIAP) inhibits caspase-3 and -7 in distinct modes." *J Biol Chem* 276(29): 27058-63.

References

Suzuki, Y., Takahashi-Niki, K., Akagi, T., Hashikawa, T. and Takahashi, R. (2004). "Mitochondrial protease Omi/HtrA2 enhances caspase activation through multiple pathways." *Cell Death Differ* 11(2): 208-16.

Tan, X., Martin, S. J., Green, D. R. and Wang, J. Y. (1997). "Degradation of retinoblastoma protein in tumor necrosis factor- and CD95-induced cell death." *J Biol Chem* 272(15): 9613-6.

Tan, X. and Wang, J. Y. (1998). "The caspase-RB connection in cell death." *Trends Cell Biol* 8(3): 116-20.

Tang, G., Yang, J., Minemoto, Y. and Lin, A. (2001). "Blocking caspase-3-mediated proteolysis of IKKbeta suppresses TNF-alpha-induced apoptosis." *Mol Cell* 8(5): 1005-16.

Thornberry, N. A., Chapman, K. T. and Nicholson, D. W. (2000). "Determination of caspase specificities using a peptide combinatorial library." *Methods Enzymol* 322: 100-10.

Thornberry, N. A. and Lazebnik, Y. (1998). "Caspases: enemies within." *Science* 281(5381): 1312-6.

Tinel, A. and Tschopp, J. (2004). "The PIDDosome, a protein complex implicated in activation of caspase-2 in response to genotoxic stress." *Science* 304(5672): 843-6.

Troy, C. M. and Shelanski, M. L. (2003). "Caspase-2 redux." *Cell Death Differ* 10(1): 101-7.

Tsai, K. Y., Hu, Y., Macleod, K. F., Crowley, D., Yamasaki, L. and Jacks, T. (1998). "Mutation of E2f-1 suppresses apoptosis and inappropriate S phase entry and extends survival of Rb-deficient mouse embryos." *Mol Cell* 2(3): 293-304.

References

Tusher, V. G., Tibshirani, R. and Chu, G. (2001). "Significance analysis of microarrays applied to the ionizing radiation response." *Proc Natl Acad Sci U S A* 98(9): 5116-21.

Van Antwerp, D. J., Martin, S. J., Verma, I. M. and Green, D. R. (1998). "Inhibition of TNF-induced apoptosis by NF-kappa B." *Trends Cell Biol* 8(3): 107-11.

Varfolomeev, E. E. and Ashkenazi, A. (2004). "Tumor necrosis factor: an apoptosis JuNKie?" *Cell* 116(4): 491-7.

Vaux, D. L., Cory, S. and Adams, J. M. (1988). "Bcl-2 gene promotes haemopoietic cell survival and cooperates with c-myc to immortalize pre-B cells." *Nature* 335(6189): 440-2.

Veis, D. J., Sorenson, C. M., Shutter, J. R. and Korsmeyer, S. J. (1993). "Bcl-2-deficient mice demonstrate fulminant lymphoid apoptosis, polycystic kidneys, and hypopigmented hair." *Cell* 75(2): 229-40.

Venkatesan, N. (1977). "Mechanism of inhibition of DNA synthesis by cycloheximide in Balb/3T3 cells." *Biochim Biophys Acta* 478(4): 437-53.

Verhagen, A. M., Silke, J., Ekert, P. G., Pakusch, M., Kaufmann, H., Connolly, L. M., Day, C. L., Tikoo, A., Burke, R., Wrobel, C., Moritz, R. L., Simpson, R. J. and Vaux, D. L. (2002). "HtrA2 promotes cell death through its serine protease activity and its ability to antagonize inhibitor of apoptosis proteins." *J Biol Chem* 277(1): 445-54.

Wajant, H., Pfizenmaier, K. and Scheurich, P. (2003). "Tumor necrosis factor signaling." *Cell Death Differ* 10(1): 45-65.

Wang, C. Y., Mayo, M. W., Korneluk, R. G., Goeddel, D. V. and Baldwin, A. S., Jr. (1998). "NF-kappaB antiapoptosis: induction of TRAF1 and TRAF2 and c-IAP1 and c-IAP2 to suppress caspase-8 activation." *Science* 281(5383): 1680-3.

References

Wang, J. Y. (2000). "Regulation of cell death by the Abl tyrosine kinase." *Oncogene* 19(49): 5643-50.

Wei, M. C., Zong, W. X., Cheng, E. H., Lindsten, T., Panoutsakopoulou, V., Ross, A. J., Roth, K. A., MacGregor, G. R., Thompson, C. B. and Korsmeyer, S. J. (2001). "Proapoptotic BAX and BAK: a requisite gateway to mitochondrial dysfunction and death." *Science* 292(5517): 727-30.

Wu, G., Chai, J., Suber, T. L., Wu, J. W., Du, C., Wang, X. and Shi, Y. (2000). "Structural basis of IAP recognition by Smac/DIABLO." *Nature* 408(6815): 1008-12.

Xiao, B., Spencer, J., Clements, A., Ali-Khan, N., Mittnacht, S., Broceno, C., Burghammer, M., Perrakis, A., Marmorstein, R. and Gamblin, S. J. (2003). "Crystal structure of the retinoblastoma tumor suppressor protein bound to E2F and the molecular basis of its regulation." *Proc Natl Acad Sci U S A* 100(5): 2363-8.

Yang, Q. H. and Du, C. (2004). "Smac/DIABLO selectively reduces the levels of c-IAP1 and c-IAP2 but not that of XIAP and livin in HeLa cells." *J Biol Chem* 279(17): 16963-70.

Yoshida, M., Usui, T., Tsujimura, K., Inagaki, M., Beppu, T. and Horinouchi, S. (1997). "Biochemical differences between staurosporine-induced apoptosis and premature mitosis." *Exp Cell Res* 232(2): 225-39.

Zha, J., Harada, H., Yang, E., Jockel, J. and Korsmeyer, S. J. (1996). "Serine phosphorylation of death agonist BAD in response to survival factor results in binding to 14-3-3 not BCL-X(L)." *Cell* 87(4): 619-28.

Zou, H., Li, Y., Liu, X. and Wang, X. (1999). "An APAF-1.cytochrome c multimeric complex is a functional apoptosome that activates procaspase-9." *J Biol Chem* 274(17): 11549-56.

7   Acknowledgements

8   Lebenslauf

Name, Vorname: Masselli, Anja

Geburtsdatum: 25.07.1976

Geburtsort: Göttingen

Staatsangehörigkeit: deutsch

1983 – 1987   Besuch der Grundschule in Bad Sooden-Allendorf

1987 - 1996   Besuch der Rhenanus-Schule Bad Sooden-Allendorf (Gesamtschule mit gymnasialer Oberstufe)

1996   Abitur an der gymnasialen Oberstufe der Rhenanus-Schule Bad Sooden-Allendorf

1996 – 1998   Studium der Biochemie an der Universität Regensburg

1998   Vordiplom an der Universität Regensburg

1998 – 2001   Studium der Biochemie/Molekularbiologie an der Friedrich-Schiller-Universität Jena

2000 – 2001   Diplomarbeit am Max-Planck-Institut für Biophysikalische Chemie in Göttingen, in der Abteilung Neurobiologie von Herrn Prof. Dr. Reinhardt Jahn

2001   Erlangung des Hochschulgrades "Diplom-Biochemikerin" an der Friedrich-Schiller-Universität Jena; Gesamtnote „ausgezeichnet".

2001 – 2005   Doktorarbeit an der *University of California San Diego* (UCSD) im *Department of Molecular Biology*, in der Arbeitsgruppe von Frau Prof. Dr. Jean Y. J. Wang

9 Selbstständigkeitserklärung

Ich erkläre hiermit, dass ich die vorliegende Arbeit selbstständig und nur unter Verwendung der angegebenen Hilfsmittel und Quellen angefertigt habe.

Jena, den 28. Mai 2005